

Dissertation zur Erlangung des Doktorgrades  
der Fakultät für Chemie und Pharmazie  
der Ludwig-Maximilians-Universität München

**Functional characterization of the N-terminal  
glycine of the GxGD aspartyl protease active  
site motif in presenilin 1**

Blanca Isabel Pérez Revuelta  
aus  
Salamanca, Spanien

2008

### Erklärung

Diese Dissertation wurde im Sinne von § 13 Abs. 4 der Promotionsordnung vom 29. Januar 1998 von Prof. Dr. Christian Haass und von Prof. Dr. Ralf-Peter Jansen vor der Fakultät für Chemie and Pharmazie vertreten.

### Ehrenwörtliche Versicherung

Diese Dissertation wurde selbständig, ohne unerlaubte Hilfe erarbeitet.

München, am 16.10.08

.....  
(Blanca I. Pérez Revuelta)

Dissertation eingereicht am 16.10.08

1. Gutachter: Prof. Dr. Ralf-Peter Jansen

2. Gutachter: Prof. Dr. Christian Haass

Mündliche Prüfung am 9.12.08

To my father, my mother and my sister.

The results in this dissertation are partially presented in the following publication:

**Generation of Abeta 38 and Abeta 42 is independently and differentially affected by FAD-associated presenilin 1 mutations and gamma secretase modulation.**

Page RM, Baumann K, Tomioka M, Pérez Revuelta, BI, Fukumori A, Jacobsen H, Flohr A, Luebbbers T, Ozmen L, Steiner H, Haass C.

*J Biol Chem* 2008 Jan 11;283(2):677-83

## ABBREVIATIONS

<b>aa</b>	Amino acid
<b>A<math>\beta</math></b>	Amyloid- $\beta$ peptide
<b>AD</b>	Alzheimer's disease
<b>ADAM</b>	A disintegrin and metalloproteinase
<b>AICD</b>	APP intracellular domain
<b>APH-1</b>	Anterior pharynx-defective phenotype
<b>APLP</b>	APP like protein
<b>APP</b>	$\beta$ -amyloid precursor protein
<b>APS</b>	Ammonium persulfat
<b>BACE</b>	$\beta$ -site APP-cleaving enzyme
<b>BSA</b>	Bovine serum albumin
<b>CD44</b>	Cluster of differentiation 44
<b>CD44<math>\beta</math></b>	CD44 beta peptide
<b>CD44-ICD</b>	CD44 intracellular domain
<b><i>C.elegans</i></b>	<i>Caenorhabditis elegans</i>
<b>CHAPSO</b>	3-[(3-cholamidopropyl)dimethyl-ammonio]-2-hydroxy-1-propanesulfonate
<b>CTF</b>	C-terminal fragment
<b>DDM</b>	n-dodecyl-D-maltoside
<b>DMSO</b>	Dimethyl sulphoxide
<b>DNA</b>	Deoxyribonucleic acid
<b>DTT</b>	1,4 Dithiothreitol
<b><i>E.coli</i></b>	<i>Escherichia coli</i>
<b>EDTA</b>	Ethylene diamine tetraacetic
<b>EGFR</b>	Epidermal-growth-factor-receptor
<b>ER</b>	Endoplasmic reticulum
<b>FAD</b>	Familial AD
<b>Fen</b>	Fenofibrate
<b>F-NEXT</b>	Flag tagged NEXT
<b>Flu</b>	Flurbiprofen
<b>GSM</b>	$\gamma$ -Secretase modulator
<b>HEK</b>	Human embryonic kidney cells
<b>HOP-1</b>	Homologue of PS
<b>ICD</b>	Intracellular domain
<b>IL1R2</b>	Interleukin1 receptor type II
<b>IP</b>	Immunoprecipitation
<b>kDa</b>	Kilodalton
<b>MEF</b>	Mouse embryonic fibroblast
<b>MMP</b>	Membrane-associated matrix metalloproteinase
<b>MS</b>	Mass spectrometry
<b>Nap</b>	Naproxen
<b>N<math>\beta</math></b>	Notch beta peptide
<b>NCT</b>	Nicastrin
<b>NEXT</b>	Notch extracellular truncation
<b>NICD</b>	Notch intracellular domain
<b>NSAID</b>	Non-steroidal anti-inflammatory drug
<b>NTF</b>	N-terminal fragment
<b>PAGE</b>	Polyacrylamide gel electrophoresis
<b>PBS</b>	Phosphate buffer saline
<b>PCR</b>	Polymerase chain reaction

ABBREVIATIONS

<b>PEN-2</b>	PS enhancer 2
<b>PS</b>	Presenilin
<b>RNA</b>	Ribonucleic acid
<b>RNAi</b>	RNA interference
<b>SAP</b>	Shrimp alkaline phosphatase
<b>S1,S2,S3,S4</b>	Site 1, site 2, site 3, site 4
<b>sAPP</b>	Soluble APP
<b>sCD44</b>	Soluble CD44
<b>SDS</b>	Sodium dodecyl sulfate
<b>SEL-12</b>	Suppressor / enhancers of lin-12
<b>SPE-4</b>	Spermatogenesis defective-4
<b>SPP</b>	Signal peptide peptidase
<b>SPPL</b>	SPP like protein
<b>Sul</b>	Sulindac sulfide
<b>sw</b>	Swedish mutant
<b>TBS</b>	Tris buffer saline
<b>TEMED</b>	N,N,N',N'-tetramethylethylenediamine
<b>TFPP</b>	Type 4 prepilin peptidase
<b>TNF-<math>\alpha</math></b>	Tumor necrosis factor- $\alpha$
<b>wt</b>	Wild type

<b>1</b>	<b>Introduction</b>	<b>11</b>
1.1	<i>Alzheimer's disease</i>	11
1.2	<i>Genetics of Alzheimer's disease</i>	13
1.3	<i>Molecular cell biology of Alzheimer's disease</i>	16
1.3.1	Amyloid $\beta$ precursor protein (APP)	16
1.3.1.1	APP processing	17
1.3.2	$\alpha$ - and $\beta$ -Secretase	21
1.3.3	$\gamma$ -Secretase	22
1.3.3.1	Components of the $\gamma$ -secretase complex	24
1.3.3.1.1	Presenilin	24
1.3.3.1.2	Nicastrin	25
1.3.3.1.3	PEN-2	25
1.3.3.1.4	APH-1	26
1.3.3.2	$\gamma$ -Secretase assembly	26
1.3.3.3	Substrates of the $\gamma$ -secretase complex	27
1.3.3.3.1	Notch	28
1.3.3.3.2	CD44	29
1.3.3.4	Substrate recognition by $\gamma$ -secretase	30
1.3.3.5	$\gamma$ -Secretase as a therapeutical target	32
1.4	<i>The GxGD protease family</i>	33
1.5	<i>Aim of the study</i>	35
<b>2</b>	<b>Materials and methods</b>	<b>37</b>
2.1	<i>Machines and software</i>	37
2.1.1	Equipment and instrument	37
2.1.2	Recombinant DNA techniques	38
2.1.3	Cell culture	38
2.1.4	Protein analysis	39
2.1.5	Sandwich immunoassay	39
2.1.6	Mass spectrometry	39
2.2	<i>Recombinant DNA techniques</i>	40
2.2.1	Constructs and vectors	40
2.2.2	Primers and template DNA	41
2.2.3	PCR reaction mixtures	41
2.2.4	PCR programs	41
2.2.5	Two-step PCR	42
2.2.6	Isolation and purification of PCR products	42
2.2.6.1	Materials	42
2.2.6.2	Agarose gel electrophoresis	42
2.2.6.3	Isolation and purification of PCR products from agarose gels	42
2.2.7	Enzymatic modification of cDNA fragments	43
2.2.7.1	Enzymes and vectors	43
2.2.7.2	Restriction enzyme treatment	43
2.2.7.3	Alkaline phosphatase treatment	43
2.2.7.4	Ligation of cDNA fragments	43
2.2.8	Transformation of <i>E.coli</i>	44
2.2.8.1	Materials	44
2.2.8.2	Preparation of competent cells	44
2.2.8.3	Transformation of <i>E.coli</i>	44
2.2.9	Preparation of plasmid DNA from <i>E.coli</i>	45

2.2.9.1	Materials	45
2.2.9.2	Small-scale plasmid DNA preparation (mini-prep)	45
2.2.9.3	Mini-prep analysis	45
2.2.9.4	Large scale plasmid DNA preparation (maxi-prep)	45
2.2.9.5	DNA sequencing	46
2.3	<i>Cell culture and cell lines</i>	46
2.3.1	Materials	46
2.3.2	Cell lines and culture medium	47
2.3.3	Cell culture	47
2.3.4	Transfection of mammalian cells	48
2.3.4.1	Materials	48
2.3.4.2	Transfection mixture	48
2.3.4.3	Transient co-transfection	48
2.3.4.4	Stable transfection	48
2.3.4.5	Drug treatment of cells	49
2.4	<i>Antibodies</i>	49
2.4.1	Monoclonal antibodies	49
2.4.2	Polyclonal antibodies	50
2.4.3	Secondary antibodies	50
2.5	<i>Protein analysis</i>	50
2.5.1	Total cell lysate	50
2.5.1.1	Materials	50
2.5.1.2	Cell lysate preparation	51
2.5.1.3	Protein quantitation	51
2.5.2	Membrane lysate	51
2.5.2.1	Materials	51
2.5.2.2	Preparation and solubilization of membrane	51
2.5.3	Immunoprecipitation	52
2.5.3.1	Materials	52
2.5.3.2	Immunoprecipitation from total cell lysate	52
2.5.3.3	Immunoprecipitation from conditioned media	53
2.5.4	<i>In vitro</i> $\gamma$ -secretase assay	54
2.5.4.1	Materials	54
2.5.4.2	Membrane preparation and <i>in vitro</i> $\gamma$ -secretase assay	54
2.5.5	Sample preparation for SDS-PAGE	55
2.5.5.1	Materials	55
2.5.5.2	Sample preparation	55
2.6	<i>SDS-Polyacrylamide gel electrophoresis (PAGE)</i>	56
2.6.1	Tris-glycine gels	56
2.6.1.1	Materials	56
2.6.1.2	Gel preparation	56
2.6.1.3	Electrophoresis	57
2.6.2	Tris-tricine gels	57
2.6.2.1	Materials	57
2.6.2.2	Electrophoresis	57
2.6.3	Modified Tris-bicine-urea gel	58
2.6.3.1	Materials	58
2.6.3.2	Gel preparation	58
2.6.3.3	Electrophoresis	59
2.7	<i>Western Blotting</i>	59
2.7.1	Materials	59
2.7.2	Blotting procedure	59
2.7.3	Blocking procedure	60



2.7.4	Primary antibody incubation .....	60
2.7.5	Secondary antibody incubation .....	60
2.7.6	Detection.....	60
2.8	<i>Sandwich immunoassay</i> .....	61
2.8.1	Materials .....	61
2.8.2	Sandwich immunoassay.....	61
2.9	<i>Mass Spectrometry (MS)</i> .....	62
2.9.1	Materials .....	62
2.9.2	Mass spectrometry analysis .....	62
<b>3</b>	<b>Results</b> .....	<b>63</b>
3.1	<i>Most PS1 G382 mutants do not undergo endoproteolysis and do not support APP processing</i> .....	63
3.1.1	PS1 G382A mutant produces AICD and A $\beta$ <i>in vitro</i> .....	66
3.1.2	PS1 G382A alters the cleavage specificity of the $\gamma$ -cleavage sites .....	67
3.1.3	PS1 G382A mutant shows an altered response to NSAIDs.....	70
3.2	<i>Impact of PS1 G382 mutants on the processing of other <math>\gamma</math>-secretase substrates</i> 80	
3.2.1	PS1 G382A supports processing of APPsw-6myc in PS1/PS2 -/- MEF cells 81	
3.2.2	PS1 G382A supports processing of Notch1 in PS1/PS2 -/- MEF cells.....	83
3.2.3	PS1 G382A supports Notch2 processing in PS1/PS2 -/- MEF cells .....	85
3.2.4	PS1 G382A mutant supports processing of Notch3 in PS1/PS2 -/- MEF cells 87	
3.2.5	PS1 G382 mutants do not support Notch4 processing in PS1/PS2 -/- MEF cells 89	
3.2.6	PS1 G382 mutants do not support processing of CD44 in PS1/PS2-/- MEF cells 91	
3.3	<i>Proteasomal turn over of NICD generated by PS1 wt, PS1 G382A and PS1 L383F is similar</i> .....	93
<b>4</b>	<b>Discussion</b> .....	<b>97</b>
4.1	<i>Most of the PS1 G382 mutants inhibit PS1 endoproteolysis</i> .....	97
4.2	<i>PS1 G382A has reduced <math>\gamma</math>-secretase activity possibly due to a distorted docking site</i> 98	
4.2.1	PS1 G382 mutants are inactive regarding APP processing except PS1 G382A mutant.....	98
4.2.2	PS1 G382A has an altered response to NSAIDs.....	98
4.2.3	PS1 G382A processes APP and Notch1-3 homologues but not Notch4 and CD44 100	
4.2.4	NICD generated by PS1 G382A and PS1 L383F mutants have a similar proteasomal turn over .....	101
4.2.5	PS1 G382 may form part of the $\gamma$ -secretase substrate docking site.....	102
4.3	<i>Putative structural placement of PS1 G382</i> .....	105
4.4	<i>PS1 G382 may form part of a putative helix-packing motif</i> .....	107
4.5	<i>The GxGD and PALP motif may be located close together in PS</i> .....	108
4.6	<i>Outlook</i> .....	110
<b>5</b>	<b>Summary</b> .....	<b>112</b>
<b>6</b>	<b>References</b> .....	<b>114</b>



# 1 Introduction

## 1.1 Alzheimer's disease

Alzheimer's disease (AD), named after the German psychiatrist Alois Alzheimer (figure 1), is the most common neurodegenerative dementia observed in people older than 65 years in the world and is expected to affect to ~16 million cases in the year 2050 in Europe (1). About 100 years ago Alzheimer described delusions, hallucinations, dementia, disorientation and loss of memory, as the clinical symptoms of the disease suffered by the 51 years old Auguste D. (figure 1) the first reported AD patient. Neuropathological post-mortem studies of her brain by silver staining identified neuritic plaques and neurofibrillary tangles (2) as the two principal hallmarks of the disease.

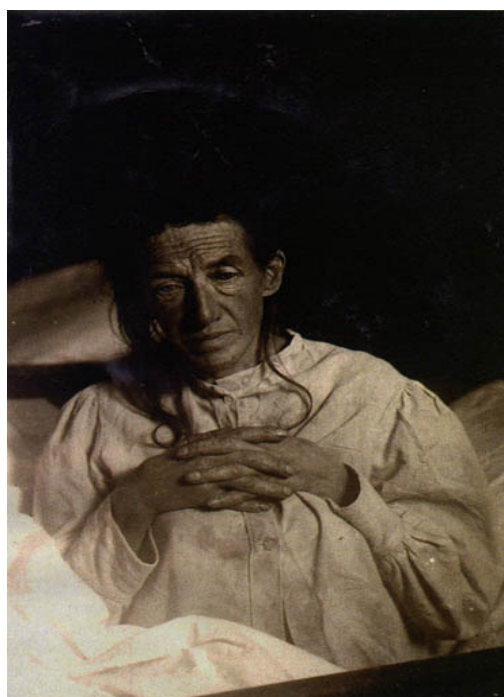


Figure 1. Photographs of Alois Alzheimer (left) and the first documented AD patient, Auguste D. (right).

Nowadays, using electron microscopy or immunohistochemical staining for synaptic markers has shown a decrease in the synaptic density in the AD brain (3,4). Moreover, the decrease in the synapse number is deproportionated to the loss of neurons. This suggests that the loss of synaptic endings precedes the demise of the neurons leading to the cognitive impairment, which is the major hallmark in AD.

Biochemical analysis showed that the neurofibrillary tangles present in AD brain, that occupy much of the perinuclear cytoplasm, are made of abnormal filaments, the so-called paired helical filaments (PHF). These have a diameter of 10 nm, and are formed by a hyperphosphorylated form of the microtubule-associated protein tau (5). The physiological role of tau is probably the stabilization of axonal microtubuli by bridging and stabilizing the tubulin-tubulin interfaces along protofilaments (6,7) but in AD, hyperphosphorylation of tau leads to its dissociation from the microtubules and aggregation into PHFs (8) (figure 2) perturbing probably the cell's transport machinery.

The second pathological hallmark in AD brain are neuritic plaques, which are generally found in the limbic and association cortices (9). These plaques contain extracellular deposits of amyloid- $\beta$  ( $A\beta$ ) peptide (10,11) and are surrounded by activated microglia and astrocytes (12) (figure 2). These amyloid plaques are composed of heterogeneous ~4 kDa  $A\beta$  peptide species derived from the amyloid precursor protein (APP) (13,14) (mainly  $A\beta$ 38,  $A\beta$ 40,  $A\beta$ 42,  $A\beta$ 43) and contain the highly aggregation-prone  $A\beta$ 42 as predominant constituent (15,16). Short N-terminal truncated species have also been found in the amyloid plaques (17).

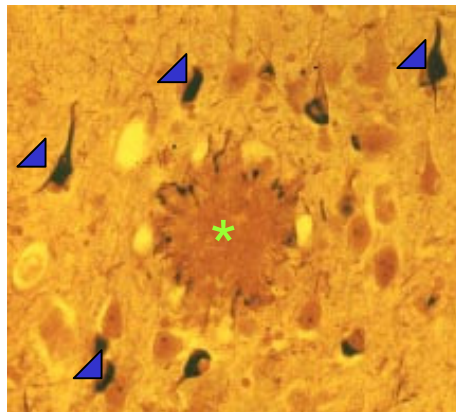


Figure 2: AD neuropathology as revealed by silver staining.  $A\beta$  containing plaques (green asterisk) and neurofibrillary tangles (blue head arrows).

Large  $A\beta$  plaques have been associated with local synaptic abnormalities even with the breakage of neuronal processes (18) but recent studies have also shown that small  $A\beta$  oligomers, dimers and trimers of  $A\beta$ , block hippocampal long-term potentiation, a measure of synaptic plasticity, *in vivo* (19). This block in the long-term potentiation reduces the density of dendritic spines and number of electrophysiologically active synapses thus interfering with the memory of a learned behavior in healthy adult rats (20,21). This

suggests that A $\beta$  oligomers might play an important role in AD pathogenesis. The large A $\beta$  aggregates could actually be inert or even protective to neurons by reducing the amount of the soluble A $\beta$  oligomers as it has been proposed for other protein-folding disorders as for example in Huntington's disease (22). Nevertheless, large A $\beta$  plaques, as mentioned above, have been associated with local synaptic abnormalities. Whether the large insoluble A $\beta$  aggregates or the A $\beta$  oligomers are the cause of AD is currently under debate.

From these three hallmarks in AD, decrease in synaptic density, neurofibrillary tangles, and amyloid plaques, it is the number of neurofibrillary tangles which correlates better with the severity of the dementia than the number of amyloid plaques, although the best correlation occurs between measurements of synaptic density and degree of dementia (23,24).

## **1.2 Genetics of Alzheimer's disease**

The main risk to develop AD is aging. Most of the AD cases registered worldwide are not causally linked to a genetic factor and these cases are called "sporadic" AD. Although sporadic AD counts for most of the AD cases, the reason for it is still unclear. Sporadic AD may be caused by a decrease in the clearance of the A $\beta$  peptide from the extracellular space by the A $\beta$  degrading proteases insulin degrading enzyme (IDE) and neprylisin (25,26) or by an increase of  $\beta$ -secretase cleavage due to an increase in  $\beta$ -secretase expression (27).

The genetically linked AD cases (familial AD, FAD) have a prevalence of ~5% of all AD cases, and manifest with an earlier age of onset (~ 60 years old) than the "sporadic" AD cases (28).

Mutations in the  $\beta$ -amyloid precursor protein (APP), presenilin 1 (PS1) and presenilin 2 (PS2) genes have been identified as the genetic causes of FAD (29-32). Most of the mutations, if not all, in these genes lead to larger production in A $\beta$ 42 species, which are more prone to aggregation (33,34) changing the ratio between A $\beta$ 42/A $\beta$ 40.

Mutations in the APP are placed near its processing sites leading to AD by altering its proteolytic processing (figure 3) (see section 1.3.1.2). APP is processed by three

proteases termed  $\alpha$ -secretase,  $\beta$ -secretase and  $\gamma$ -secretase (figure 5 and figure 6 and section 1.3.2). Mutations near the  $\gamma$ -secretase cleavage site increase the production of A $\beta$ 42 (35) whereas the mutations near the  $\beta$ -secretase cleavage site increase the production of both A $\beta$ 40 and A $\beta$ 42. This is the case of the rare Swedish APP mutation where two amino acids, KM are mutated to NL (36,37). Mutations within the A $\beta$  domain, near the  $\alpha$ -secretase site, increase the aggregation properties of the A $\beta$  peptides generated (38).

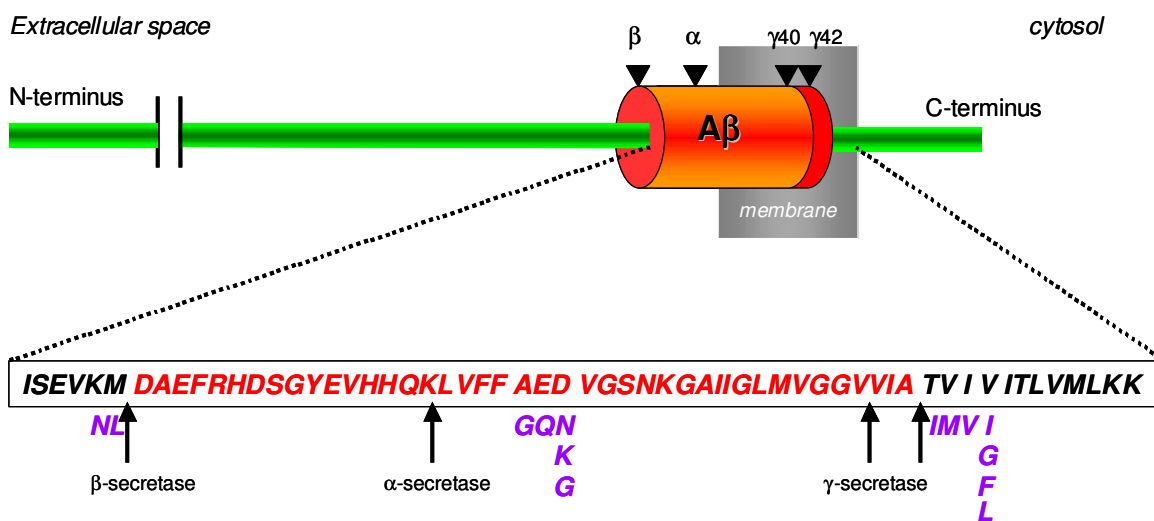


Figure 3. Schematic representation of FAD mutations in APP. The amino acid sequence of the A $\beta$  domain is enlarged. Arrows indicate the position of the  $\alpha$ ,  $\beta$  and  $\gamma$ -secretase cleavage sites. FAD mutations are displayed in purple.

The APP gene is located on chromosome 21 (13,14,39,40). Interestingly, patients with trisomy 21 (Down syndrome) also develop AD neuropathology during middle adult years. The vast majority of Down patients often display plaques composed of A $\beta$ 42 in their adolescence (41). Microgliosis, astrocytosis as well as neurofibrillary tangles appear in the late 20s or 30s and progressive loss of cognitive functions after the age of 35 (41,42). Recently, it has also been discovered that an extra copy of the APP gene causes FAD, further supporting the hypothesis that increased A $\beta$  production is the cause of the disease (43).

Mutations in the PS1 and PS2 genes, located on chromosome 14 and 1 respectively, increase the ratio A $\beta$ 42/A $\beta$ 40 (44-51). More than 150 FAD mutations have been described in PS1 and 11 mutations in PS2 (Source:<http://www.molgen.ua.ac.be/ADMutations/>). The

mutations occurs through the entire PS molecule (figure 4) and lead to a miscleavage of the APP substrate increasing the ratio of A $\beta$ 42 to A $\beta$ 40 (46,49) suggesting that PS mutations change the mode of APP processing.

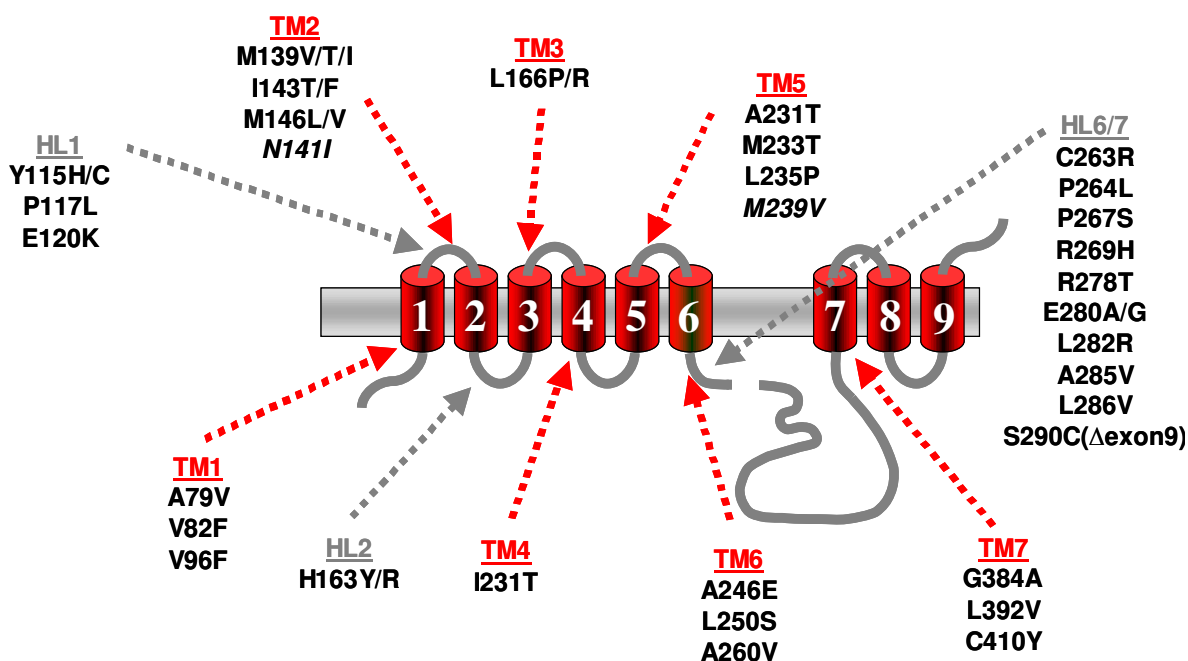


Figure 4. Schematic depiction of a selection of FAD-associated mutations occurring in PS1 and PS2. Arrows indicate the location of the FAD mutations, which occur in the entire molecule. FAD-associated PS2 mutations are depicted in italics. TM: Transmembrane domain; HL: Hydrophilic loop.

The major genetic risk factor for late-onset AD is the  $\epsilon$ 4 allele of apolipoprotein E (52). This allele is present in subjects with AD and its inheritance may increase the risk of developing AD to above fivefold (28). The mechanism by which ApoE4 is related to AD is still unclear but ApoE4 protein has been found in A $\beta$  deposits in AD brain tissue, so it might contribute to enhance A $\beta$  deposition (28). However, a recent study has shown that ApoE4 plays a role in facilitating the proteolytic clearence of soluble A $\beta$  from the brain (53).

### **1.3 Molecular cell biology of Alzheimer's disease**

#### **1.3.1 Amyloid $\beta$ precursor protein (APP)**

APP is a member of a family of conserved type I proteins that comprise the *C.elegans* APL-1 (54), *Drosophila melanogaster* APPL (55) and the mammals APP like protein 1 and 2 (APLP1 and APLP2) (56).

The expression of APP and APLP2 is very similar. Both genes are strongly expressed in brain, kidney and lung, whereas the expression of APLP1 is much more restricted to the brain (57). APP is a 110 to 140 kDa protein (58), occurring in three major isoforms due to alternative splicing. These are referred to as APP695, APP751 and APP770 splice variants according to the number of residues (59,60). The 751 and 770 splice variants are expressed in both neuronal and non-neuronal cells while the 695 variant is predominantly expressed in neurons (61). Apart from their different tissue expression, another difference between these splice variants is that the splice variant 695 lacks the 56 amino acid Kunitz-type serine protease inhibitor domain (60).

The physiological function of APP is still unclear. Studies in mice that lack APP showed that these mice are viable and fertile (62). Aged mice deficient in APP are smaller than wild type mice and show impairment in behaviour and long-term potentiation (62,63). The subtle phenotype of APP deficient mice can indicate the compensation for the loss of APP by the presence of other APP family members. Indeed this is the case, whereas the mice deficient for APLP1 and APLP2 showed no major phenotype, the double knockout mice APP/APLP2 and APLP1/APLP2 lead to death shortly after birth. On the other hand, APP/APLP1 mice are viable (64,65). These data suggest a key physiological role for APLP2 and indicate redundancy between APLP2 and both other family members (64,65). A recent study has suggested a critical function for APP for proper migration of neuronal precursors cells during the development of the mammalian brain (66).



### **1.3.1.1 APP processing**

APP is posttranslationally modified along its trafficking path through the secretory pathway (67) towards the plasma membrane. Full length APP is subjected to sequential cleavages mediated by  $\alpha$ -,  $\beta$ - and  $\gamma$ -secretases (section 1.3.2 and 1.3.3). These sequential cleavages give rise to two different processing pathways of APP.

In the amyloidogenic pathway (figure 5), full length APP is first cleaved within its ectodomain by  $\beta$ -secretase. This cleavage, releases a soluble fragment called soluble APP-beta (sAPP $\beta$ ) to the extracellular space (67,68) and leaves a 99 amino acid long C-terminal fragment ( $\beta$ -CTF) in the membrane (58).  $\beta$ -CTF becomes subsequently a substrate for  $\gamma$ -secretase. Due to the action of the  $\gamma$ -secretase, A $\beta$  is secreted to the extracellular space and the APP intracellular domain (AICD) is released into the cytosol (figure 5).

Initially it was believed that A $\beta$  production is a pathogenic event. This view was changed when it was demonstrated in 1992 that A $\beta$  production was a normal physiological process, and that the peptide is detectable in both cerebrospinal fluid and plasma in healthy subjects (69-72).

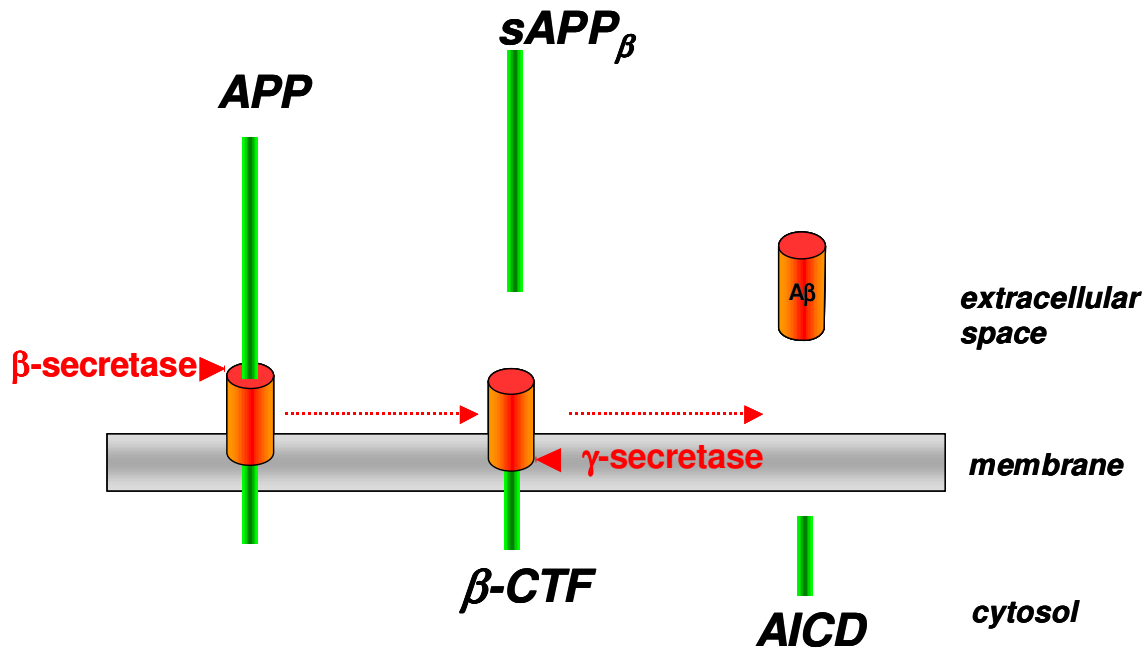


Figure 5. Schematic representation of the amyloidogenic processing pathway of APP. The APP ectodomain is first shedded by  $\beta$ -secretase to release sAPP $\beta$ . The remaining membrane-bound  $\beta$ -CTF is then further processed by  $\gamma$ -secretase releasing A $\beta$  to the extracellular space and the APP intracellular domain (AICD) to the cytosol.

In the non-amyloidogenic pathway (figure 6), the ectodomain of APP is first shedded by  $\alpha$ -secretase resulting in the release of the soluble APP-alpha, sAPP $\alpha$ , to the extracellular space, which has neuroprotective and memory enhancing effects (73). This  $\alpha$ -cleavage takes place between residues 16 and 17 of the A $\beta$  domain thus precluding the formation of the A $\beta$  peptide (67,74). After the  $\alpha$ -secretase cleavage has taken place, the resultant 83 amino acid membrane-bound C-terminal fragment or  $\alpha$ -C-terminal fragment ( $\alpha$ -CTF) (74) is further processed by  $\gamma$ -secretase.  $\gamma$ -Secretase cleavage of  $\alpha$ -CTF releases the p3 fragment (75,76) to the extracellular space and AICD (APP intracellular domain) to the cytosol (figure 6).

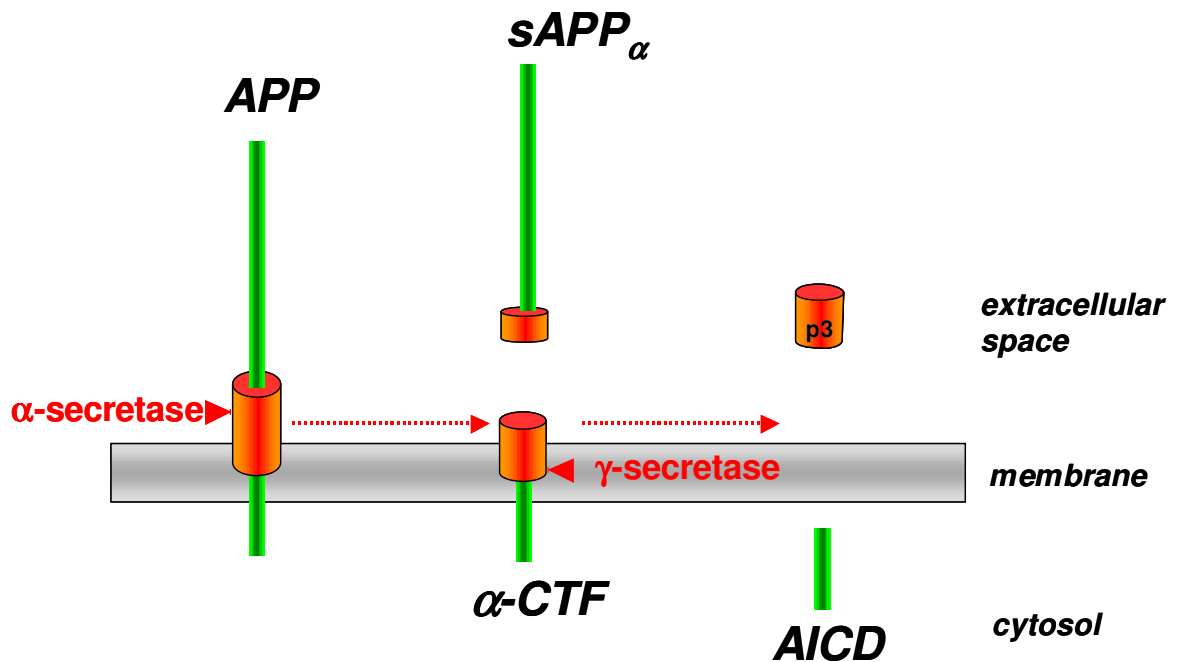


Figure 6. Schematic representation of the non-amyloidogenic processing pathway of APP. Ectodomain shedding of APP by  $\alpha$ -secretase occurs within the A $\beta$  domain. The remaining membrane-bound  $\alpha$ -CTF is then further processed by  $\gamma$ -secretase releasing the p3 peptide to the extracellular space and the APP intracellular domain (AICD) to the cytosol.

$\gamma$ -Secretase processes APP in its TMD at two major positions, the gamma-site ( $\gamma$ -site), which is heterogeneous giving rise to different A $\beta$  species (77) and the also heterogeneous epsilon-site ( $\epsilon$ -site) which releases the 50 or 51 amino acid long residue APP intracellular domain or AICD (78-81) (Figure 7). Other  $\gamma$ -secretase substrates as for example Notch and CD44 are processed in a similar manner (see section 1.3.3.3.1 and 1.3.3.3.2).

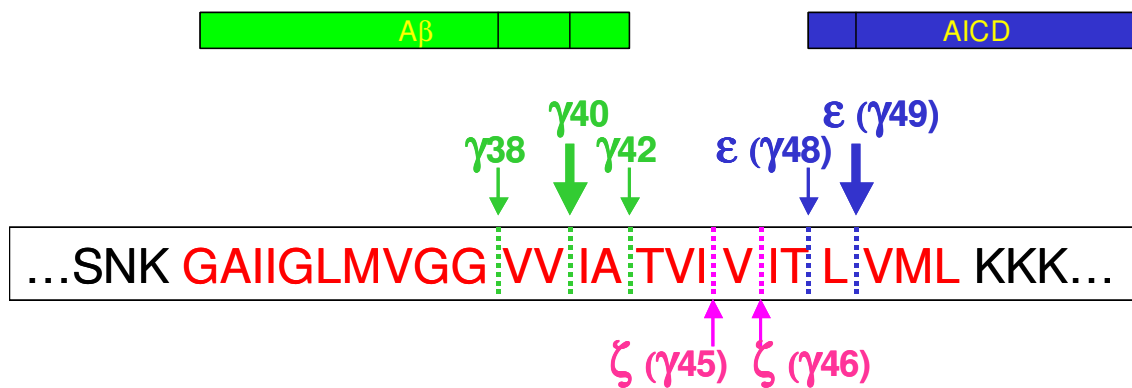


Figure 7. Schematic depiction of APP processing by  $\gamma$ -secretase. Amino acid residues of the APP TMD are depicted in red. Heterogeneous cleavages at the  $\gamma$ -site are depicted in green which give rise to the different A $\beta$  species shown in green.  $\epsilon$ -Site cleavages are depicted in blue, which give rise to AICD shown in blue.  $\zeta$ -Site cleavages are depicted in pink. Big arrows indicate the major cleavages.

Recent evidence suggested that  $\gamma$ -secretase cleaves APP in a step-wise manner with the  $\epsilon$ -cleavage occurring first, followed by the  $\zeta$ -cleavage (82,83) (figure 7) and finally the  $\gamma$ -cleavage (83-85) (figure 8). The major  $\epsilon$ -cleavage is at position  $\gamma$ 49 (78-81). By subsequent cleavage from position  $\gamma$ 49 every three amino acids, A $\beta$ 40 is produced (figure 8 A) (84). The minor  $\epsilon$ -cleavage is at position  $\gamma$ 48 (78-81,86). The cleavage every three amino acids from this position results in the production of A $\beta$ 42 (figure 8 B). This three amino acid cleavage sequence could explain the production of the main A $\beta$  species, A $\beta$ 40 and A $\beta$ 42. Thus, A $\beta$ 40 and A $\beta$ 42 appear to be the result of two product lines.

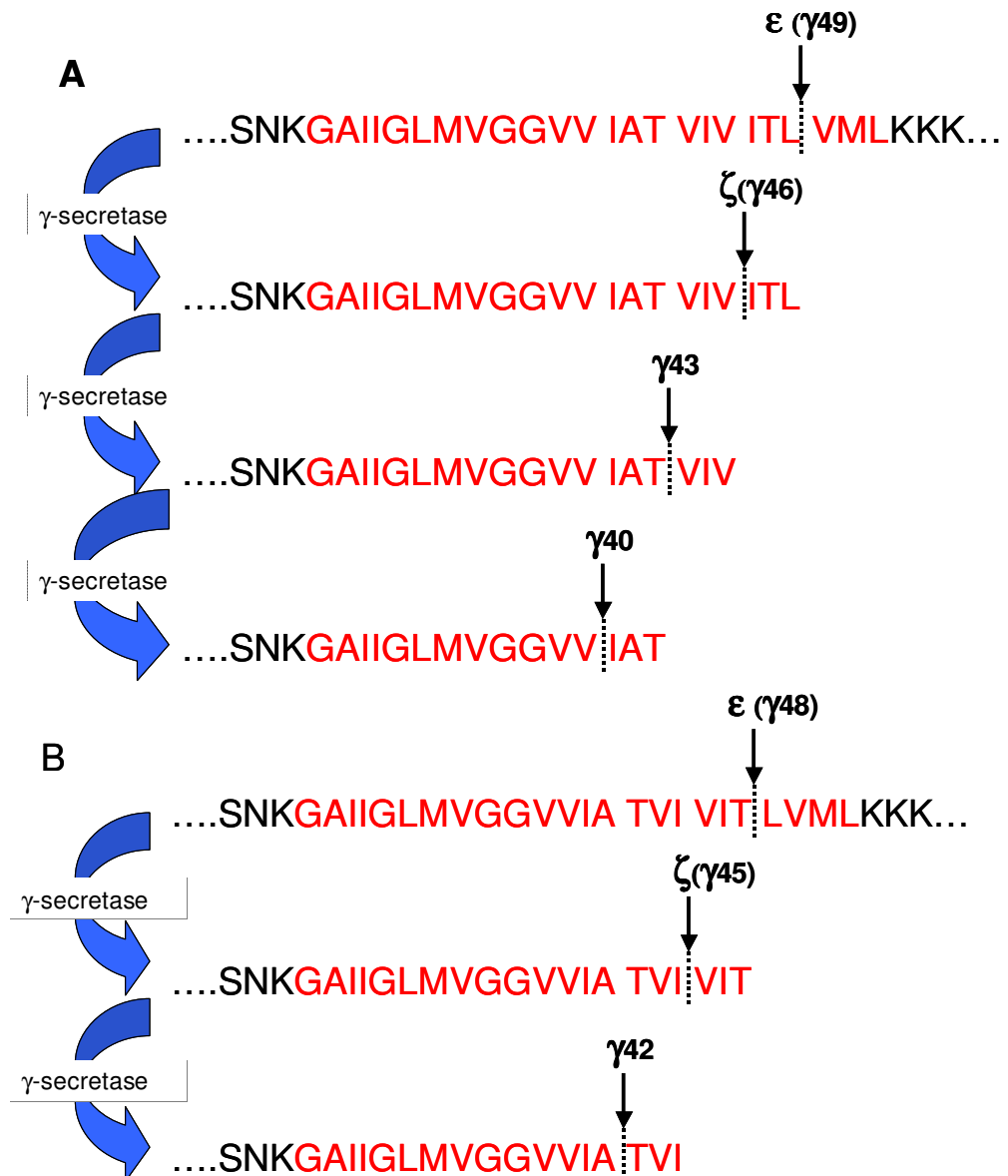


Figure 8. Sequential cleavage of the APP by  $\gamma$ -secretase. Amino acid residues of the APP TMD are depicted in red. In panel A, sequential cleavage of APP beginning at  $\gamma$ 49 is depicted. In panel B, sequential cleavage of APP at  $\gamma$ 48 is shown.

### 1.3.2 $\alpha$ - and $\beta$ -Secretase

Various members of the ADAM (a disintegrin and metalloproteinase) family cleave APP at the  $\alpha$ -secretase site. ADAMs are type I integral membrane proteins with a catalytic domain containing the HEXXH zinc-binding metalloproteinase active site motif (87).

ADAMs play an important role in diverse biological processes such as fertilization (88-90) neurogenesis (91) heart development (92,93) and the activation of the EGFR growth factors and immune regulators such as TNF- $\alpha$  (94). Members of this family, ADAM 17 or TACE (Tumour necrosis factor- $\alpha$  convertase), ADAM 10 and ADAM 9 show  $\alpha$ -secretase activity (95-97). Indeed, knockout and RNAi experiments targeting endogenous TACE, ADAM 10 and ADAM 9 have shown that all three enzymes are involved in the  $\alpha$ -secretase cleavage of APP (97,98).

$\beta$ -Secretase was identified by different groups as BACE1 ( $\beta$ -site APP cleaving enzyme) (99-103). Homozygous BACE1 knockout mice do not produce any A $\beta$  species consistent with BACE1 being the enzyme responsible for the  $\beta$ -cleavage of APP (104,105). BACE1 is a type I membrane protein selectively expressed in neurons. BACE1 contains the typical DTGS and DSGT, aspartyl protease active site motifs (101). BACE1 cleaves APP at amino acid 1 of the A $\beta$  domain, at amino acid 11 (101,106) and 34 (107).

The physiological role of BACE1 was not clear until recently because BACE1 knockout mice showed no major phenotype (105). Recently, however, neuregulin-1 type III has been identified as a BACE1 substrate and it has been shown that BACE1 is required for myelination in the central and peripheral nervous system and correct bundling of axons via processing of neuregulin-1 (108,109). Additional substrates of BACE1 apart from APP, are P-selectin glycoprotein ligand 1, (110) and sialyl-transferase ST6gal1 (111).

Soon after the discovery of BACE1, a homologous aspartyl protease was identified, BACE2 (112,113). BACE2 process APP at the  $\beta$ -secretase site (114,115) but cleaves with more efficiency near the  $\alpha$ -secretase cleavage site (115,116). This suggests that BACE2 acts as an alternative  $\alpha$ -secretase lowering the A $\beta$  production.

### 1.3.3 $\gamma$ -Secretase

$\gamma$ -Secretase is the enzyme responsible for the final cleavage of APP, which occurs within its transmembrane domain (TMD). Biochemical and genetic studies have shown that  $\gamma$ -secretase is a complex composed of four subunits, presenilin (PS), nicastrin (NCT), anterior pharynx defective phenotype-1 (APH-1) and presenilin enhancer-2 (PEN-2) (figure 9). The four subunits are all integral membrane proteins and necessary and

sufficient for  $\gamma$ -secretase activity (117-120) and are in most likely 1:1:1:1 stoichiometry in the complex (121).

The calculated molecular weight of these four components together is  $\sim$ 200 kDa. Nevertheless, different molecular weights have been reported, from 150 to 2000 kDa (118,122-127), pointing to the interesting possibility that the  $\gamma$ -secretase complex could exist as a dimer or higher oligomeric forms, or that  $\gamma$ -secretase contains other additional components.  $\gamma$ -Secretase catalyses the peptide bond hydrolysis of a substrate in a hydrophobic environment of the lipid bilayer and represents an example of an I-Clip (Intramembrane-cleaving protease). A low resolution electron microscopy structure has suggested that the complex is an almost spherical particle with  $\sim$ 100 Å diameter containing a 20-40 Å hydrophilic cavity and 20 Å pores at the top and the bottom of the complex, which could represent exit for the products (128). Consistent with a hydrophilic cavity, PS1 TMD6 and TMD7 which carry the catalytic aspartates of  $\gamma$ -secretase have been shown to be water accessible (129,130).

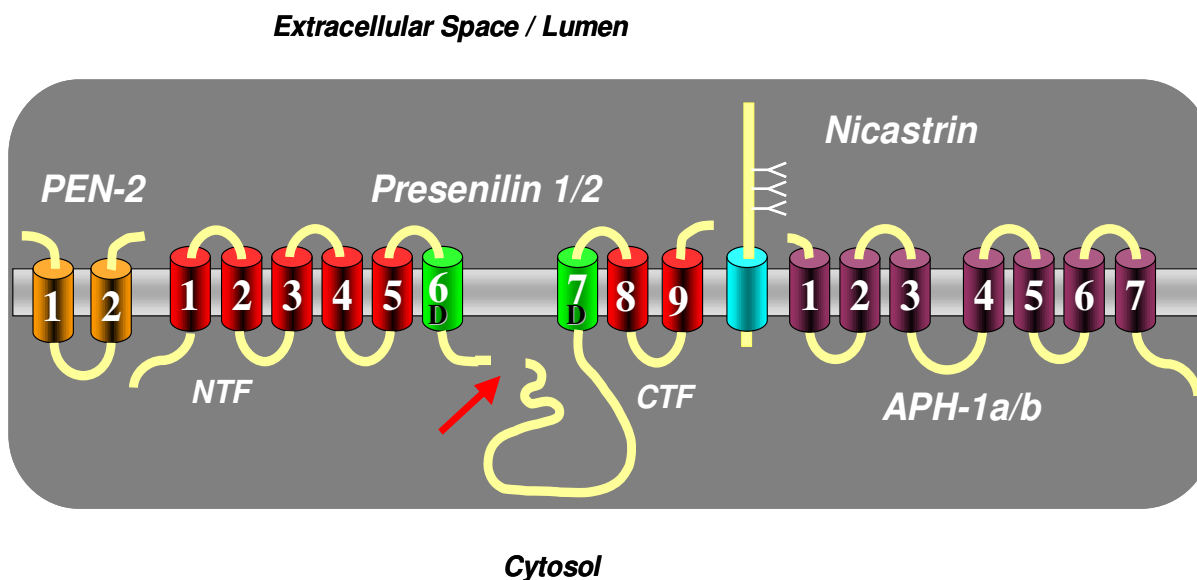


Figure 9. Schematic representation of the  $\gamma$ -secretase complex and its components. Presenilins (PS) 1/2 are depicted in red with the TMD6 and TMD7 highlighted in green. PEN-2 is coloured in yellow and Nicastrin is depicted in light blue. APH-1 homologues (APH-1a/b) are depicted in maroon. The red arrow points to the endoproteolytic cleavage site in PS1/2.

### **1.3.3.1 Components of the $\gamma$ -secretase complex**

#### **1.3.3.1.1 Presenilin**

Membrane topology studies showed that PS is a polytopic 9 transmembrane domain protein with the N-terminus and the large loop facing the cytosolic side and the C-terminus facing the extracellular side (131-133) (Figure 9). PS is endoproteolyzed within its cytoplasmic loop generating N-terminal and C-terminal fragments (134) which remain stably associated as heterodimers (122,123,135) (figure 9). This endoproteolysed form is part of the  $\gamma$ -secretase complex and is more stable than the full length molecule (136,137).

Two homologues of PS, PS1 and PS2, exist in mammals, which do not exist within the same  $\gamma$ -secretase complex (123,138,139). These two molecules show 63% of sequence homology and are known as the catalytic subunit of  $\gamma$ -secretase. The first evidence that PS is the catalytic subunit of  $\gamma$ -secretase came from studies with PS1 knockout mice which showed a strongly reduced  $\gamma$ -secretase activity (140,141). Aspartyl protease inhibitors also inhibited the  $\gamma$ -secretase activity (77,142), helping to identify two conserved aspartate residues in TMD6 and TMD7. The mutagenesis of these two aspartates abrogates the enzyme activity (143-145). Cross-linking studies using  $\gamma$ -secretase transition state aspartyl protease inhibitors analogues showed that these compounds specifically bind to the PS1 heterodimer (146,147).

Apparently, PS is an unusual aspartyl protease as it does not contain the classical aspartyl protease motif, D(T/S)G(T/S) but rather a novel active site motif, the GxGD motif around the critical aspartate in TMD7 (148). This GxGD motif has been shown to be important for protease activity and for substrate discrimination (148,149) (see chapter 1.4).

PS endoproteolysis is abrogated when one of the critical aspartates of the active site is mutated indicating that PS endoproteolysis might be an autocatalytic mechanism (143). Further work strongly suggests that this is indeed the case. Reconstitution of  $\gamma$ -secretase activity in yeast which does not contain any  $\gamma$ -secretase has shown that endoproteolysis is taking place only when the four  $\gamma$ -secretase components are present (117). Endoproteolysis, however, is not strictly required for an active  $\gamma$ -secretase complex. The FAD mutation PS1 $\Delta$ Exon9 in which the endoproteolytic cleavage site is deleted and other mutations like PS1 M292D and PS1 S141R, PS1 T245I, PS1 R278I, PS1 A434T and PS1



L435H result in an uncleaved PS holoprotein but the resulting  $\gamma$ -secretase complex still retains activity (150,151). On the other hand, several PS1 G384 mutants undergo endoproteolysis but are inactive except for PS1 G384A (148).

PS has also been proposed to have different functions apart from being the catalytic subunit of  $\gamma$ -secretase. It has been proposed that uncleaved PS forms passive ER  $\text{Ca}^{2+}$  ion channels. This would explain the calcium signalling abnormalities that have been observed in PS FAD mutations (152,153). Apart from forming  $\text{Ca}^{2+}$  ion channels, PS, has been shown to affect intracellular trafficking of APP, Notch (154-157), tyrosinase (158) tyrosine receptor kinase (141)  $\beta$ - and  $\delta$ -catenin (159,160), telencephaline and  $\alpha$ - and  $\beta$ -synuclein.

#### **1.3.3.1.2 Nicastrin**

Nicastrin (NCT) was identified as a  $\gamma$ -secretase complex component by co-immunoprecipitation studies, which showed that it interacts with PS1 and PS2 (161) (figure 9). NCT is a type I membrane glycoprotein with an apparent molecular weight of ~110 kDa. It has a conserved DYIGS motif, which is important for  $\gamma$ -secretase maturation and activity. Mutations in this motif reduce the PS/NCT interaction as well as A $\beta$  production (162-164). NCT undergoes complex glycosylation (N- and O-glycosylation) through the secretory pathway giving the mature form of NCT, which characterizes a mature  $\gamma$ -secretase complex (154,161). Biochemical studies have shown that NCT might act as a first docking site for  $\gamma$ -secretase substrates acting as a receptor for membrane-retained fragments i.e of the shedded substrates, by binding to the free N-terminus (165) (see section 1.3.3.4) although these findings have recently been challenged (166).

#### **1.3.3.1.3 PEN-2**

PEN-2 (Presenilin enhancer-2) was identified in a genetic screen for PS enhancers in a *C. elegans* strain partially deficient in Sel-12, the *C.elegans* homologue of PS1 (167) and was shown to be a  $\gamma$ -secretase complex component by co-immunoprecipitation and RNAi studies (139). PEN-2 is a small 12 kDa hairpin-like membrane protein, which binds to the TMD4 of PS1 (168,169) (figure 9). PEN-2 is required for the maturation of the  $\gamma$ -secretase complex, in particular for triggering the endoproteolysis of the PS protein (120) and for the

stabilization of the NTF and CTF fragments of PS in the complex after endoproteolysis has occurred (170,171). The contribution of PEN-2 to the catalytic function of  $\gamma$ -secretase, if any, however, remains elusive.

#### **1.3.3.1.4 APH-1**

Like PEN-2, APH-1 was identified in a genetic screen carried out in *C.elegans* for PS enhancers as a 20 kDa 7 TMD protein (167,172,173). APH-1 interacts with NCT and with PS (174) (figure 9).

In humans two homologues of APH-1 exist, APH-1a and APH-1b, the former occurring in two splice variants, APH-1aS and APH-1aL (167,173). All these variants, like PS1 and PS2, do not co-exist in the same  $\gamma$ -secretase complex (138,175). Thus, three different PS1 and PS2  $\gamma$ -secretase complexes exist, each differing in the APH-1 homologue present, giving a total of six  $\gamma$ -secretase complexes. These complexes, when they contain a PS1 or PS2 FAD mutant as catalytic subunit, do not show any difference in the pathogenic activity, independently of the APH-1 homologue found in these complexes (176). APH-1 has been shown to be important for  $\gamma$ -secretase complex formation acting as an assembly scaffold for the complex (177-180). As for PEN-2, the contribution of APH-1 to the catalytic activity of  $\gamma$ -secretase, if any, has not been elucidated yet.

#### **1.3.3.2 $\gamma$ -Secretase assembly**

RNAi and knockout studies have given insight of the  $\gamma$ -secretase complex formation. Several studies showed a selective association between APH-1 and immature N-glycosylated NCT in the absence of PS (163,178,181). Knockdown of NCT and APH-1 by RNAi showed a decrease in PS and PEN-2 levels (127,163). On the other hand, a knockout of PS does not change the levels of NCT and APH-1 but PEN-2 levels are decreased (139). Furthermore, knockdown of PEN-2 expression was accompanied by an accumulation of PS holoprotein (170,182).

Taken together this data suggests that the assembly of the  $\gamma$ -secretase complex begins with the formation of a NCT/APH-1 complex (177,178). This association serves as a scaffold for the assembly of the other two  $\gamma$ -secretase complex components. After the

APH-1/NCT scaffold is formed, PS binds forming a ternary complex. The addition of PEN-2 as the last component triggers the endoproteolysis of PS (120). Biochemical studies have shown that the APH-1/NCT scaffold and also the ternary complex containing PS occurs on immature NCT, suggesting that and  $\gamma$ -secretase complex formation takes place in the ER (180,183). Once the complex is formed is subsequently released from the ER to the Golgi compartments, where O-glycosylation of NCT takes place. The mature  $\gamma$ -secretase complex continues its way through the secretory pathway and reaches its functional sites, the plasma membrane and the late compartments of the secretory pathway (154,180,184).

Little is known about the control of  $\gamma$ -secretase complex formation. Mainly,  $\gamma$ -secretase subunits, which failed to become incorporated into the  $\gamma$ -secretase complex, are rapidly degraded by the proteasome pathway (137,185). Rer1 (Retention in endoplasmic reticulum 1) is a protein involved in the retrieval of unassembled subunits of multimeric complexes in the ER (186). Recent studies have reported that Rer1 can bind to immature N-glycosylated NCT (187) or to unassembled PEN-2 (188). These data indicate the existence of a quality control system of the  $\gamma$ -secretase assembly to ensure that only fully assembled complexes, and not unassembled subunits, leave the ER.

### ***1.3.3.3 Substrates of the $\gamma$ -secretase complex***

A large number of  $\gamma$ -secretase substrates have been discovered in the past years (table 1). These are generally type I transmembrane proteins which the ectodomain has been shedded. So far, an unconfirmed exception is the polytopic glutamate receptor subunit 3, which does not undergo ectodomain shedding in order to be a  $\gamma$ -secretase substrate (189).

All  $\gamma$ -secretase substrates, APP, Notch (1-4) and CD44 (cluster of differentiation 44) that were investigated in this thesis follow a similar processing pathway (See figures 10 and 11).

APP	APLP1(190)	APLP2(190)	mNotch1(191)	mNotch2(191)
mNotch3(191)	mNotch4(191)	CD44(192)	Delta(193)	Jagged2(193)
N-Cadherin(194)	E-Cadherin(194)	ErbB4(195)	LRP(196)	Nectin $\alpha$ (197)
DCC(198)	Syndecan3(199)	p75NTR(200)	IRE 1 $\alpha$ (201)	Ephrin B (202)
IL1R2(203)				

Table 1:  $\gamma$ -Secretase substrates that have been discovered in the past years.

#### 1.3.3.3.1 Notch

Notch is a major physiological substrate of  $\gamma$ -secretase. Notch signaling is required for all metazoans to specify cell fate and regulate other cell decisions during development and in adulthood (204,205). The alteration of this signaling has been associated with different cancers and stroke (206). The involvement of  $\gamma$ -secretase in Notch signaling was finally shown by genetic studies in *C.elegans* to be facilitated by Sel-12, the PS1 homologue in *C.elegans* (207).

Notch is a type I transmembrane receptor protein with a molecular weight of 300 kDa (208). Notch exists in four homologues in human, Notch1-4, which are processed in a similar way (209). During trafficking through the secretory pathway (Figure 10), Notch is cleaved by furin at site 1 (S1). The resultant two fragments remain associated with each other forming the mature receptor, reaching the plasma membrane (208,210). At the plasma membrane, Notch receptors are activated by type I transmembrane ligands known as DSL (Delta, Serrate and Lag 2). Upon ligand binding the ectodomain of the Notch receptor is shedded by TACE at the S2 cleavage site. The resultant membrane-anchored stub, termed NEXT (Notch extracellular truncated) is then further processed by  $\gamma$ -secretase at site 3 (S3) within the TMD. This S3 cleavage releases the Notch intracellular domain (NICD), which translocates to the nucleus and activates genes important for cell fate decisions (204,205). This S3 cleavage resembles the  $\epsilon$ -cleavage site in APP processing. Furthermore, there is a S4 cleavage site also within the Notch TMD. This S4

cleavage is analogous to the  $\gamma$ -cleavage of APP at amino acids 40/42 and releases the Notch  $\beta$  peptide ( $N\beta$ ) to the extracellular space (211).

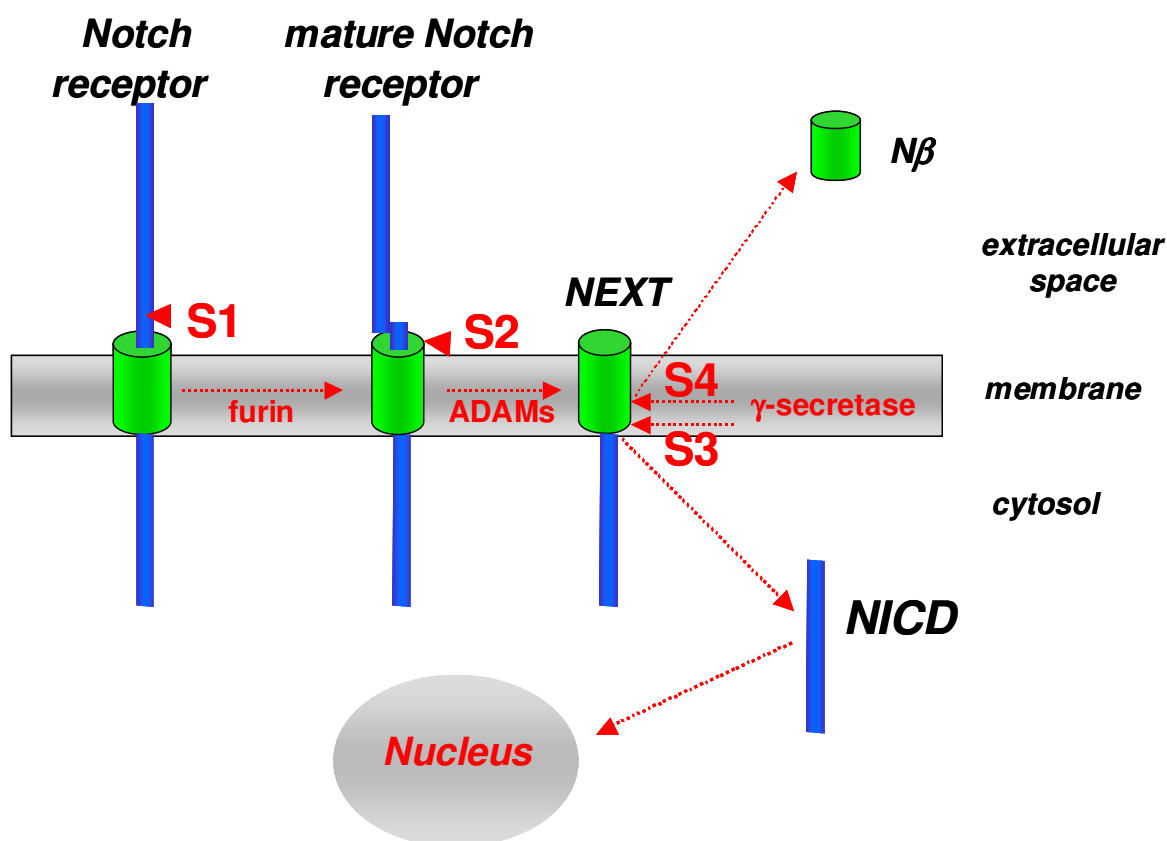


Figure 10. Schematic representation of Notch processing. S1 cleavage by furin occurs in the Golgi network and the mature Notch receptor reaches the plasma membrane, upon ligand activation (not shown) the ectodomain is released by ADAM at S2 cleavage. NEXT is then further processed by  $\gamma$ -secretase at the S3 and S4 cleavage sites releasing  $N\beta$  to the extracellular space and NICD to the cytosol. NICD translocates to the nucleus to regulate gene transcription of Notch target genes.

#### 1.3.3.3.2 CD44

CD44 is a highly glycosylated type I membrane cell surface adhesion protein and the main cell surface receptor for hyaluronan, the principal glycosaminoglycan component of the extracellular matrix. CD44 is expressed in most tissues and is implicated in pathological and physiological processes such as cancer invasion and metastasis, wound healing, cell migration and proliferation (212-214).

The ectodomain of CD44 is first cleaved by ADAM 10, ADAM 17 or membrane-associated matrix metalloproteinases (MMPs) MT1-MMP, resulting in a secreted CD44 form (sCD44) (215-217). The release of sCD44 regulates the interaction between CD44 and the

extracellular matrix during cell migration (218). This ectodomain cleavage is highly prevalent in tumours (219). Following ectodomain shedding, the CD44 stub or CD44-CTF is cleaved by  $\gamma$ -secretase within the plasma membrane releasing the CD44 intracellular domain (CD44-ICD) (192) which translocates to the nucleus and induces expression of the CD44 transcript itself (220) and CD44 $\beta$  to the extracellular space (figure 11).

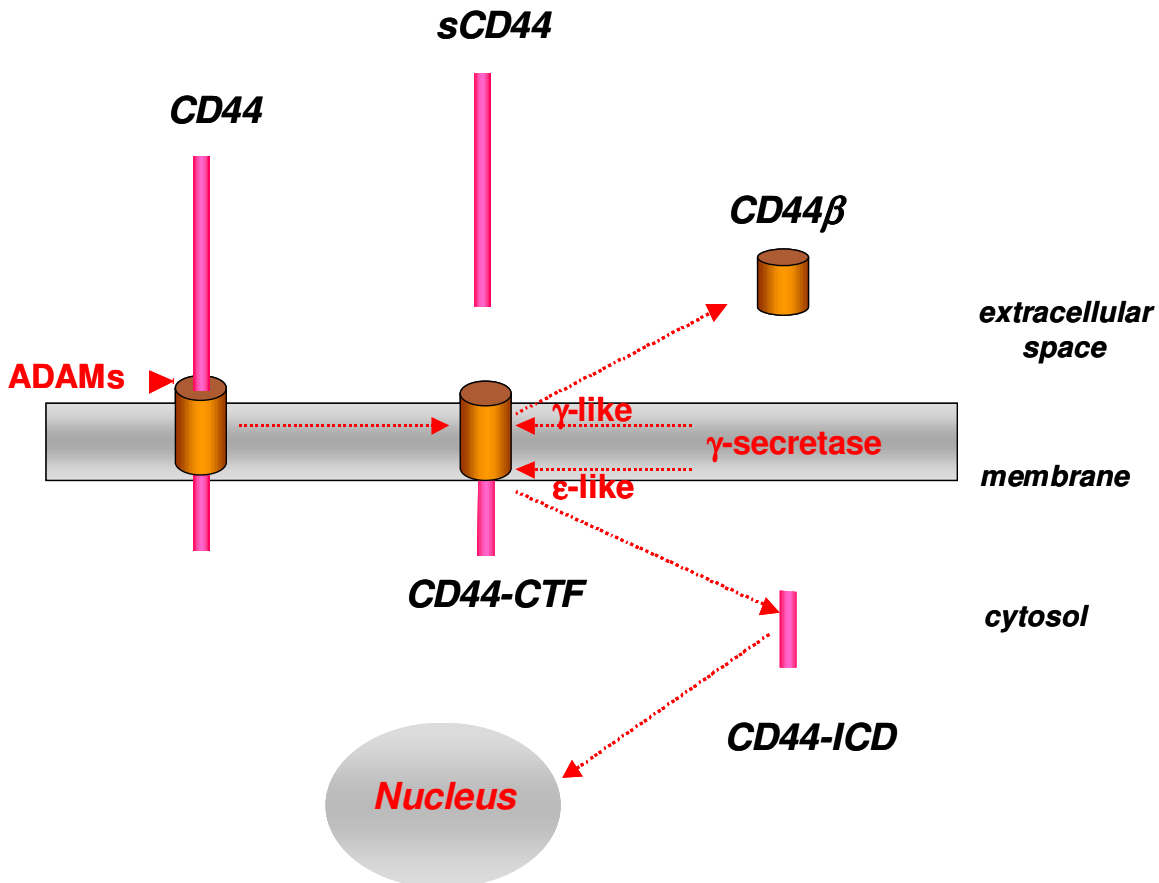


Figure 11. Schematic representation of CD44 processing. The CD44 ectodomain is released to the extracellular space by ADAMs. The membrane bound CTF is further processed by  $\gamma$ -secretase, releasing CD44 $\beta$  to the extracellular space and CD44-ICD, which translocates to the nucleus.

#### 1.3.3.4 Substrate recognition by $\gamma$ -secretase

As type I membrane proteins,  $\gamma$ -secretase substrates have their N-terminus facing the extracellular domain and their C-terminus facing the cytosol and undergo shedding of their large ectodomain by  $\alpha$ - and  $\beta$ -secretase (221). This shedding event creates a new N-terminus in the substrate that is subsequently recognized by the ectodomain of NCT thus recruiting the substrates into the  $\gamma$ -secretase complex (165). The interaction of the new N-

terminus of the substrate with the NCT ectodomain depends on the spatial distance and steric compatibility of their respective binding sites. Important for binding to the free N-terminal amino acid from the substrate is residue E333 of the NCT ectodomain (165). This interaction allows NCT to recruit the different  $\gamma$ -secretase substrates that have been already shedded (165). However, this substrate recognition mechanism has been challenged very recently (166). Within the  $\gamma$ -secretase complex, in the PS molecule, a second recognition site of the substrate which is different from the active site, the so-called, “docking site” has been proposed (222,223). This “docking site” of the substrate has been recently shown to be three amino acids away from the active site (224). Taken together, these findings suggest a two step mechanism for the delivery of the substrate to the active site for its processing (figure 12). First, the shedded substrate is recognized by NCT and the substrate is subsequently translocated to the docking site. From there, it is transferred to the active site for its cleavage. The mechanism by which the substrate is transferred from the recognition site to the docking site has, however, not been elucidated yet.

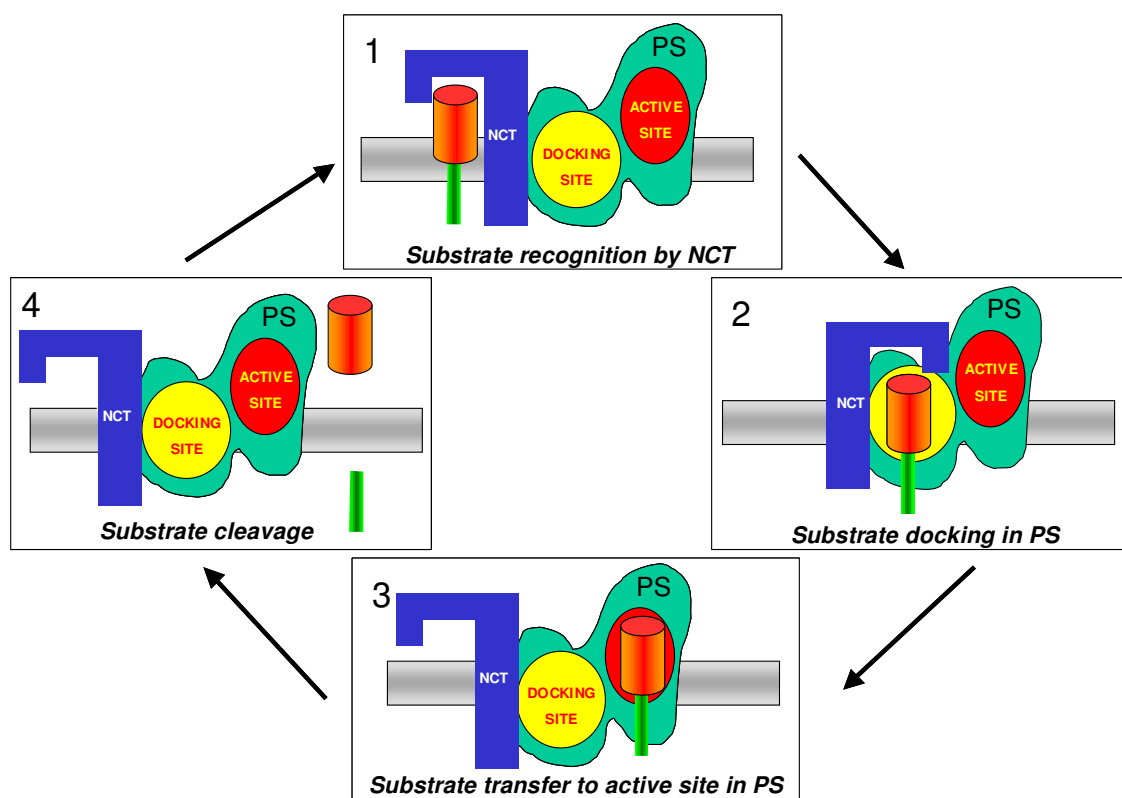


Figure 12. Model of  $\gamma$ -secretase substrate recognition and cleavage. The shedded substrate is first recognized by NCT (blue) (1) and then transferred to the docking site in PS (yellow) (2), from where it is moved to the active site (red) (3) for processing (4). Adapted from Shah et al (165).

### **1.3.3.5 $\gamma$ -Secretase as a therapeutic target**

The most straightforward therapeutical approach to attack the progression of AD would be to inhibit  $\beta$ - and  $\gamma$ -secretase, the two enzymes responsible for A $\beta$  production. The identification and development of  $\beta$ -secretase inhibitors has been difficult as its active site is more open and less hydrophobic than in other aspartyl proteases (225). Moreover, some  $\beta$ -secretase inhibitors have been reported to be a substrate of P-glycoprotein transport resulting in the drug being pump out from the the blood-brain barrier and therefore not being able to reach BACE1 in the brain (226-228). In contrast,  $\gamma$ -secretase inhibitors have been quickly identified and further developed. The big drawback of the  $\gamma$ -secretase inhibitors is that indiscriminately block cleavages within the TMDs of  $\gamma$ -secretase substrates, blocking the formation of ICDs (229). This lack of selectivity gives rise to undesirable side effects such as alteration of T cell development (230), increase of goblet cell number in the intestine as well as alteration of the intestine tissue morphology (231), effects that are due to the block of Notch processing and signalling. It will be therefore interesting the development of new  $\gamma$ -secretase inhibitors that selective inhibits APP processing but not Notch. Nevertheless, these  $\gamma$ -secretase inhibitors have been suggested for the treatment of different tumours because of their ability to inhibit Notch signalling as increasing evidence suggests that Notch signalling is frequently dysregulated in human neoplasms (232).

Modulation of  $\gamma$ -secretase cleavage might provide a safer way in treating AD than using  $\gamma$ -secretase transition state analogues. It has been shown that a subset of non-steroidal anti-inflammatory drugs (NSAIDs) can modulate  $\gamma$ -secretase activity by reducing the production of longer A $\beta$  species (A $\beta$ 42) while increasing the production of shorter species (A $\beta$ 38) in PS1 wt (233). The mechanism by which the modulation of  $\gamma$ -secretase by these compounds occurs is still not known, although it is likely that they directly act on the protease by a non-competitive mechanism (234-236) that might change the PS1 conformation (237). Interestingly,  $\epsilon$ -cleavage is not affected by this  $\gamma$ -secretase modulation. This makes these  $\gamma$ -secretase modulators a more promising alternative to complete inhibition of  $\gamma$ -secretase activity in the treatment of AD as they do not interfere with Notch or other signalling pathways mediated by ICDs release from  $\gamma$ -secretase cleavage (233,234,238).

Another therapeutical approach would be to target the potential modulatory subunits of  $\gamma$ -secretase. Two proteins, CD147 and TMP21 have been recently suggested as two



potential modulatory subunits of  $\gamma$ -secretase (239,240). CD147 is a cell-surface protein that stimulates matrix metalloproteinase secretion (241), which has been co-purified with  $\gamma$ -secretase. RNAi experiments have shown that ablation of CD147 results in an increase of A $\beta$  production, suggesting that CD147 normally down-regulates A $\beta$  production (239). Nevertheless, a new study has proposed that CD147 modulates the A $\beta$  production not by regulating  $\gamma$ -secretase activity but by the extracellular degradation of A $\beta$  by stimulating MMP production (242). TMP21, a trafficking protein, has also been co-purified with  $\gamma$ -secretase and RNAi experiments have shown that knockdown of TMP21 increases A $\beta$  production whereas no changes in AICD production were observed, suggesting that TMP21 regulates the  $\gamma$ -cleavage without affecting the  $\epsilon$ -cleavage (240). However, further research could not fully reproduce the above data of TMP21 (243). TMP21 was not present in the mature  $\gamma$ -secretase complex and only a minor increase of A $\beta$ 40 was observed upon knockdown experiments (243). However, an enhanced APP maturation, APP surface accumulation and a significantly increase in A $\beta$ 42 secretion was observed (243). Further experiments are needed in order to elucidate the exact role of these two proteins within the  $\gamma$ -secretase complex and APP trafficking.

#### **1.4 The GxGD protease family**

The GxGD motif found in PS surrounding one of the critical aspartates is functionally conserved during evolution as it is found in a subset of I-Clips such as the signal peptide peptidase (SPP) family, the SPP-like subfamily with SPPL2a, SPPL2b and SPPL3 as members (244-247) and the type 4 prepilin peptidase (TFPP) in prokaryotes (248). Mutational analysis within the GxGD motif in PS1 which is the prototype of these proteases (see section 1.3.3.1.1), has shown the importance of the glycine neighbouring the critical aspartate for enzyme activity as a big side chain amino acid abrogates the activity of PS1 except when a minor change is introduced as alanine (148) which is a FAD mutation changing the ratio A $\beta$ 42/A $\beta$ 40 (148). The importance of the amino acid in position x within the GxGD motif for substrate selection has also been confirmed (149). Exchanging the PS1 GLGD motif with the GFGD motif from SPE-4 the most distant PS homologue in *C.elegans* was found to allow APP processing whereas Notch processing was heavily impaired suggesting the importance of this amino acid for substrate selection

(149). Taking together, these evidences points to the importance of this functionally conserved motif and found a novel aspartyl protease family, the GxGD family (148).

The TFPPs, one of the members of this GxGD family, are eight TMDs integral cytoplasmic membrane proteins with two critical aspartate residues located close to TM3 and TM6. Mutagenesis of these critical aspartates brings about a loss of activity of the protease (249). TFPPs are responsible for the processing of the highly conserved type 4 leader peptide present at the N-terminus of the secreted proteins known as type 4 prepilins and type 4 prepilin-like proteins (250). The processing has been postulated to be on the cytoplasmic side of the membrane and the resultant type 4 pili are polymerised forming the pilus, which are surface organelles that are necessary for genetic transfer between bacteria pathogens and for virulence (251).

The other family member, SPP/SPPL are polytopic membrane proteins that span the membrane nine times that, however, unlike PS, do not undergo endoproteolysis. In addition, they do not need other cofactors for their activity (figure 13) (246). Topologically, SPP/SPPL are oriented in an opposite direction as PS (246,252) and consistent with this topology their substrates are type II transmembrane proteins (253). SPP might be a homodimer and the dimerization may be important for the activity of the protease (254,255). Mutagenesis of the critical aspartate of the GxGD motif in SPP leads to a loss of proteolytic activity (246) in concordance with the mutagenesis of the critical aspartate of the GxGD motif in PS and TFPP (143,249). Knockdown of SPP in zebrafish results in cell death in the central nervous system (256). Remarkably, expression of an aspartate mutant of SPP in zebrafish, reproduce the phenocopy of the knockdown phenotype.

SPP mediates the clearance of the signal peptides of the nascent proteins from the ER membrane after their liberation by signal peptidase (257). In addition, it is involved in the processing of the hepatitis C virus core protein (258) and the generation of cell surface histocompatibility antigen (HLA)-E epitopes in humans (259). Recently two substrates for SPPL have been identified, TNF $\alpha$  involved in the transcriptional regulation of IL-12 (260,261) and Bri protein (262) implicated in British familial dementia (263). Aspartic protease transition state analogues inhibit not only  $\gamma$ -secretase but also SPP and SPPL and affect the intramembrane cleavage of signal peptides as well as the intramembrane proteolysis of TNF $\alpha$  (260,264) thus potentially inhibiting the release of biologically important peptides.

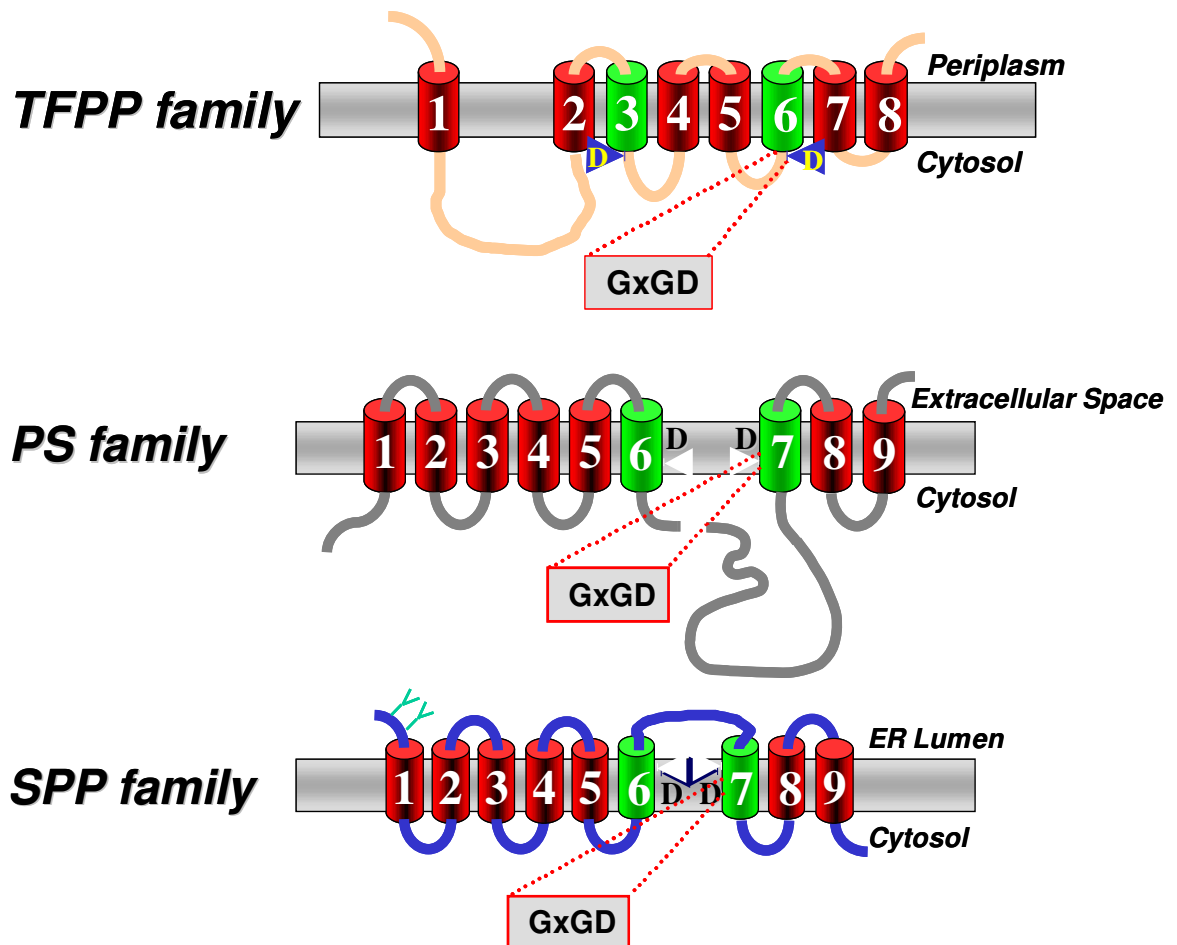


Figure 13: Schematic comparison of the TFPP, PS and the SPP family. Note the opposite topological orientation of PS and SPP. The TMDs that harbour the critical aspartates are highlighted in green.

### 1.5 Aim of the study

A novel class of aspartyl proteases has been discovered which do not carry the typical motif for these proteases, (D(T/S)G(T/S)), but rather a novel signature motif, the GxGD motif (148). One of these proteases carrying this motif is PS that is one of the key proteases in AD as it contributes to the formation of the AD-causing A $\beta$  peptide. This novel protease motif has been found in other aspartyl proteases such as the signal peptide peptidase family (SPP family) or in the prokaryotic TFPP family, suggesting functional conservation of the motif during evolution (148). Previous mutational analysis of the glycine neighbouring the critical aspartate in PS1 has shown a loss of activity of the protease except when the glycine is substituted to a small side chain amino acid like

alanine (148). Moreover, mutational analysis of the amino acid in the position x of PS1 has shown the importance of this motif for  $\gamma$ -secretase substrate selectivity (149). However, the functional role of the GxGD motif is still not known. In particular, it is unclear why glycines are invariant residues of it. The aim of the study was to investigate the functional role of the N-terminal glycine of the GxGD motif. This glycine has been proposed to be important based on its sequence conservation among the PS, SPP and TFPP families. To investigate the functional role of this glycine a mutational analysis approach was carried out, using a mutagenesis approach for PS.

## 2 Materials and methods

### 2.1 Machines and software

#### 2.1.1 Equipment and instrument.

Shaker (KM2)	Edmund Buhler
Rotator (Rotator shaker genie 2)	Scientific Industries
Thermo-shaker (Thermomixer 5439 compact)	Eppendorf
Magnet stirler (IKAMAG REO)	IKA Labortechnik
Vortex (Vortex Genie 2)	Scientific Industries
Microwave	Bosch
Heatblock	Liebisch
Centrifuge for Eppendorf tubes (Biofuge pico)	Heraeus, Kendro
Centrifuge for Eppendorf tubes/4 °C (Biofuge pico)	Heraeus, Kendro
Centrifuge/ 4 °C/ swing rotor (Megafuge 1.0R)	Heraeus, Kendro
Centrifuge/ 4 °C/ swing rotor (Multifuge 3L-R)	Heraeus, Kendro
Centrifuge (J-20XP)	Beckman
Rotors: Type JA10	
Ultracentrifuge (L7-55)	Beckman, Sorvall
Rotors: Ti 50, Ti 70	
Ultracentrifuge (LE-80K)	Beckman
Rotors: Ti 50, Ti 70	
Table Ultracentrifuge (optima ultracentrifuge) Rotor: TLA-55	Beckman
Scale (Analytical +200g-0.0001g)	Ohaus
Scale (Standard 2000g-0.01g)	Ohaus
pH-Meter (Inolab pH Level 1)	WTW
Photometer (SmartSpec™ 3000)	Bio-Rad
Disposable cuvette (10x4x45 mm)	Sarstedt
Quarz cuvette (10x10x45 mm)	Hellma
Incubator 37 °C (Function line)	Heraeus
Incubator 56 °C	Heraeus
Freezer -20 °C	Elektrolux
Freezer -20 °C	Liebherr
Fridge +4 °C	Elektrolux
Fridge +4 °C	Siemens
Autoclave (Tuttnauer 3850 EL)	Systec
Water deionizing machine (Milli-Q academic)	Millipore
Pipettier (Accu-Jet)	Brand
Pipettes (P2, P20, P200, P1000)	Gilson
Disposable pipetts (2 ml, 5 ml, 10 ml, 25 ml)	Sarstedt
Pipette tips (2 µl, 20 µl, 200 µl, 1 ml)	Sarstedt
Disposable tubes (0.2 ml; 0.5 ml; 1.5 ml; 2 ml; 15 ml; 50 ml)	Sarstedt
Centrifuge tubes (1.5 ml)	Beckman

Centrifuge J-20XP (rotor JA10)		Ultracentrifuges L7-55 and LE-80K (rotor 50Ti)		Table ultracentrifuge (rotor TLA-55)		Centrifuge for Eppendorf tubes, Biofuge pico	
xg	rpm	xg	rpm	xg	rpm	xg	rpm
1500	6000	100000	45000	100000	55000	1000	3200
						3000	6000
						16000	13000

Table 2. Velocities for each centrifuge used in this thesis.

## 2.1.2 Recombinant DNA techniques

PCR-machine (Gene Amp PCR system 2400)  
37°C incubator (Function line)  
37°C shaker (Certomat BS-1)

Electrophoresis chamber (Model: B1A; Model: B2)

UV-Lamp (White/Ultraviolet Transilluminator)  
Camera (CCD Video Camera Module)  
Software (Quickscore plus II)  
Printer (p91)

Perkin Elmer  
Heraeus  
B. Braun Biotech  
International  
Owl Separation  
Systems, Inc  
UVP  
Raiser  
MS Laborgeräte  
Mitsubishi

## 2.1.3 Cell culture

Clean bench (Hera Safe HS12)  
CO<sub>2</sub>-Incubator (Hera cell)  
Gas burner (Gas profi 1<sup>SCS</sup>)  
Centrifuge (Megafuge 1.0)  
Water bath (Typ 1002; Typ 1003)  
Microscope (Wilovert S 10x 4/10/20)  
N<sub>2</sub>-Tank (Chronos)  
Freezer -80°C (HFU 86-450)  
Cloning ring (8x8 mm)  
Sterile serological pipettes (2 ml, 5 ml 10 ml, 25 ml)  
Sterile filter pipette tips (2 µl, 20 µl, 200 µl, 1 ml)  
Pasteur pipettes  
Disposable culture dish (60x15 mm, 100x17 mm, 24 well, 12 well)  
Microtube (2 ml) PP  
Cell lifter

Heraeus, Kendro  
Heraeus, Kendro  
WLD-Tec  
Heraeus, Kendro  
GFL  
Hund  
Messer Griesheim  
Heraeus, Kendro  
Bellco  
Sarstedt  
Sarstedt  
VWR International  
Nunc  
Sarstedt  
Costar

### 2.1.4 Protein analysis

Electrophoresis chambers: Mini-PROTEAN 3 electrophoresis cell	Bio-Rad
X-Cell Sure Lock™ Mini Cell	Novex, Invitrogen
Dual gel caster	Hofer
Mighty small II for 8x9CM gels	Amersham Biosc.
Transfer chamber: Mini trans-blot transfer cell	Bio-Rad
Power supply (Power Pac 300)	Bio-Rad
Power supply EPS 3501 XC	Amersham
	pharmacia biotech
Power supply EPS 1001	GE health care Bio-Sciences
	Agfa
Film developer (Curix 60)	Epson
Scanner: Epson Perfection 4870 Photo	
FluorChem™ 8900	Alpha Innotech
NIH imager	NIH

### 2.1.5 Sandwich immunoassay

Streptavidin coated 96 well plate	MSD
Multichannel pipette	Eppendorf
Sector Imager 2400	MSD
MSD Workbench software	MSD
Graph Pad Prism 4 software	GraphPad software

### 2.1.6 Mass spectrometry

Sample plate, SS, numbers and circles	Applied Biosystems
Mass spectrometer Voyager-DE STR	Applied Biosystems
Voyager control panel 5.10.2	Applied Biosystems
Data Explorer TM 4.3	Applied Biosystems
GPMW 5.02	Lighthouse data

## 2.2 Recombinant DNA techniques

### 2.2.1 Constructs and vectors

Name of the construct	Cloning sites	Vector	
PS1 wt	Eco RI	pcDNA 3.1 zeo (+)	§1
PS1 D385A	BamHI/XhoI	pcDNA 3.1 zeo (+)	§2
PS1 G382A	EcoRI/XhoI	pcDNA 3.1 zeo (+)	
PS1 G382I	EcoRI/XhoI	pcDNA 3.1 zeo (+)	
PS1 G382P	EcoRI/XhoI	pcDNA 3.1 zeo (+)	
PS1 G382W	EcoRI/XhoI	pcDNA 3.1 zeo (+)	
PS1 G382K	EcoRI/XhoI	pcDNA 3.1 zeo (+)	
PS1 G382D	EcoRI/XhoI	pcDNA 3.1 zeo (+)	
H <sub>6</sub> X-PS1 wt	BamHI/XhoI	pcDNA 4/His C	§3
H <sub>6</sub> X-PS1 D385A	BamHI/XhoI	pcDNA 4/His C	§4
H <sub>6</sub> X-PS1 G382A	EcoRI/XhoI	pcDNA 4/His C	
H <sub>6</sub> X-PS1 G382I	EcoRI/XhoI	pcDNA 4/His C	
H <sub>6</sub> X-PS1 G382P	EcoRI/XhoI	pcDNA 4/His C	
H <sub>6</sub> X-PS1 G382W	EcoRI/XhoI	pcDNA 4/His C	
H <sub>6</sub> X-PS1 G382K	EcoRI/XhoI	pcDNA 4/His C	
H <sub>6</sub> X-PS1 G382D	EcoRI/XhoI	pcDNA 4/His C	
APPsw-6myc	Clal	pCS2 (+)	§5
F-NEXT		pcDNA 3.1 hygro (+)	§6
mN2ΔE	Clal	pCS2 (+)	§7*
mN3ΔE	Clal	pCS2 (+)	§8
mN4ΔE	Clal	pCS2 (+)	§9
CD44ΔE-Flag	Hind/XhoI	pSecTag 2/HygroB	§10

Table 3: cDNA constructs. Overview of the constructs and the vectors as well as the restriction enzymes sites, which were used to clone the constructs in the respective vectors.

§1-§4: These constructs were provided by Dr. Harald Steiner.

§5: This construct was provided by Dr. Alison Goate (265)

§6: NEXT construct was provided by Dr. Raphael Kopan (266) and modified by Dr Masayasu Okochi (267).

§7-§9: These constructs were provided by Dr. Raphael Kopan (191).

§10: This construct was provided by Dr. Sven Lammich (192).

\*This construct additionally carries the M1697L mutation in order to prevent generation of NICD-sized fragments due to an alternative translation from a methionine within the transmembrane domain (191)



## 2.2.2 Primers and template DNA

Construct	Primer Pairs	cDNA template
PS1 wt	F: 5'-CCG-AAT-TCA-AGA-AAG-AAC-CTC-AA-3' R: 5'-CGC-CTC-GAG-GCA-AAT-ATG-CTA-GAT-ATA-3'	PS1 wt
PS1 G382A	F: 5'-AGG-GGA-GTA-AAA-CTT-GCA-TTG-GGA-GAT-TTC-ATT-TTC-3' R: 5'-AAT-GAA-ATC-TCC-CAA-TGC-AAG-TTT-TAC-TCC-CCT-TTC-3'	PS1 wt
PS1 G382I	F: 5'-AGG-GGA-GTA-AAA-CTT-ATA-TTG-GGA-GAT-TTC-ATT-TTC-3' R: 5'-AAT-GAA-ATC-TCC-CAA-TAT-AAG-TTT-TAC-TCC-CCT-TTC-3'	PS1 wt
PS1 G382P	F: 5'-AGG-GGA-GTA-AAA-CTT-CCA-TTG-GGA-GAT-TTC-ATT-TTC-3' R: 5'-AAT-GAA-ATC-TCC-CAA-TGG-AAG-TTT-TAC-TCC-CCT-TTC-3'	PS1 wt
PS1 G382W	F: 5'-AGG-GGA-GTA-AAA-CTT-TGG-TTG-GGA-GAT-TTC-ATT-TTC-3' R: 5'-AAT-GAA-ATC-TCC-CAA-CCA-AAG-TTT-TAC-TCC-CCT-TTC-3'	PS1 wt
PS1 G382K	F: 5'-AGG-GGA-GTA-AAA-CTT-AAA-TTG-GGA-GAT-TTC-ATT-TTC-3' R: 5'-AAT-GAA-ATC-TCC-CAA-TTT-AAG-TTT-TAC-TCC-CCT-TTC-3'	PS1 wt
PS1 G382D	F: 5'-AGG-GGA-GTA-AAA-CTT-GAC-TTG-GGA-GAT-TTC-ATT-TTC-3' R: 5'-AAT-GAA-ATC-TCC-CAA-GTC-AAG-TTT-TAC-TCC-CCT-TTC-3'	PS1 wt

Table 3. Forward (F) and reverse (R) primer pairs used for the construction of the different PS1 G382 mutants are shown.

## 2.2.3 PCR reaction mixtures

cDNA template (200 ng)	1 $\mu$ l
Forward Primer (1 $\mu$ g/ $\mu$ l)	1 $\mu$ l
Reverse Primer (1 $\mu$ g/ $\mu$ l)	1 $\mu$ l
10xPCR reaction buffer complete (Peq Lab)	10 $\mu$ l
dNTPs (10 mM, Roche)	2 $\mu$ l
Pwo DNA polymerase (1U/ $\mu$ l, Peq Lab)	2.5 $\mu$ l
dH <sub>2</sub> O	82.5 $\mu$ l
Final volume	100 $\mu$ l

The PCR reaction mixture used for the construction of the PS1 G382 mutants is shown.

## 2.2.4 PCR programs

94 °C	4 min	
94 °C	1 min	15 cycles
55 °C	1 min	
72 °C	2 min	
72 °C	10 min	
4 °C	$\infty$	

The PCR program used for constructing the PS1 G382 mutants mutants is shown.

## 2.2.5 Two-step PCR

Two-step PCR was performed to introduce mutations in the construct. The first PCR was performed using the indicated primer pairs (see section 2.2.2). The PCR products were isolated and purified as described (see section 2.2.6.3). Aliquots of purified PCR products were mixed (1:1) and this mixture was used as template for the second PCR. The second PCR was performed using the outer primer pairs.

## 2.2.6 Isolation and purification of PCR products

### 2.2.6.1 Materials

**TBE-buffer:**

9 mM Tris, 2 mM EDTA in dH<sub>2</sub>O

**6x DNA-loading buffer:**

30% Glycerol, 0.25% bromophenolblue and 0.25% xylene cyanol FF in dH<sub>2</sub>O

**Agarose** (Amersham Biosciences)

**1 kb DNA ladder** (Gibco Invitrogen Corporation)

**Nucleo Spin Extraction Kit** (Macherey-Nagel)

**Ethidiumbromide** (Sigma)

### 2.2.6.2 Agarose gel electrophoresis

After the PCR, DNA loading buffer was added to the PCR reaction mixture to a one-fold final concentration. PCR products were loaded on a 1% agarose gel in TBE buffer containing 0.2 µg/µl ethidiumbromide and separated by electrophoresis at 150 volts. 1 kb DNA ladder was loaded in parallel to the PCR products as size standard (see section 2.2.6.1).

### 2.2.6.3 Isolation and purification of PCR products from agarose gels

The right-sized PCR products, confirmed under the UV-lamp, were cut out from the agarose gel and purified from the agarose gel using the Nucleo Spin Extraction Kit following the manufacturer's instructions (see section 2.2.6.1). The purified DNA fragments were used as template for the second PCR or treated with restriction enzymes (see section 2.2.7.1) to allow their subcloning.

## 2.2.7 Enzymatic modification of cDNA fragments

### 2.2.7.1 Enzymes and vectors

**Restriction Enzymes:**

**EcoRI** (10U/ $\mu$ l) (MBI Fermentas)

**XhoI** (10U/ $\mu$ l) (MBI Fermentas)

**Alkaline phosphatase:**

**Shrimp alkaline phosphatase** (SAP;1U/ $\mu$ l) (Roche)

**Ligase:**

**T4 DNA ligase** (5U/ $\mu$ l) (Roche)

**Vectors:**

**pcDNA 3.1/zeo (+)** (Invitrogen)

**pcDNA 4/HisC** (Invitrogen)

### 2.2.7.2 Restriction enzyme treatment

The purified DNA fragments were digested with 10U of the corresponding restriction enzymes and the appropriate reaction buffer supplied by the manufacturer. The mixture was adjusted to a final volume of 30  $\mu$ l with dH<sub>2</sub>O and incubated at 37°C overnight. Three  $\mu$ g of the appropriate vector were also digested with the corresponding restriction enzymes (see section 2.2.7.1) for 2 h at 37°C. After the digestion reaction cDNA fragments were isolated by agarose electrophoresis (see section 2.2.6.2) and purified with Nucleo Spin Extraction Kit (see section 2.2.6.3).

### 2.2.7.3 Alkaline phosphatase treatment

Linearized vectors were treated with SAP (see section 2.2.7.1) to dephosphorylate DNA ends in order to avoid self-ligation. 1U of SAP per 10-15  $\mu$ g of vector was used with reaction buffer from the manufacturer. The mixture was incubated at 37°C for 1 h followed by incubation at 65°C for inactivation of the enzyme for 20 min.

### 2.2.7.4 Ligation of cDNA fragments

Ligation of cDNA fragments to the linearized vectors was performed using 2U of T4 ligase (see section 2.2.7.1) and a ratio of 1:6 (Vector: cDNA fragments) with the reaction buffer from the manufacturer in a final volume of 20  $\mu$ l. The mixture was incubated for 1h at room temperature. The ligation mixture was then used for *E.coli* transformation (see section 2.2.8).

## 2.2.8 Transformation of *E.coli*

### 2.2.8.1 Materials

**LB medium (Low salt Luria-Bertani Medium):**

1% Tryptone; 0.5% yeast extract; 0.5% NaCl in dH<sub>2</sub>O (adjust to pH 7.0) autoclaved at 120°C/ 1.2 bar for 20 min.

**Transformation buffer:**

50 mM CaCl<sub>2</sub>; 15 % glycerol; 10 mM PIPES buffer, pH 6.6, autoclaved and stored at 4°C.

**LB agarose plates with ampicillin:**

LB medium; 1.5% agarose with 100 µg/ml of ampicillin, autoclaved at 120°C/ 1 bar for 20 min.

**Competent *E.coli* strain:**

DH5α

### 2.2.8.2 Preparation of competent cells

DH5α cells were cultured overnight in LB medium (see section 2.2.8.1). Cells were diluted with fresh LB medium and adjusted to OD A<sub>600</sub>=0.05. 5 ml were inoculated to 400 ml LB medium and grown for 2-3 hours to an OD A<sub>600</sub> of 0.2. Cells were then chilled on ice for 10 min and centrifuged at 1500xg for 10 min at 4°C. The cells were resuspended in 200 ml of transformation buffer (see section 2.2.8.1), chilled on ice for 20 min and centrifuged again at 1500xg for 10 min at 4°C. Cells were then resuspended in 20 ml of transformation buffer. Aliquots of the suspension were frozen in liquid N<sub>2</sub> and stored at -80°C until further use.

### 2.2.8.3 Transformation of *E.coli*

75-100 µl of competent cells were added to the ligation mixture (see section 2.2.8.1). The mixture was then incubated for 20 min on ice followed by a heat-shock treatment of 42°C for 30 seconds and further incubation for 2 min on ice. 300 µl of fresh LB medium was added to the ligation mixture and was incubated at 37°C for 45 min shaking. The mixture was then plated onto LB-agarose plates containing 100 µg/ml of ampicillin (see section 2.2.8.1) and incubated overnight at 37°C.

## **2.2.9 Preparation of plasmid DNA from *E.coli***

### **2.2.9.1 Materials**

**LB medium**

(See section 2.2.8.1)

**NucleoSpin plasmid** (Macherey-Nagel)

**Nucleobond AX 500 kits** (Macherey-Nagel)

**TE buffer:**

10 mM Tris pH 7.6; 1 mM EDTA pH 8.0 in dH<sub>2</sub>O

### **2.2.9.2 Small-scale plasmid DNA preparation (mini-prep)**

*E.coli* colonies from the LB-agarose plates were picked and inoculated into 2 ml of fresh LB medium containing 100 µg/ml of ampicillin and incubated overnight at 37°C with shaking. 1.5 ml of the culture was then used for a small scale plasmid DNA isolation using the NucleoSpin plasmid kit following the manufacturer's instruction (see section 2.2.9.1). The plasmid DNA obtained was resuspended in 40 µl of TE buffer (see section 2.2.9.1).

### **2.2.9.3 Mini-prep analysis**

5 µl of miniprep DNA were digested with the corresponding restriction enzymes (see section 2.2.7.1) in order to identify positive *E.coli* clones carrying the correct plasmid. After the restriction digest, the DNA fragments were separated in an agarose gel (see section 2.2.6.2). The positive clone containing the correct size of insert was selected and used for large-scale DNA preparation (see section 2.2.9.4).

### **2.2.9.4 Large scale plasmid DNA preparation (maxi-prep)**

10 µl of the overnight culture from the positive clone identified by miniprep analysis was inoculated to 200 ml of LB medium containing 100 µg/ml of ampicillin and incubated overnight with shaking at 37°C. Plasmid DNA was isolated using the Nucleobond AX 500 kit following the manufacturer's instructions (see section 2.2.9.1). Purified plasmid DNA was resuspended in 200-500 µl of TE buffer (see section 2.2.9.1). DNA concentration was measured by photometry at OD A<sub>260</sub>.

### 2.2.9.5 DNA sequencing

All cDNA constructs were sequenced by GATC Biotech AG (Konstanz, Germany) to verify successful site-directed mutagenesis and to rule out second-site mutations.

## 2.3 Cell culture and cell lines

### 2.3.1 Materials

**Dulbecco's modified Eagle's medium (DMEM) high glucose** (Gibco Invitrogen corporation)

**Fetal bovine serum (FBS)** (PAA)

**L-glutamine** (Gibco Invitrogen corporation)

**Penicillin/Streptomycin (Pen/Strep)** (Gibco Invitrogen corporation)

**Geneticin (G418)** (Gibco Invitrogen corporation)

**Zeocin (Zeo)** (Gibco Invitrogen corporation)

**Trypsin-EDTA** (Gibco Invitrogen corporation)

**PBS:**

140 mM NaCl; 10 mM Na<sub>2</sub>HPO<sub>4</sub> 2H<sub>2</sub>O; 1.75 mM KH<sub>2</sub>PO<sub>4</sub>; 2.7 mM KCl autoclaved and stored at room temperature

**R,S Flurbiprofen** (Calbiochem; Cat No: 344079): 250 mM stock solution dissolved in DMSO and stored at -20°C

**Sulindac sulfide** (Sigma; Cat No: S3131): 250 mM stock solution dissolved in DMSO and stored at -20°C

**Fenofibrate** (Sigma; Cat No: F6020): 250 mM stock solution dissolved in DMSO and stored at -20°C

**S Naproxen** (Sigma; Cat No: N8280): 250 mM stock solution dissolved in DMSO and stored at -20°C

**DMSO** (Merck)

**Lactacystin** (Calbiochem): 10 mM stock solution dissolved in DMSO and stored at -20°C

### 2.3.2 Cell lines and culture medium

Cell lines	Antibiotics
PS1/PS2 -/- MEF	Pen/Strep/G418
HEK293	Pen/Strep
HEK293/sw	Pen/Strep/G418
HEK293/sw/H <sub>6</sub> X-PS1wt	Pen/Strep/G418/Zeo
HEK293/sw/H <sub>6</sub> X-PS1 D385A	Pen/Strep/G418/Zeo
HEK293/sw/H <sub>6</sub> X-PS1 G382A	Pen/Strep/G418/Zeo
HEK293/sw/H <sub>6</sub> X-PS1 G382I	Pen/Strep/G418/Zeo
HEK293/sw/H <sub>6</sub> X-PS1 G382P	Pen/Strep/G418/Zeo
HEK293/sw/H <sub>6</sub> X-PS1 G382W	Pen/Strep/G418/Zeo
HEK293/sw/H <sub>6</sub> X-PS1 G382K	Pen/Strep/G418/Zeo
HEK293/sw/H <sub>6</sub> X-PS1 G382D	Pen/Strep/G418/Zeo

### 2.3.3 Cell culture

Mouse embryonic fibroblasts (MEF) derived from PS1/PS2 double knock out mice (268) were cultured in DMEM Glutamax supplemented with 10% FBS, 1% L-glutamine, 1% of Pen/Strep and 200 µg/ml of G418 under 5% CO<sub>2</sub> and at 37°C (see section 2.3.1). For inoculation, cells were washed with PBS and trypsinized for 5 min. An appropriate amount of cells was transferred to a new plate with fresh medium. Human embryonic kidney cells (HEK) 293 cells stably expressing human APP carrying the Swedish mutation (HEK/sw) (36) were cultured and spread as before. HEK/sw cells stably expressing the H<sub>6</sub>X-PS1 constructs (see section 2.2.1) were cultured in DMEM Glutamax supplemented with 10% FBS, 1% L-glutamine, 1% Pen/Strep, 200 µg/ml of G418 and 0.2 µg/ml of zeocin and spread as before (see section 2.3.1). Untransfected HEK cells were cultured in DMEM Glutamax supplemented with 10% FBS, 1% L-glutamine and 1% Pen/Strep under 5% CO<sub>2</sub> at 37°C (see section 2.3.1).

## 2.3.4 Transfection of mammalian cells

### 2.3.4.1 Materials

**OptiMEM** medium (Gibco Invitrogen corporation)  
**Lipofectamine 2000** transfection reagent (Invitrogen)

### 2.3.4.2 Transfection mixture

culture dishes	volume of culture medium	total cDNA	Lipofectamine 2000
10 cm	10 ml	16 µg	40 µl

### 2.3.4.3 Transient co-transfection

One tenth of PS1/PS2 <sup>-/-</sup> MEF cells from a confluent 10 cm dish were spread into a 10 cm dish containing 10 ml of culture medium without antibiotics. On the next day, cells were transiently co-transfected with the respective combinations of two cDNAs (encoding substrate and protease) using lipofectamine 2000 (see section 2.3.4.1). In total, 16 µg of cDNAs (8 µg/cDNA) and 40 µl of lipofectamine 2000 per dish were used. First, cDNAs and lipofectamine 2000 were mixed with 1 ml of OptiMEM (see section 2.3.4.1) and incubated for 5 min at room temperature. Both solutions were mixed, incubated for 20 min at room temperature and then gently added onto the cells. 24 hours after transfection, the medium was replaced with 4.5 ml of fresh OptiMEM (see section 2.3.4.1) and conditioned for another 16 hours.

### 2.3.4.4 Stable transfection

To establish stable cell lines, HEK293 or HEK/sw cells were transfected with the corresponding cDNA as described before (see section 2.3.4.3). One day after transfection, cells were split 1:10 to 1:1000. Two days after transfection, zeocin was added at final concentration of 0.2 mg/ml to select the resistant cells for 2-3 weeks. Single cell clones were isolated using cloning-cylinders, transferred to a 24 well plate and cultured. Single cells clones were checked for expression levels of the transfected cDNA by immunoblotting and a representative single cell clone with a robust expression was selected as working clone.



### 2.3.4.5 Drug treatment of cells

For proteasome inhibition experiments, a 10 mM stock of lactacystin (269) was prepared in DMSO. The drug was then diluted to the desired final concentration for the treatment of cells in a 10 cm dish in 4.5 ml of DMEM GlutaMAX media containing FBS, L-glutamine and Pen/Strep and the drug containing medium was gently added to the cells. For non-steroidal anti-inflammatory drug (NSAID) treatment of cells in a 10 cm dish, a 250 mM stock solution of each drug was prepared in DMSO. The drug was diluted to the desired final concentration in 4.5 ml of DMEM GlutaMAX media containing FBS. Medium was gently added to the cells and incubated for 24 hours. Medium was removed and fresh media containing the desired NSAID concentration was again added and incubated for another 24 hours. For fenofibrate treatment, a lipid regulating drug (270) cells were incubated for 8 hours with the desired drug concentration as before.

## 2.4 Antibodies

### 2.4.1 Monoclonal antibodies

Antibody	Epitope	Reference/supplier	IP	Blot	SIA
PS1N	PS1 N-terminus	(Capell et al., 1997)		1:5000	
6E10	A $\beta$ aa 1-16	Signet Laboratories		1:10000	
M2	FLAG peptide	Sigma		1:1000	
9E10	C-Myc peptide	Santa Cruz Biotechnology		1:2000	
Xpress	Xpress peptide	Invitrogen	1:150		
2D8-biotin	A $\beta$ aa 1-16	(Shirotani et al., 2007)			1:1000
A $\beta$ 38- Ruthenium tag	A $\beta$	MSD			1:1000
A $\beta$ 40- Ruthenium tag	A $\beta$ aa 34-40	(Brockhaus et al., 1998) Roche			1:1000
A $\beta$ 42- Ruthenium tag	A $\beta$ aa 36-42	(Brockhaus et al., 1998) Roche			1:1000
4G8	A $\beta$ aa 17-24	Covance	5 $\mu$ l 4G8/15 $\mu$ l beads (MS)		

IP: Immunoprecipitation; SIA: Sandwich immunoassay; MS: Mass spectrometry

## 2.4.2 Polyclonal antibodies

Antibody	Epitope	Reference/supplier	IP	Blot
3027	PS1 aa 263-407	(Walter et al., 1997)		1:1000
N1660	NCT aa 693-709	Sigma		1:5000
6687	APP last 20 aa	(Steiner et al., 2000)		1:1000
3552	A $\beta$ aa 1-40	(Yamasaki et al., 2006)	1:300	
Cleaved Notch1	NICD aa V1744	Cell signalling Technology		1:1000
$\beta$ -catenin	$\beta$ -catenin aa 571-781	BD Transduction laboratories		1:8000

## 2.4.3 Secondary antibodies

Antibody	Epitope	Reference/supplier	Blot
Anti-rabbit-HRP	Rabbit IgG	Promega	1:10000
Anti-mouse-HRP	Mouse IgG	Promega	1:10000
Anti-mouse-AP	Mouse IgG	Promega	1:5000

## 2.5 Protein analysis

### 2.5.1 Total cell lysate

#### 2.5.1.1 Materials

**PBS:**

See section 2.3.1

**STEN-lysis buffer:**

50 mM Tris pH 7.6; 150 mM NaCl; 2 mM EDTA; 1% NP-40 in dH<sub>2</sub>O

**BSA solution:**

2 mg/ml Albumin from bovine serum in dH<sub>2</sub>O (Sigma)

**Complete Mini protease inhibitor cocktail tablets** (Roche)

**BIO-RAD protein assay** (BIO-RAD)

### **2.5.1.2 Cell lysate preparation**

Confluent cells were washed with PBS buffer (see section 2.3.1), collected and pelleted in Eppendorf tubes by centrifugation for 5 min at 1000xg at 4°C. Cells from a 10 cm dish were lysed with 500 µl of STEN-lysis buffer (see section 2.5.1.1) with 1x complete mini protease inhibitor cocktail (see section 2.5.1.1) and incubated for 20 min on ice. The cell lysate was then ultracentrifuged for 20 min at 100000xg at 4°C, the supernatant was transferred to a new Eppendorf tube, and the protein concentration of the cell lysate was measured by the Bradford protein assay from BIO-RAD (see section 2.5.1.3).

### **2.5.1.3 Protein quantitation**

Total cell lysate protein concentration was measured by the Bradford assay. 1 µl of total cell lysate was mixed with 1 ml of BIO-RAD protein assay solution (see section 2.5.1.1), diluted with dH<sub>2</sub>O (1:5), incubated for 5 min at room temperature and the OD A<sub>595</sub> was measured with a photometer, in parallel, 2 µl of 2 mg/ml BSA were measured as standard.

## **2.5.2 Membrane lysate**

### **2.5.2.1 Materials**

**PBS:**

See section 2.3.1

**Hypotonic buffer:**

10 mM MOPS, 10 mM KCl in dH<sub>2</sub>O, pH 7.0

**Co-IP buffer:**

150 mM Na-citrate pH 6.4 in dH<sub>2</sub>O.

**10% CHAPSO:**

10% CHAPSO in dH<sub>2</sub>O

**BSA solution:**

See section 2.5.1.1

**Complete Mini protease inhibitor cocktail tablets** (Roche)

**Needle 23G** (B-Braun)

### **2.5.2.2 Preparation and solubilization of membrane**

The cell pellet of a 10 cm dish was resuspended in 500 µl of hypotonic buffer containing protease inhibitor cocktail (see section 2.5.2.1) and incubated on ice for 20 min. The cell

suspension was passed 10 times through a syringe equipped with a 23G needle and centrifuged 15 min at 1000xg at 4°C to pellet nuclei and unbroken cells. The resultant post nuclear supernatant was transferred to a new Eppendorf tube and centrifuged for 45 min at 16000xg at 4°C to pellet the membranes. The membrane fraction was then solubilized with 1% CHAPSO in Co-IP buffer containing protease inhibitor cocktail (see section 2.5.2.1) for 20 min at 4°C and ultracentrifuged for 30 min at 100000xg at 4°C to pellet the unsolubilized membranes. The supernatant was transferred to a fresh Eppendorf tube and the protein concentration was measured by the Bradford assay as described (see section 2.5.1.3).

## 2.5.3 Immunoprecipitation

### 2.5.3.1 Materials

**PBS:**

See section 2.3.1

**Protein A Sepharose (PAS)**

1 g PAS / 10 ml STEN; 2 mg/ml BSA

**STEN-NaCl:**

50 mM Tris pH 7.6; 500 mM NaCl; 2 mM EDTA pH 8.0; 0.2% NP-40 in dH<sub>2</sub>O

**STEN-SDS:**

50 mM Tris pH 7.6; 150 mM NaCl; 2 mM EDTA pH 8.0; 0.1% SDS; 0.2% NP-40 in dH<sub>2</sub>O

**STEN:**

50 mM Tris pH 7.6; 150 mM NaCl; 2 mM EDTA pH 8.0; 0.2% NP-40 in dH<sub>2</sub>O

**TBS:**

10 mM Tris pH 7.4; 150 mM NaCl

**Anti-FLAG M2 agarose** (Sigma)

**Anti-c-myc agarose** (Sigma)

### 2.5.3.2 Immunoprecipitation from total cell lysate

Immunoprecipitations from total cell lysate were performed to analyse CD44-ICD formation. Anti c-myc agarose were washed three times with PBS (see section 2.5.3.1) and 25 µl of those were added to the total cell lysate (see section 2.5.1) and were incubated overnight at 4°C with shaking. Beads were collected by centrifugation at 3000xg for 5 min at 4°C and washed three times with 1 ml of PBS. After the washes, the supernatant was carefully removed and 20 µl of SDS-SB was added to the beads (see section 2.5.6.1).

### ***2.5.3.3 Immunoprecipitation from conditioned media.***

Secreted A $\beta$ , N $\beta$  and CD44 $\beta$  were analysed by combined immunoprecipitation/immunoblotting from conditioned media. The conditioned media (optiMEM) (see section 2.3.4.1) from PS1/PS2 -/- MEF cells transiently co-transfected with the corresponding cDNAs, were collected into a Falcon tube and centrifuged at 3000xg for 5 min to pellet cells present in the media. For A $\beta$ , 4 ml of media were precleared with 20  $\mu$ l of PAS (see section 2.5.3.1) for 30 min at 4°C. After centrifugation at 3000xg for 5 min at 4°C, the precleared conditioned media was transferred to a new Falcon tube and 25  $\mu$ l of PAS and anti-A $\beta$  antibody 3552 (see section 2.4.2) were added and incubated overnight at 4°C with shaking. The immunoprecipitates were washed with 1 ml of STEN-NaCl, STEN-SDS and STEN (see section 2.5.3.1) and 20  $\mu$ l of urea-SDS-SB was added to the beads (see section 2.5.6.1).

For N $\beta$  and CD44 $\beta$ , 4 ml of the conditioned media (optiMEM) was directly subjected to immunoprecipitation with 25  $\mu$ l of FLAG-M2 agarose (see section 2.5.3.1) previously washed with PBS. N $\beta$  was immunoprecipitated overnight at 4°C whereas CD44 $\beta$  was immunoprecipitated at 4°C for 4 hours. In both cases, after the corresponding times, beads were washed 3 times with 1 ml of TBS (see section 2.5.3.1). After the last wash, the supernatant was carefully removed and 20  $\mu$ l of urea-SDS-SB was added to the beads. To analyse A $\beta$  from HEK293/sw cells stably expressing the different PS1 constructs (see section 2.5.3.1), DMEM + GlutaMax media were conditioned for 16 hours. Secreted A $\beta$  species were immunoprecipitated as described above, eluted with urea-SDS-SB or Tris-bicine-urea-SB (see section 2.5.6.1).

## 2.5.4 *In vitro* $\gamma$ -secretase assay

### 2.5.4.1 Materials

**PBS:**

See section 2.3.1

**Hypotonic buffer:**

See section 2.5.2.1

**Na-citrate buffer:**

150 mM Na-citrate pH 6.4 in dH<sub>2</sub>O

**Washing buffer:**

0.5% CHAPSO; 150 mM Na-citrate pH 6.4 in dH<sub>2</sub>O

**10% CHAPSO:**

see section 2.5.2.1

**Purified recombinant C100-His<sub>6</sub> (271)**

**Phosphatidylcholine (Sigma)**

**DTT (Biomol)**

**BSA:**

See section 2.5.1.1

**Complete Mini protease inhibitor cocktail tablets (Roche)**

**Reaction mix:**

150 mM Na-citrate, pH 6.4; 0.25% CHAPSO; 0.5 mg/ml phosphatidylcholine; 10 mM DTT; 0.1 mg/ml BSA and complete mini protease inhibitor cocktail.

### 2.5.4.2 Membrane preparation and *in vitro* $\gamma$ -secretase assay

Stable HEK293/sw cells stably expressing the H<sub>6</sub>X-PS1 constructs (see section 2.2.1) were used to analyse *de novo* AICD generation. Cells from a confluent 10 cm dish were washed with PBS, recollected into an Eppendorf tube, and centrifuged for 5 min at 1000xg at 4°C to pellet the cells. The pellet was then resuspended in 500  $\mu$ l of hypotonic buffer (see section 2.5.2.1) containing 1x complete mini protease inhibitor cocktail (see section 2.5.4.1) and incubated on ice for 20 min. Cell suspension was then passed 10 times through a syringe equipped with a 23G needle followed by centrifugation for 15 min at 1000xg at 4°C. The supernatant was transferred into a new Eppendorf tube and further centrifuged for 45 min at 16000xg at 4°C to collect the membrane fraction. The membrane pellet was solubilised with Na-citrate buffer containing 1% CHAPSO (see section 2.5.4.1) and 1x complete mini protease inhibitor cocktail and incubated for 20 min on ice. After 30 min centrifugation at 100000xg at 4°C, protein concentrations of the samples were determined by the Bradford assay (see section 2.5.3.1). The volume of membrane suspensions of the different cell lines to be used for the *in vitro*  $\gamma$ -secretase assay was adjusted depending on the protein concentration. Samples were then precleared with bridge antibody coupled to PAS (see section 2.5.3.2) for 30 min at 4°C to avoid unspecific binding to the beads. The precleared lysate was subjected to immunoprecipitation with

Xpress antibody (see section 2.4.1) for 2 hours at 4 °C with shaking. After 3 washes with washing buffer (see section 2.5.4.1) containing complete mini protease inhibitor cocktail, 20 µl of reaction mix (see section 2.5.4.1) was added to the beads and incubated with 1 µl of C100-His<sub>6</sub> (see section 2.5.4.1) overnight at 37 °C to allow AICD generation.

## 2.5.5 Sample preparation for SDS-PAGE

### 2.5.5.1 Materials

**Urea-SDS-sample buffer (SB):**

62.5 mM Tris pH 6.8; 2% SDS; 10% glycerol; 2.5% β-mercaptoethanol; 2 M urea; bromophenolblue in dH<sub>2</sub>O

**SB for modified Tris-bicine-urea gel:**

0.72 M Bis-Tris; 0.32 M bicine; 2% SDS; 5% β-mercaptoethanol; 30% sucrose; bromophenolblue in dH<sub>2</sub>O

**Prestained protein standard; See Blue Plus 2** (Invitrogen)

### 2.5.5.2 Sample preparation

To detect NCT; PS1<sub>NTF</sub>, PS1<sub>CTF</sub>; APP<sub>CTFs</sub>; APP<sub>sw-6myc</sub>; AICD; F-NEXT; NICDs; mN2ΔE; mN3ΔE; mN4ΔE; CD44<sub>CTFs</sub>; CD44-ICD; total cell lysates were analysed by immunoblotting. 25-50 µg of proteins were denatured by adding urea-SDS-SB (see section 2.5.6.1) and boiling for 10 min at 65 °C before applying them to the gel. Samples were separated by SDS-PAGE (section 2.6). 12% Tris-glycine SDS-PAGE (see section 2.6.1) was used to separate CD44<sub>CTFs</sub> and CD44-ICD; 10 % Tris-glycine-urea SDS-PAGE was used to separate NCT, PS1<sub>NTF</sub>, PS1<sub>CTF</sub>, APP<sub>sw-6myc</sub> (CTFs and AICD) (see section 2.6.1); 7% Tris-glycine SDS-PAGE was used to separate NICDs, F-NEXT, mN2ΔE, mN3ΔE and mN4ΔE (see section 2.6.1). To detect AICD and Aβ derived from *in vitro* γ-secretase assays, urea-SDS-SB was added to the reaction mixture and boiled for 10 min at 95 °C. AICD and Aβ were separated in a 10%-20% Tris-tricine gel (see section 2.6.2). Immunoprecipitated Aβ from stably transfected HEK/sw cells and Aβ, Nβ, CD44β from transiently transfected MEF cells on PAS or anti-FLAG M2 agarose, were released from the beads and denatured by adding urea-SDS-SB or SB for modified Tris-bicine-urea gel (see section 2.5.6.1) and boiling for 10 min at 95 °C. Total Aβ, Nβ and CD44β, were separated in a 10%-20% Tris-tricine gel. A modified Tris-bicine-urea gel was used to separate Aβ<sub>38</sub>/Aβ<sub>40</sub>/Aβ<sub>42</sub> species. To detect APP<sub>CTFs</sub> co-immunoprecipitated with γ-secretase complex, immunoprecipitates were boiled for 10 min at 65 °C in urea-SDS-SB.

APP<sub>CTFs</sub> were separated on a 10-20% Tris-tricine gel and  $\gamma$ -secretase complex components were separated on a 10% Tris-glycine-urea gel.

## 2.6 SDS-Polyacrylamide gel electrophoresis (PAGE)

### 2.6.1 Tris-glycine gels

#### 2.6.1.1 Materials

**Lower Tris (4x):**

1.5 M Tris pH 8.8; 0.4% SDS; in dH<sub>2</sub>O

**Upper Tris (4x):**

0.5 M Tris pH 6.8; 0.4% SDS in dH<sub>2</sub>O

**Acrylamide (SERVA):**

40% (w/v) acrylamide/bis-acrylamide 37.5:1 in dH<sub>2</sub>O

**8 M urea solution:**

8 M urea in dH<sub>2</sub>O

**APS:**

10% (w/v) ammonium persulfat in dH<sub>2</sub>O

**Tris-glycine gel running buffer:**

25 mM Tris; 200 mM glycine; 0.1% SDS in dH<sub>2</sub>O

**N,N,N',N'-tetramethylethylenediamine (TEMED)** (Merck)

#### 2.6.1.2 Gel preparation

For one thick (1.5mm) mini gel:

	7% separating gel	12% separating gel	stacking gel	10% urea separating gel	urea stacking gel
<b>8 M urea</b>	-	-	-	2.6 ml	2.5 ml
<b>40% acrylamide</b>	1.31 ml	2.25 ml	487.5 $\mu$ l	1.875 ml	487.5 $\mu$ l
<b>4x lower Tris</b>	1.875 ml	1.875 ml	-	1.875 ml	-
<b>4x upper Tris</b>	-	-	1.25 ml	-	1.25 ml
<b>dH<sub>2</sub>O</b>	4.315 ml	3.37 ml	3.4 ml	1.125 ml	0.91 ml
<b>APS</b>	15 $\mu$ l	15 $\mu$ l	15 $\mu$ l	15 $\mu$ l	15 $\mu$ l
<b>TEMED</b>	15 $\mu$ l	15 $\mu$ l	15 $\mu$ l	15 $\mu$ l	15 $\mu$ l



### **2.6.1.3 Electrophoresis**

Gels were set in Mini-PROTEAN 3 electrophoresis cell chamber (see section 2.1.4), filled with Tris-glycine gel running buffer (see section 2.6.1.1). The power supply Power Pac 300 (see section 2.1.4) was first set to constant voltage at 90 V until samples reached the separating gel then the voltage was raised to 120 V.

## **2.6.2 Tris-tricine gels**

### **2.6.2.1 Materials**

**10-20% Tris-tricine gel** (Invitrogen)

**Tris-tricine gel running buffer:**

100 mM Tris; 100 mM tricine; 0.1% SDS in dH<sub>2</sub>O

### **2.6.2.2 Electrophoresis**

Pre-cast Tris-tricine gel was put into X Cell Sure Lock™ Mini cell chamber (see section 2.1.4). The gel chamber was filled with Tris-tricine gel running buffer (see section 2.6.2.1), and the gel was run at constant voltage as described above (see section 2.6.1.3).

## 2.6.3 Modified Tris-bicine-urea gel

### 2.6.3.1 Materials

**Separating gel buffer:**

1.6 M Tris; 0.4 M H<sub>2</sub>SO<sub>4</sub> in dH<sub>2</sub>O

**Spacer gel buffer:**

0.8 M Bis-tris; 0.2 M H<sub>2</sub>SO<sub>4</sub> in dH<sub>2</sub>O

**Stacking gel buffer:**

0.72 M Bis-tris; 0.32 M bicine in dH<sub>2</sub>O

**Acrylamide (BIO-RAD):**

40% (w/v) Acrylamide/ bis-acrylamide 19:1 in dH<sub>2</sub>O

**APS:**

See section 2.6.1.1

**20% SDS:**

20% SDS in dH<sub>2</sub>O

**Urea**

**TEMED**

See section 2.6.1.1

**Cathode buffer:**

0.2 M Bicine; 0.25% SDS; 0.1 M NaOH in dH<sub>2</sub>O

**Anode buffer:**

0.2 M Tris; 50 mM H<sub>2</sub>SO<sub>4</sub> in dH<sub>2</sub>O

### 2.6.3.2 Gel preparation

For one thick (1.5 mm) long gel:

	separating gel	spacer gel	stacking gel
urea	4.8 g	-	-
40% acrylamide	2.75 ml	300 µl	675 µl
separating gel buffer	2.5 ml	-	-
spacer gel buffer	-	1 ml	-
stacking gel buffer	-	-	1.5 ml
20% SDS	50 µl	10 µl	15 µl
dH <sub>2</sub> O	1 ml	680 µl	740 µl
APS	40 µl	8 µl	18 µl
TEMED	5 µl	2 µl	6 µl

The length of the separating gel, spacer gel, and stacking gel were respectively, 6.7 cm; 1.25 cm and 1.7 cm.

### 2.6.3.3 Electrophoresis

Modified Tris-bicine-urea gel was put into Mighty small II for 8x9CM cell chamber (see section 2.1.4). The inner gel chamber was filled with cathode buffer whereas the outer gel chamber was filled with anode buffer (see section 2.6.3.1). The power supply (EPS) (see section 2.1.4) was first set to 90 V until the samples reached the separating gel. Then the voltage was raised to 130 V.

## 2.7 Western Blotting

### 2.7.1 Materials

**Blotting buffer:**

25 mM Tris; 20 mM glycine in dH<sub>2</sub>O

**Blocking buffer:**

0.2% I-Block (Tropix); 0.1% tween-20 in PBS

**TBST:**

10 mM Tris pH 7.4; 150 mM NaCl; 0.1% tween-20 in dH<sub>2</sub>O

**Sodium azide solution:**

5% Sodium azide in dH<sub>2</sub>O

**Filterpaper** (Schleicher&Schuell)

**Immobilon-P** (PVDF transfer membrane) (Millipore)

**Protran** (Nitrocellulose transfer membrane) (Schleicher&Schuell)

**ECL**, western blotting detection reagent (Amersham Biosciences)

**ECL plus**, western blotting detection reagent (Amersham Biosciences)

**Western-Star**, protein detection kit (Tropix)

**Super RX**, Fuji Medical X-Ray film (Fujifilm)

### 2.7.2 Blotting procedure

PVDF transfer membrane was soaked in isopropanol and washed with dH<sub>2</sub>O before soaking in blotting buffer (see section 2.7.1). For detection of the A $\beta$  and A $\beta$ -like peptides, a nitrocellulose transfer membrane was used instead of PVDF. Nitrocellulose membrane was soaked directly in blotting buffer. Gels were carefully removed from the plates. The transfer membrane was placed on the gel between two filter papers (see section 2.7.1) soaked with blotting buffer and one sponge on both sides and placed on the transfer membrane. The sandwich were put in the Mini Trans-Blot cell transfer chamber (see

section 2.1.4) filled with blotting buffer and with an ice cube block. The proteins were transferred from the gel to the transfer membrane for 1 hour at constant 400 mA.

### **2.7.3 Blocking procedure**

The transfer membrane was blocked for 1 hour at room temperature in blocking buffer (see section 2.7.1) to minimize unspecific antibody binding. Nitrocellulose membranes used for the detection of the A $\beta$  and A $\beta$ -like peptides were boiled for 5 min in PBS before blocking to increase the signal.

### **2.7.4 Primary antibody incubation**

Each primary antibody was diluted as described (see sections 2.4.1 and 2.4.2) in blocking buffer with 0.05% sodium azide (see section 2.7.1). Transfer membranes were incubated with the appropriate first antibody overnight at 4 °C with shaking.

### **2.7.5 Secondary antibody incubation**

After the incubation with the primary antibody, the membrane was washed 5 times with TBST (see section 2.7.1) for 5 min each wash. After washing the membrane was incubated with the appropriate horseradish peroxidase (HRP)-conjugated second antibody at the optimum dilution in TBST (see section 2.4.3) for 1 hour at room temperature. For detection of the A $\beta$  and A $\beta$ -like peptides, the nitrocellulose transfer membrane was incubated with alkaline phosphatase (AP)-conjugated secondary antibody at the optimum dilution in TBST (see section 2.4.3). After the incubations with the secondary antibodies, membranes were washed 5 times with TBST for 5 min each wash.

### **2.7.6 Detection**

Proteins were visualized by enhanced chemiluminescence (ECL) following the manufacturer's protocol. ECL plus reagent (see section 2.7.1) was used to detect CD44-ICD according to the manufacturer's instructions. The secreted A $\beta$  and A $\beta$ -like peptides

were detected by the Western-Star kit (see section 2.7.1) following the manufacturer's instructions. The signals were exposed on X-ray films for an appropriate time and the films were developed using a film developer machine (see section 2.1.4).

## **2.8 Sandwich immunoassay**

### **2.8.1 Materials**

**ECL-blocking buffer:**

PBS; 0.05% tween 20; 0.5% BSA

**Washing buffer I:**

PBS; 0.05% tween 20

**Washing buffer II:**

PBS

**2D8-Biotin:**

See section 2.4.1

**A $\beta$ 38-Sulpho-Ruthenium-tag antibody:**

See section 2.4.1

**A $\beta$ 40-Sulpho-Ruthenium-tag antibody:**

See section 2.4.1

**A $\beta$ 42-Sulpho-Ruthenium-tag antibody:**

See section 2.4.1

**Synthetic A $\beta$ 38, A $\beta$ 40 and A $\beta$ 42 peptides (Bachem)**

**MSD read buffer T (4x) with surfactant (MSD)**

### **2.8.2 Sandwich immunoassay**

The A $\beta$ 40 and A $\beta$ 42 antibodies (see section 2.4.1) were labelled with a Sulpho-Ruthenium-tag following the manufacturer's protocol. Streptavidin-coated 96-well plates (see section 2.1.5) were blocked for 30 min at room temperature with 100  $\mu$ l of blocking buffer (see section 2.8.1). 100  $\mu$ l of capture antibody 2D8-biotin (see section 2.4.1) diluted in blocking buffer were added to the plate and incubated for one hour at room temperature. Unbound 2D8-biotin antibody was removed by washing the plate twice with 100  $\mu$ l of washing buffer I (see section 2.8.1). 75  $\mu$ l of the sample and synthetic A $\beta$  peptides were added to each well (for detection of A $\beta$ 40 species media was diluted 1:10 in DMEM plus Pen/Strep (see section 2.3.1)). The synthetic peptides were diluted in DMEM plus Pen/Strep to 1  $\mu$ g/ $\mu$ l and then further serially diluted 1:3 down to 370 pg/ml. Then 25  $\mu$ l of the corresponding detection antibodies diluted in blocking buffer (see section 2.8.1)

were added to the wells. The plate was incubated for 2 hours at room temperature on a shaker. Wells were washed with 100  $\mu$ l of washing buffer I and washing buffer II two times each. 100  $\mu$ l of 1x read buffer was added to each well (see section 2.8.1). Light emission at 620 nm was measured using the MSD Sector Imager 2400 reader (see section 2.1.5) and the concentrations of the A $\beta$  peptides were calculated using the MSD Discovery workbench software (see section 2.1.5). For statistical analysis of the data Graph Pad Prism Software was used (see section 2.1.5).

## **2.9 Mass Spectrometry (MS)**

### **2.9.1 Materials**

**Protein G Sepharose (PGS)** (GE Healthcare)

**MS matrix:**

Trifluoroacetic acid/water/acetonitrile (1/20/20)

**MS IP buffer:**

140 mM NaCl; 0.1% N-Octyl glucopiranoside; 10 mM Tris-HCl pH 8.0; 5 mM EDTA

### **2.9.2 Mass spectrometry analysis**

Media from HEK/sw cells stably expressing the different H<sub>6</sub>X-PS1 constructs (see section 2.2.6.1) treated with the different  $\gamma$ -secretase modulators (GSM) for 8h and 48 hours (233) were recollected to analyse the different A $\beta$  species by MS. For that purpose, conditioned media was precleared with PGS (see section 2.5.3.1) for 30 min at 4°C shaking and immunoprecipitated for A $\beta$  peptides with antibody 4G8. Beads were washed with MS IP buffer (see section 2.5.3.1) for four times and two washes with dH<sub>2</sub>O. Water was aspirated and the beads were allowed to dry for at least 20 min. 10  $\mu$ l of the matrix (see section 2.9.1) were added to the beads and 0.8  $\mu$ l were added to the sample plate (see section 2.1.6). This step was done up to six times. Samples were measured in the mass spectrometer (see section 2.1.6). Data were analysed with Data Explorer TM (see section 2.1.6)

### 3 Results

#### 3.1 *Most PS1 G382 mutants do not undergo endoproteolysis and do not support APP processing*

In order to investigate the functional role of glycine 382 of the PS1 GxGD motif, a site-directed mutagenesis approach was used. The glycine residue was substituted by alanine, isoleucine, proline, tryptophan, lysine and aspartate to cover a wide range of different side chains (figure 14). To allow experimental flexibility, cDNA constructs encoding these PS1 mutations were created with an N-terminal Hexahistidine-Xpress tag (H<sub>6</sub>X) in addition to untagged variants.

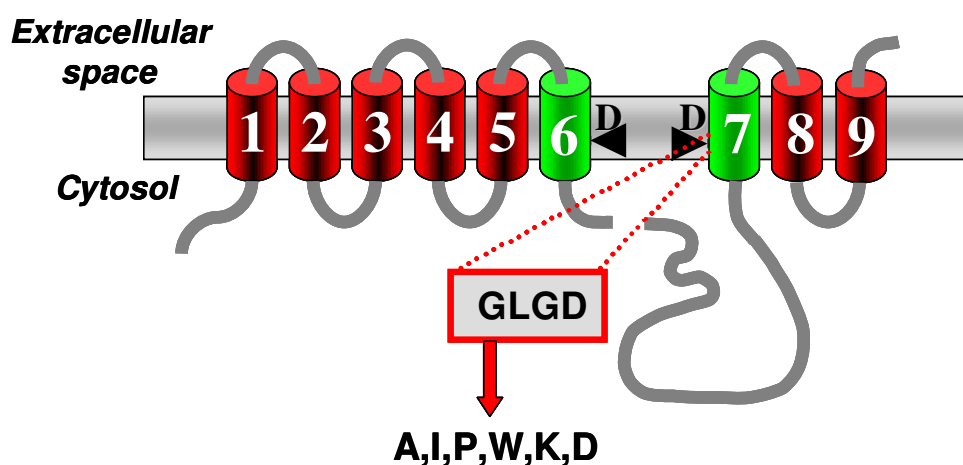


Figure 14. Schematic depiction of PS1 and the mutations introduced into the GxGD motif at G382. TMDs harbouring the active site aspartates (D) are highlighted in green.

The H<sub>6</sub>X-tagged constructs were stably expressed in human embryonic kidney 293 cells stably expressing APP carrying the Swedish mutation (HEK/sw cells). Lysates of these cells were used to verify the expression of the PS1 G382 mutants as well as  $\gamma$ -secretase complex formation. HEK cells have been widely used to study the processing of APP (36,70,75,272) and to characterize the  $\alpha$ -,  $\beta$ -secretase and  $\gamma$ -secretase activities (36,101,139,192,273,274). For these reasons and also because HEK cells are easier to transfect than neuronal cell lines, this cells were used to stably express the H<sub>6</sub>X-PS1 G382 mutants.

As shown in figure 15 (panel A),  $\gamma$ -secretase complex formation was found to be normal as judged from the unaltered maturation of NCT. Maturation of NCT only takes place when the  $\gamma$ -secretase components are correctly assembled, allowing the complex to leave

the ER and to traffic to the Golgi apparatus where NCT becomes fully mature by complex glycosylation.

Overexpression of the different PS1 constructs causes a reduction in the levels of endogenous PS1<sub>NTF</sub> demonstrating that endogenous PS1 has been replaced by the different PS1 constructs (figure 15 panel B). PS replacement is a well-established phenomenon, which demonstrates complex formation of PS with the other  $\gamma$ -secretase subunits (134,275). One striking feature that was observed is that endoproteolysis of the H<sub>6</sub>X-PS1 G382 mutants into NTF and CTF is strongly impaired similar to the H<sub>6</sub>X-PS1 D385A. This active site mutant is unable to undergo endoproteolysis and is not able to process APP<sub>sw</sub> as evident from the strong accumulation of APP<sub>CTFs</sub> and the strong reduced A $\beta$  secretion in the conditioned media. With regard to PS1 endoproteolysis, only the H<sub>6</sub>X-PS1 G382A mutant was endoproteolysed as evident from the generation of PS1<sub>NTF</sub> and PS1<sub>CTF</sub> (panel B and C).

With regard to  $\gamma$ -secretase activity, most of the H<sub>6</sub>X-PS1 G382 mutants are unable to process APP as judged from accumulation of the APP<sub>CTFs</sub> and the strongly reduced A $\beta$  production in the conditioned media (figure 15 panels D and E) similar to the H<sub>6</sub>X-PS1 D385A. Again, the only exception is H<sub>6</sub>X-PS1 G382A mutant in which the APP<sub>CTFs</sub> are processed and the A $\beta$  peptide is detected in the conditioned media (Figure 15 panels D and E). Quantitation further confirmed the loss of function of most of the PS1 G382 mutants (figure 16). As observed in figure 15, panel E, PS1 G382I also secreted A $\beta$  into the media. This A $\beta$  production was probably due to the presence of residual endogenous PS1 (figure 15 panel B). In section 3.2.1 using PS1/PS2  $-/-$  MEF cells it was confirmed that PS1 G382I is indeed inactive and does not secrete A $\beta$  peptide. Taken together these results suggest that changing the glycine to another amino acid does not affect  $\gamma$ -secretase complex formation but has an impact on endoproteolysis of PS1 and  $\gamma$ -secretase activity. When the side chain change generated is minor, then both endoproteolysis and proteolytic activity are supported, like in the case of the H<sub>6</sub>X-G382A mutant, in which a hydrogen atom (the side chain of the glycine) is changed to a methyl group (the side chain of the alanine).



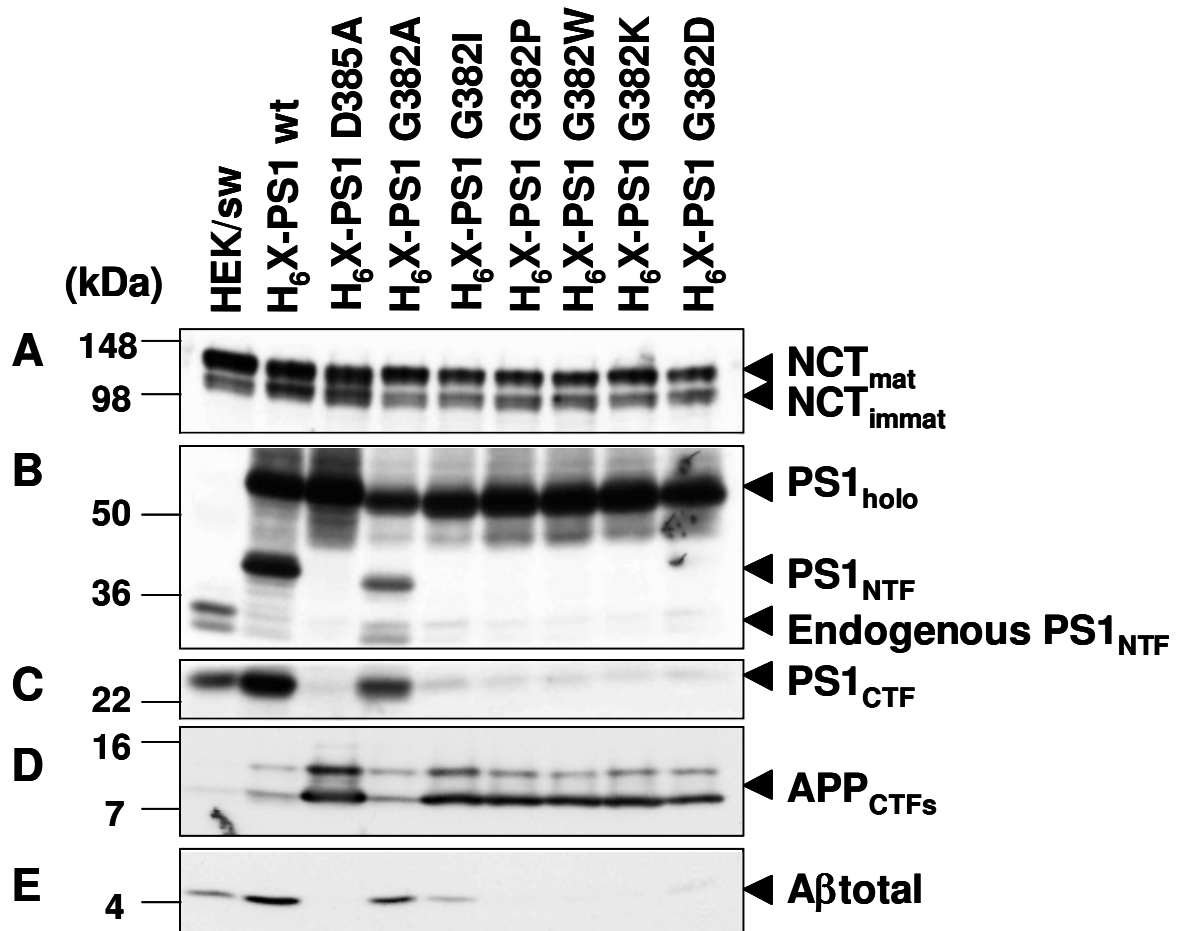


Figure 15. Cell lysates from HEK/sw cells stably expressing the indicated H<sub>6</sub>X-tagged PS1 constructs were analysed for NCT maturation by immunoblotting with antibody N1660 (panel A), for PS1 expression and endoproteolysis with antibodies PS1N and 3027 to detect PS1<sub>NTF</sub> and PS1<sub>CTF</sub> respectively (panels B and C) and for APP processing with antibodies 6687 to detect APP<sub>CTFs</sub> (panel D). Aβ was detected by combined immunoprecipitation/immunoblotting with antibodies 3552/6E10 (panel E). γ-Secretase components were separated by a 10% Tris-glycine-urea gel, while APP<sub>CTF</sub> and total Aβ were separated by a 10-20% Tris-tricine gel.

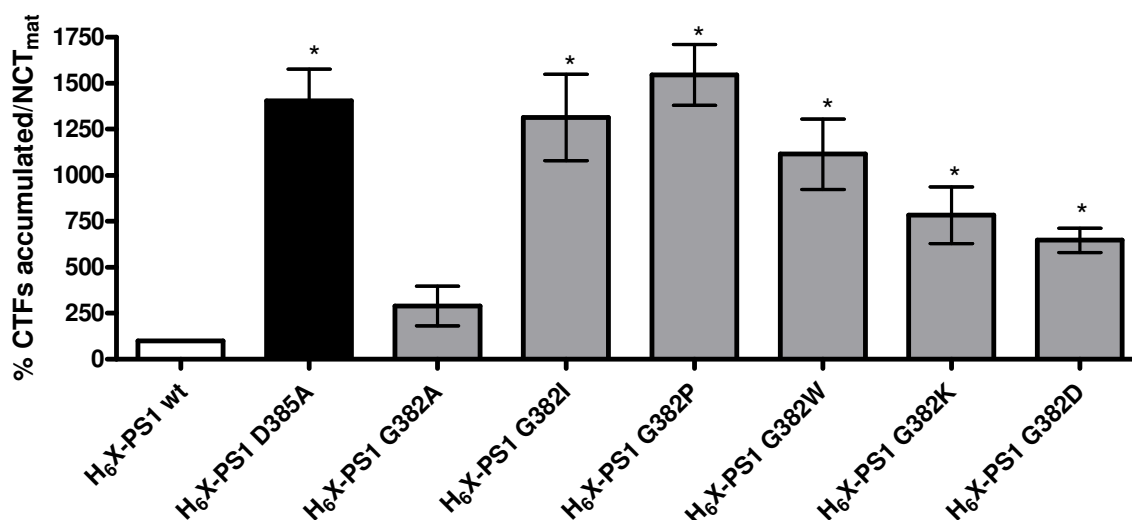


Figure 16: Signal intensity of APP<sub>CTFs</sub> accumulated by the different H<sub>6</sub>X-PS1 G382 mutants in HEK/sw cells and normalised by NCT<sub>mat</sub> protein levels. The signal intensity of APP<sub>CTFs</sub> produced by H<sub>6</sub>X-PS1 wt was set to 100%. Data were statistically analysed by paired two-tailed student's t test. (\* p<0.05). The data are representative of three independent experiments (n=3).

### 3.1.1 PS1 G382A mutant produces AICD and A $\beta$ *in vitro*

To further confirm these results, selected H<sub>6</sub>X-PS1 G382 mutants were analysed in a cell free  $\gamma$ -secretase assay with a recombinant APP substrate, C100-His<sub>6</sub> (see section 2.5.4.1).  $\gamma$ -Secretase complexes from cells stably expressing H<sub>6</sub>X-PS1 wt, H<sub>6</sub>X-PS1 D385A, H<sub>6</sub>X-PS1 G382A, and the strong mutants H<sub>6</sub>X-PS1 G382P and H<sub>6</sub>X-PS1 G382K were isolated by immunoprecipitation using an antibody against the Xpress epitope in order to avoid the potential interference by immunoprecipitation of an endogenous complex. As shown in figure 17, in agreement with the previous result, H<sub>6</sub>X-PS1 wt and the H<sub>6</sub>X-PS1 G382A mutant are able to process the recombinant APP C100-His<sub>6</sub> substrate and thereby to produce AICD and A $\beta$ . In the case of the H<sub>6</sub>X-PS1 G382A mutant, processing of C100-His<sub>6</sub> was somewhat diminished since the levels of AICD and A $\beta$  produced by this mutant were lower compared to the respective levels produced by H<sub>6</sub>X-PS1 wt. This suggests that the change from glycine to alanine partially impairs the activity of the protease. Both H<sub>6</sub>X-PS1 G382P and H<sub>6</sub>X-PS1 G382K mutants showed only residual  $\gamma$ -secretase activity, if any, also in agreement with the previous result obtained in living cells. Thus, only the H<sub>6</sub>X-PS1 G382A mutant and the H<sub>6</sub>X-PS1 wt were active *in vitro*. Taken together, this

assay confirms the partial activity of the H<sub>6</sub>X-PS1 G382A mutant and the inactivity of the H<sub>6</sub>X-PS1 G382P and H<sub>6</sub>X-PS1 G382K mutants observed in figure 15.

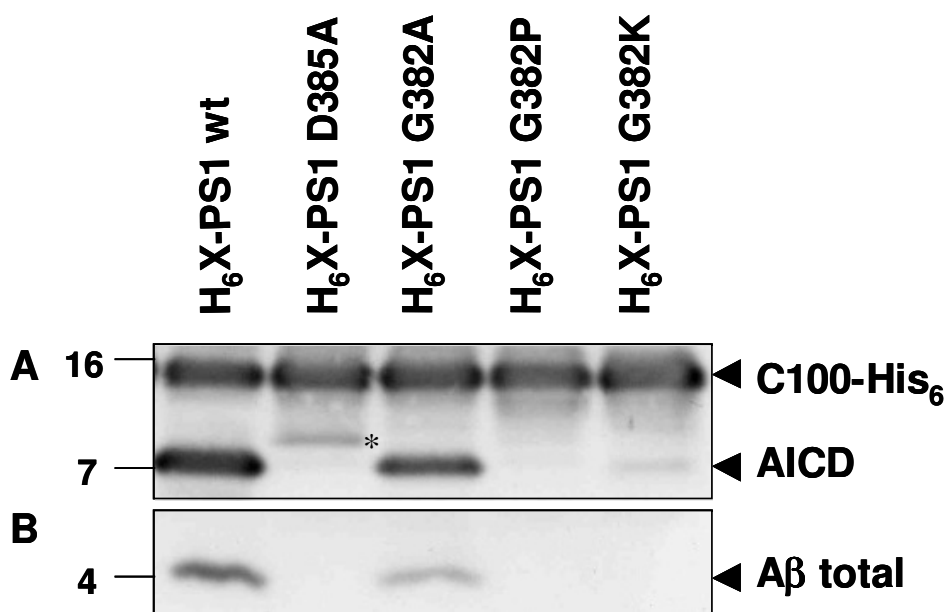


Figure 17.  $\gamma$ -Secretase complexes from the HEK/sw cells stably expressing the indicated constructs were immunoprecipitated with anti-Xpress antibody and incubated with recombinant C100-His<sub>6</sub> substrate overnight at 37°C. Samples were separated on a 10-20% Tris-tricine gel and AICD and A $\beta$  were detected by immunoblotting with antibodies 6687 (panel A) and 6E10 (panel B) respectively. Asterisk denotes a band produced probably by the action of other proteases on C100-His<sub>6</sub>.

### 3.1.2 PS1 G382A alters the cleavage specificity of the $\gamma$ -cleavage sites

Because H<sub>6</sub>X-PS1 G382A supports APP processing and generates A $\beta$ , the potential impact of this mutation on the formation of the different A $\beta$  species was studied next. Since glycine 384 of the GxGD motif was previously identified as a FAD-associated mutation (G384A), which strongly elevates A $\beta$ 42 production (148), it was next investigated whether PS1 G382A could also alter the  $\gamma$ -cleavage specificity and thereby increase the production of long A $\beta$  species.

A $\beta$  species from conditioned media from HEK/sw cells stably transfected with H<sub>6</sub>X-PS1 wt, H<sub>6</sub>X-PS1 D385A and H<sub>6</sub>X-PS1 G382A were isolated by immunoprecipitation and separated by a Tris-bicine-urea gel system, which allows the separation of the different A $\beta$  species (276). The qualitative A $\beta$  peptide analysis of the media showed a slight increase in the short A $\beta$ 38 species for H<sub>6</sub>X-PS1 G382A in comparison to H<sub>6</sub>X-PS1 wt whereas a

decrease in A $\beta$ 39 was observed for H<sub>6</sub>X-PS1 G382A in comparison to H<sub>6</sub>X-PS1 wt (figure 18 panel A). Although this Tris-bicine-urea gel system is not sensitive enough to detect small changes in A $\beta$  species, the analysis indicated also an increase in longer species (A $\beta$ 42/A $\beta$ 43) although not as strong as for the FAD PS1 L166P mutation (figure 18 panels A and B). In order to use a more sensitive assay and to verify this finding, the same samples from H<sub>6</sub>X-PS1 wt and H<sub>6</sub>X-PS1 G382A were subjected to a sandwich immunoassay allowing the quantification of the levels of the A $\beta$  species, A $\beta$ 38, A $\beta$ 40 and A $\beta$ 42, present in the conditioned media, as well as to mass spectrometry analysis (MS). Data from the A $\beta$  sandwich immunoassay showed for the H<sub>6</sub>X-PS1 G382A mutant an increase in the A $\beta$ 38/A $\beta$ total ratio, and a slight increase in A $\beta$ 42/A $\beta$ total ratio (figure 19). In the H<sub>6</sub>X-PS1 G382A mutant, A $\beta$ 40/A $\beta$ total ratio was slightly lower than H<sub>6</sub>X-PS1 wt (figure 19). This is consistent with the partial loss of  $\gamma$ -secretase activity of this mutant.

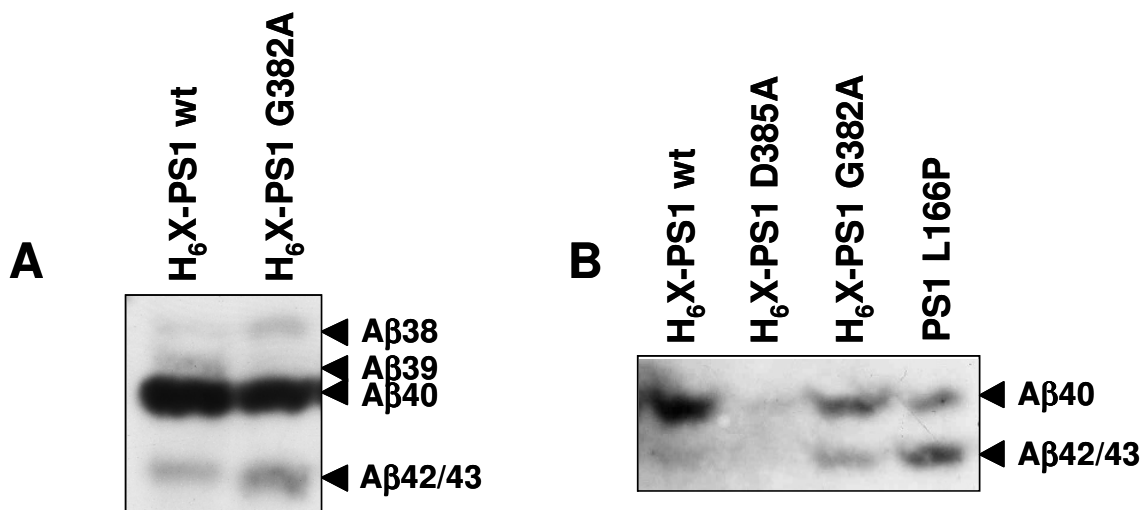


Figure 18. Panel A, A $\beta$  species from conditioned media from HEK/sw cells stably expressing H<sub>6</sub>X-PS1 wt and H<sub>6</sub>X-PS1 G382A were immunoprecipitated with antibody 3552 overnight at 4°C. Panel B, A $\beta$  species from conditioned media from HEK/sw cells stably expressing H<sub>6</sub>X-PS1 wt, H<sub>6</sub>X-PS1 D385A and H<sub>6</sub>X-PS1 G382A and PS1 L166P were immunoprecipitated with antibody 3552 overnight at 4°C. Immunoprecipitates were subjected to Tris-bicine-urea SDS-PAGE to separate the different A $\beta$  species. A $\beta$  species were detected by immunoblotting with antibody 6E10.

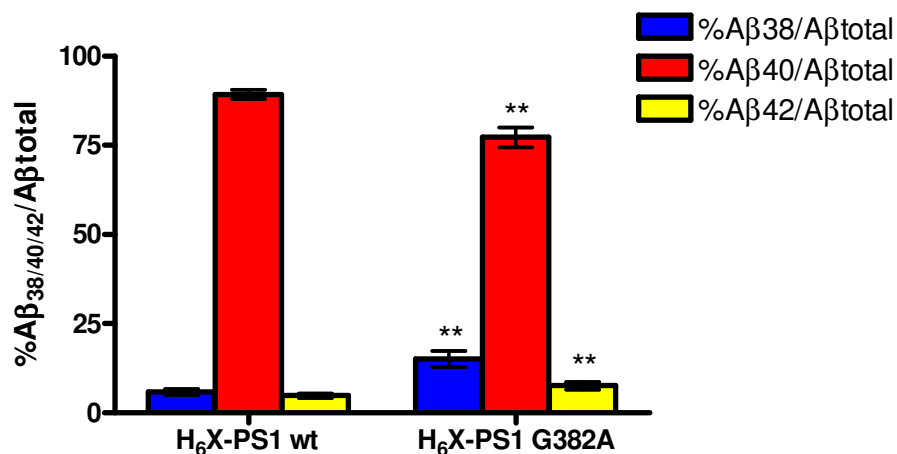


Figure 19: Sandwich immunoassay of A $\beta$  species isolated from conditioned media of HEK/sw cells media stably expressing H<sub>6</sub>X-PS1 wt and H<sub>6</sub>X-PS1 G382A. A $\beta$ 38/A $\beta$ total, A $\beta$ 40/A $\beta$ total, A $\beta$ 42/A $\beta$ total ratios were determined. Data represent the average of five independent experiments. Error bars indicate the standard error of the mean. Statistical significance was calculated by paired two-tailed student's t test (\*\* p<0.01).

MS analysis reveals the different A $\beta$  species generated in each sample although is not a quantitative method (figure 20). In the mass spectrum of H<sub>6</sub>X-PS1 G382A an extra peak corresponding to the A $\beta$ 43 species was observed (figure 20 panel B). This species was not observed for H<sub>6</sub>X-PS1 wt (figure 20 panel A). In addition, the A $\beta$ 39 peak present in the mass spectrum for H<sub>6</sub>X-PS1 wt was almost not detected for H<sub>6</sub>X-PS1 G382A in agreement with the Tris-bicine-urea gel analysis (figure 18). Therefore, the H<sub>6</sub>X-PS1 G382A mutant produces an additional A $\beta$  longer species, A $\beta$ 43. This suggests that the increase of longer species observed for this mutant that was indicated by the Tris-bicine-urea gel analysis (Figure 18 panels A and B) is due to an increased production of A $\beta$ 43.

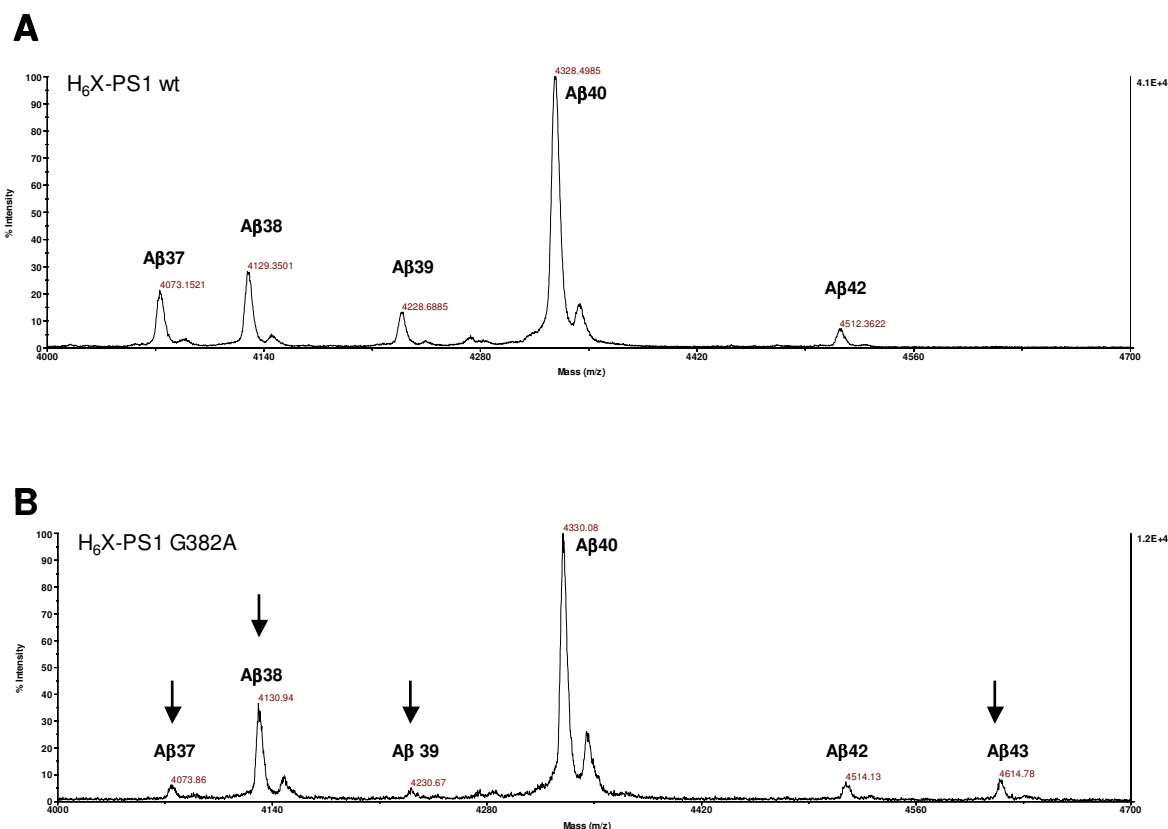


Figure 20. Representative MALDI-TOF MS of A $\beta$  peptides immunoprecipitated from conditioned media of HEK/sw cells expressing H<sub>6</sub>X-PS1 wt (Panel A) and H<sub>6</sub>X-PS1 G382A (Panel B). Arrows indicate the major peak changes.

A $\beta$ species	Peptide sequence	Calculated mass	Observed mass	
			H <sub>6</sub> X-PS1wt	H <sub>6</sub> X-PS1 G382A
A $\beta$ 37	DAEFRHDSGYEVHHQKLVFFAEDVGSNKGAIIGLMVGG	4074.55	4073.15	4073.86
A $\beta$ 38	DAEFRHDSGYEVHHQKLVFFAEDVGSNKGAIIGLMVGGG	4131.6	4129.35	4130.94
A $\beta$ 39	DAEFRHDSGYEVHHQKLVFFAEDVGSNKGAIIGLMVGGV	4230.73	4228.69	4230.67
A $\beta$ 40	DAEFRHDSGYEVHHQKLVFFAEDVGSNKGAIIGLMVGGVV	4329.86	4328.50	4330.08
A $\beta$ 42	DAEFRHDSGYEVHHQKLVFFAEDVGSNKGAIIGLMVGGVIA	4514.1	4512.36	4515.13
A $\beta$ 43	DAEFRHDSGYEVHHQKLVFFAEDVGSNKGAIIGLMVGGVVIAT	4615.21	-	4614.78

Table 4. Calculated and observed masses of the different A $\beta$  species found in the media of HEK/sw cells expressing H<sub>6</sub>X-PS1 wt and H<sub>6</sub>X-PS1 G382A. The calculated masses were predicted by GPMW (lighthouse) program.

### 3.1.3 PS1 G382A mutant shows an altered response to NSAIDs

It has been shown previously that a subset of NSAIDs typically causes a decrease in A $\beta$ 42 levels and an increase in A $\beta$ 38 levels while A $\beta$ 40 levels remain largely unaffected suggesting that these cleavages are interdependent (233). However, a recent study of

PS1 FAD mutations revealed that the A $\beta$ 38/A $\beta$ 42 production is in fact not coupled (277) (278). Moreover, it was found that many of the FAD mutants are less responsive to NSAIDs (277-279).

It was therefore next investigated whether and how the H<sub>6</sub>X-PS1 G382A mutant might change the specificity of the  $\gamma$ -cleavage in response to NSAIDs. HEK/sw cells stably expressing H<sub>6</sub>X-PS1 wt and H<sub>6</sub>X-PS1 G382A were treated with sulindac sulfide (Sul) and flurbiprofen (Flu), two well characterized NSAIDs, which modulate the activity of  $\gamma$ -secretase thereby increasing A $\beta$ 38 and reducing A $\beta$ 42 (233,280). In addition, cells were treated with fenofibrate (Fen) a lipid-regulating drug which has been shown to act as an inverse  $\gamma$ -secretase modulator by increasing A $\beta$ 42 and decreasing A $\beta$ 38 (270) and with naproxen (Nap), an NSAID which does not affect modulation of  $\gamma$ -secretase (233). Cells were pretreated with the drugs for 24 hours, then media were changed and the incubation in the presence of the drugs was continued for another 24 hours (233). Conditioned media were then collected and immunoprecipitated A $\beta$  species were separated on a Tris-bicine-urea gel system (Figure 21). The concentrations used for these  $\gamma$ -secretase modulators (GSMs) were 40  $\mu$ M for Sul, 150  $\mu$ M for Flu, 100  $\mu$ M for Fen and 200  $\mu$ M for Nap

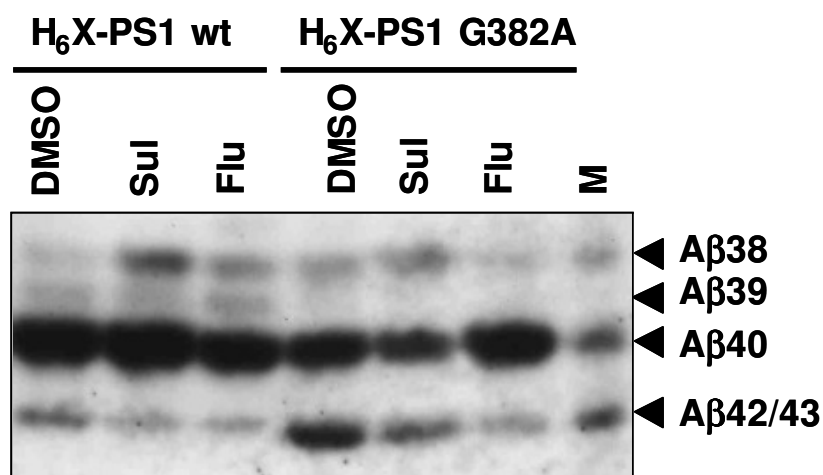


Figure 21. HEK/sw cells expressing the indicated PS1 constructs were treated with Sul (40  $\mu$ M) and Flu (150  $\mu$ M) or left untreated (DMSO). After the drug treatment, conditioned media were collected and subjected to immunoprecipitation of A $\beta$  with polyclonal antibody 3552. Immunoprecipitated A $\beta$  species were separated on a Tris-bicine-urea gel system and identified by immunoblotting with monoclonal antibody 6E10. A $\beta$ 38, A $\beta$ 40 and A $\beta$ 42 peptide standards were loaded in parallel (M)

As shown in figure 21, in H<sub>6</sub>X-PS1 wt cells, the treatment with Sul and Flu lowered the amount of A $\beta$ 42 and increased the amounts of A $\beta$ 38 species produced in comparison to DMSO-treated cells. Likewise, H<sub>6</sub>X-PS1 G382A showed a decrease in long A $\beta$  species (A $\beta$ 42/A $\beta$ 43) in response to the same GSMs. However, this decrease was not accompanied with a concomitant increase in A $\beta$ 38 species in the case of Flu treatment and with only a small increase of A $\beta$ 38 in the case of Sul treatment. To further confirm this qualitative result, aliquots of the same media were subjected to an A $\beta$  sandwich immunoassay to allow quantitation and to MS analysis.



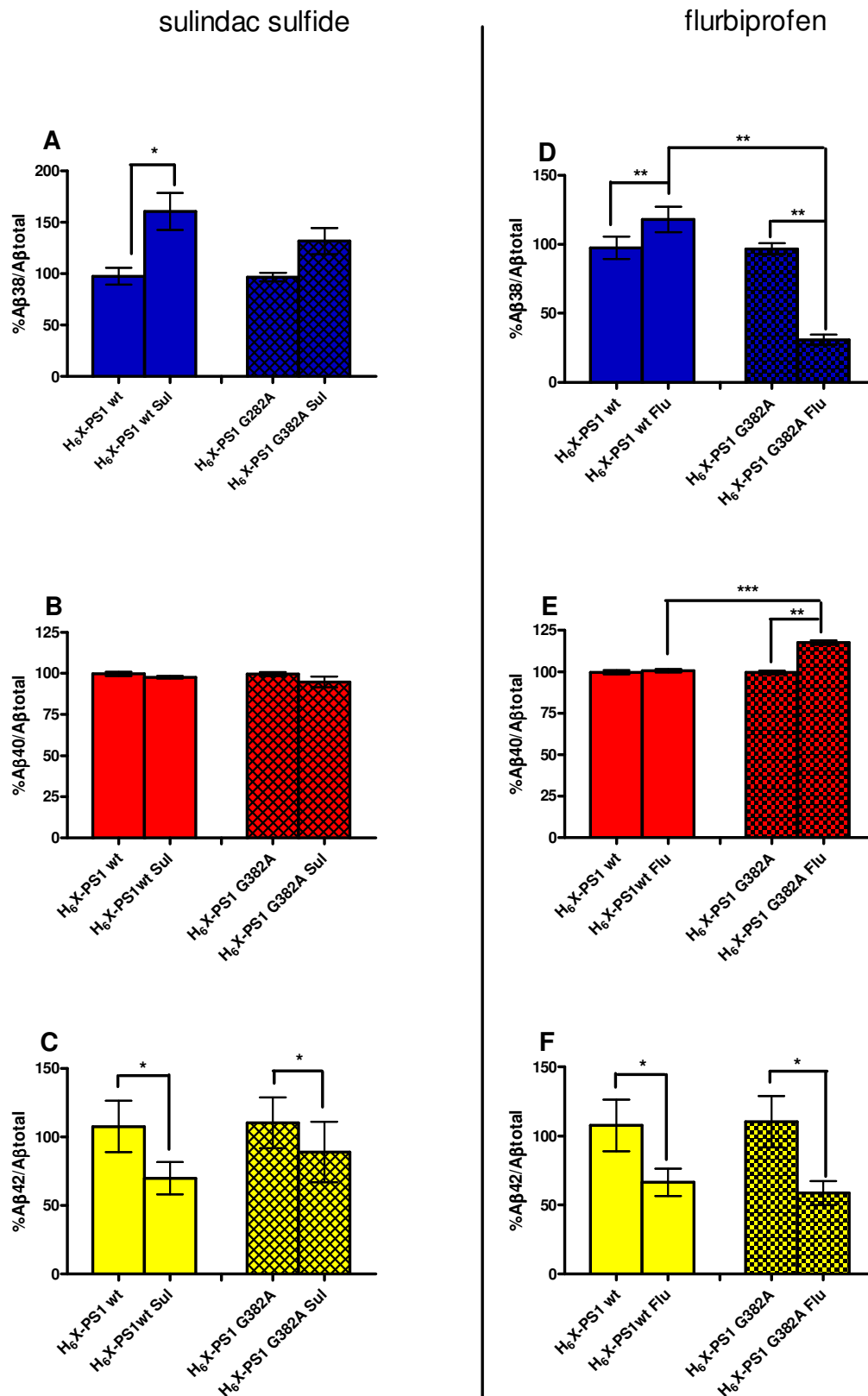


Figure 22. Effect of Sul (40  $\mu$ M) and Flu (150  $\mu$ M) treatment on A $\beta$  generation in HEK/sw cells expressing H<sub>6</sub>X-PS1 wt and H<sub>6</sub>X-PS1 G382A. A $\beta$ 38, A $\beta$ 40 and A $\beta$ 42 levels in conditioned media from HEK/sw cells stably expressing H<sub>6</sub>X-PS1 wt and H<sub>6</sub>X-PS1 G382A were measured by sandwich immunoassay and the A $\beta$ 38/A $\beta$ total, A $\beta$ 40/A $\beta$ total, A $\beta$ 42/A $\beta$ total ratios were determined. Statistical analysis of the data was performed by paired two-tailed student's t test. (\*  $p < 0.05$ ; \*\*  $p < 0.01$ ; \*\*\*  $p < 0.001$ ). The data are representative of three independent experiments (n=3).

As shown in figure 22, H<sub>6</sub>X-PS1 G382A had a typical response to Sul (i.e. an increase of the A $\beta$ 38/A $\beta$ total ratio and a decrease of the A $\beta$ 42/A $\beta$ total ratio) although its response was not as strong as for H<sub>6</sub>X-PS1 wt (Figure 22, panels A, B and C). In contrast, H<sub>6</sub>X-PS1 G382A had a robust decrease in the A $\beta$ 38/A $\beta$ total ratio in response to Flu treatment (figure 22 panel D) whereas the decrease in the A $\beta$ 42/A $\beta$ total ratio was comparable to the decrease observed for H<sub>6</sub>X-PS1 wt (figure 22 panel F). Moreover, the A $\beta$ 40/A $\beta$ total ratio was apparently also affected in the H<sub>6</sub>X-PS1 G382A mutant in response to Flu treatment consistent with the Tris-bicine-urea gel analysis (figure 21).

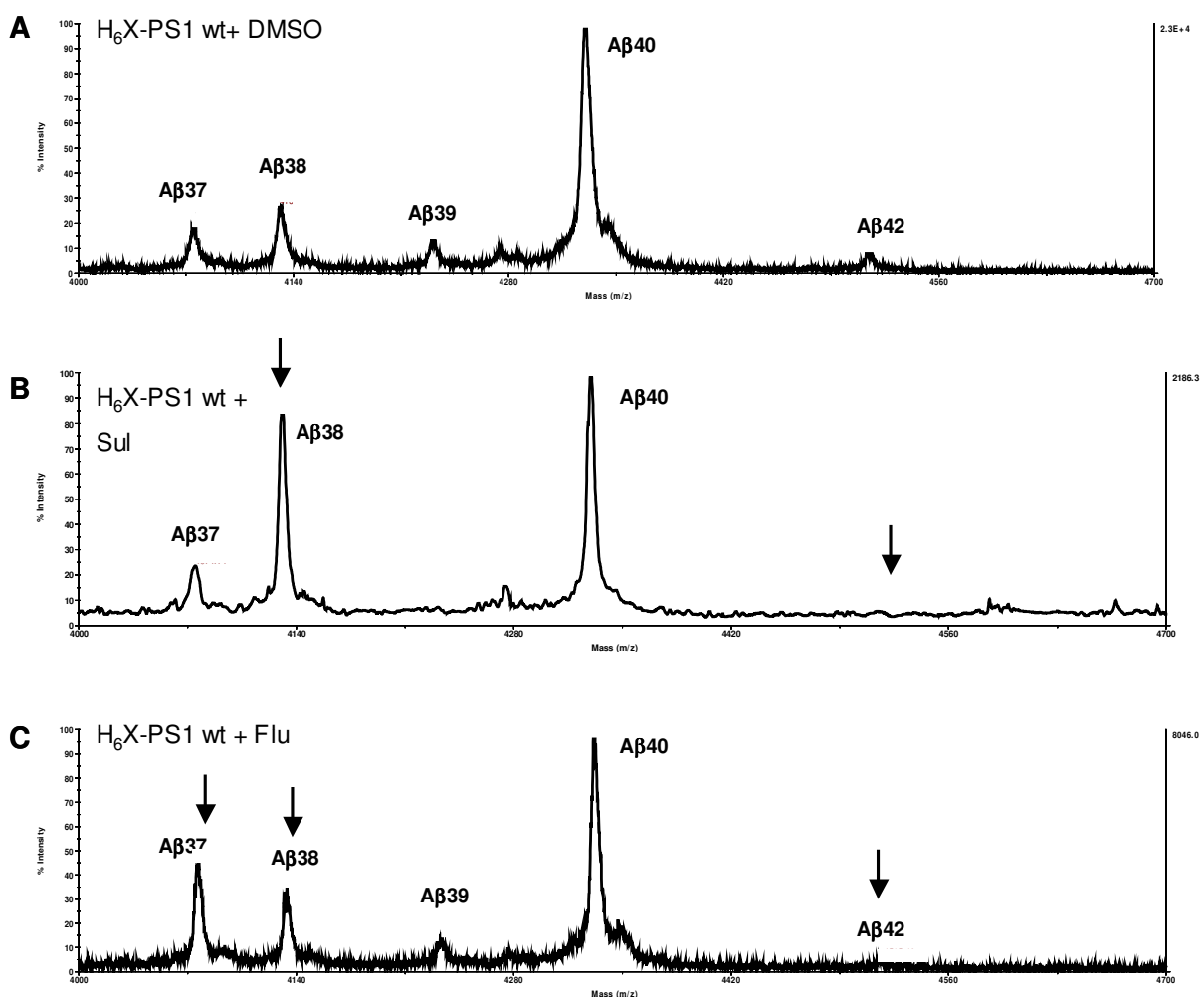


Figure 23. Representative MALDI-TOF MS of A $\beta$  peptides immunoprecipitated from media from HEK/sw cells expressing H<sub>6</sub>X-PS1 wt treated with DMSO (panel A) with Sul (panel B) and with Flu (panel C). Arrows indicate major peak changes.

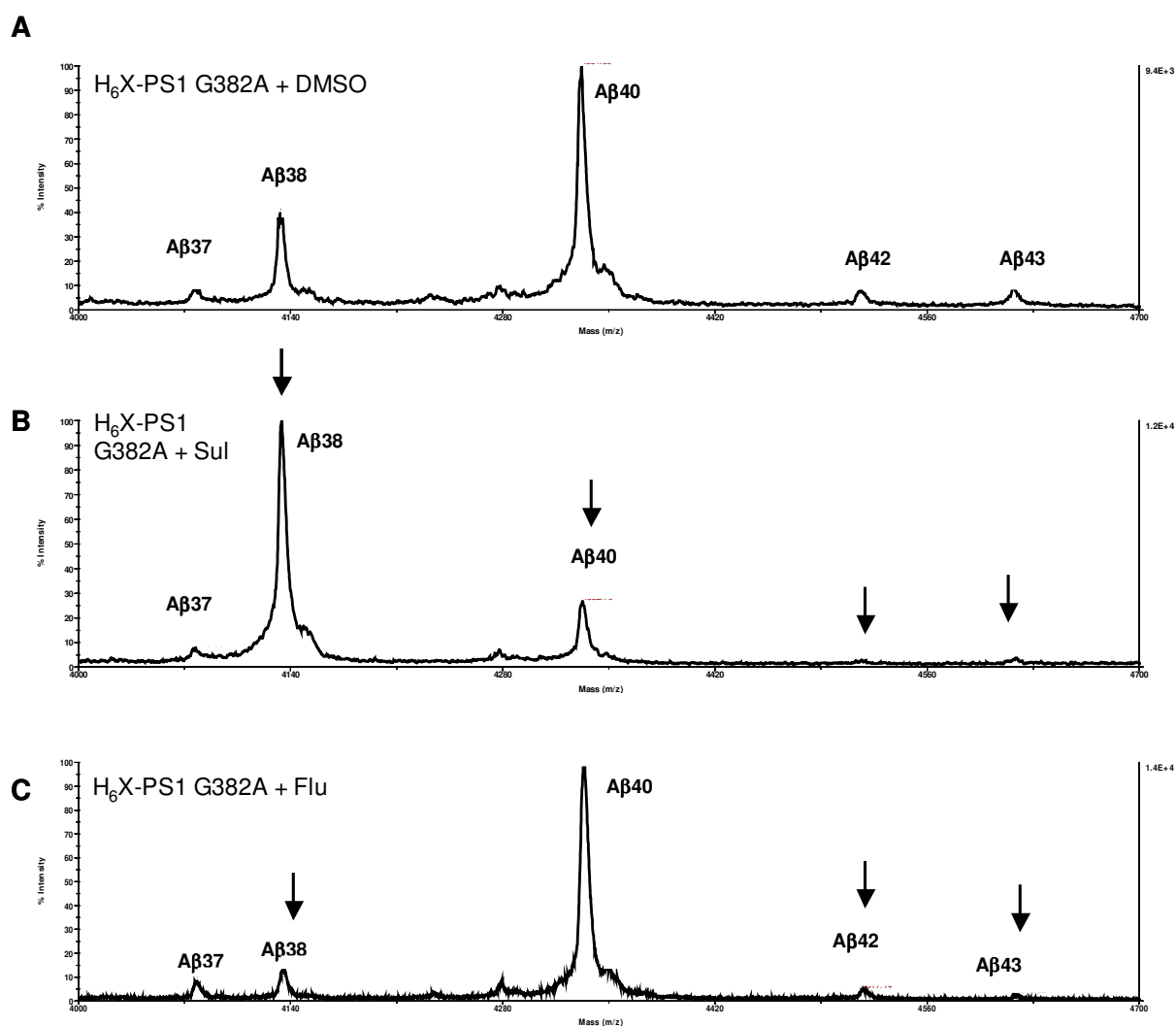


Figure 24. Representative MALDI-TOF MS of A $\beta$  peptides immunoprecipitated from conditioned media from HEK/sw cells expressing H<sub>6</sub>X-PS1 G382A treated with DMSO (panel A) with Sul (panel B) and with Flu (panel C). Arrows indicate major peak changes.

MS analysis confirmed the typical NSAID response observed for H<sub>6</sub>X-PS1 wt (figure 23) with a decrease in longer A $\beta$  species and an increase in the shorter ones (figure 23 panels B and C). Interestingly Flu causes an increase in A $\beta$ 37 in H<sub>6</sub>X-PS1 wt besides the increase in A $\beta$ 38. H<sub>6</sub>X-PS1 G382A had a typical response to NSAIDs for Sul treatment (figure 24 panel B) whereas a decrease in shorter A $\beta$  species as well as longer A $\beta$  species was observed for Flu treatment (figure 24 panel C).

The response to Fen (100  $\mu$ M) and Nap (200  $\mu$ M) treatment of the H<sub>6</sub>X-PS1 G382A was analysed next. Cells were treated for 8 hours with Fen instead of the usual 48 hours due to the fact that Fen showed high toxicity for HEK cells at 100  $\mu$ M in a 16 hours incubation. As shown in figure 25 for both H<sub>6</sub>X-PS1 wt and H<sub>6</sub>X-PS1 G382A a reduction in A $\beta$ 38 and A $\beta$ 40 species was seen upon Fen treatment with a concomitant increase in A $\beta$ 42/A $\beta$ 43

species. Nap treatment did not change any species neither in H<sub>6</sub>X-PS1 wt nor in H<sub>6</sub>X-PS1 G382A. To further confirm this qualitative result, and due to the fact that the Tris-bicine-urea gel system is not sensitive enough to detect small changes in A $\beta$  species, aliquots of the same conditioned media was subjected to a sandwich immunoassay to allow quantitation of A $\beta$  species and to MS.

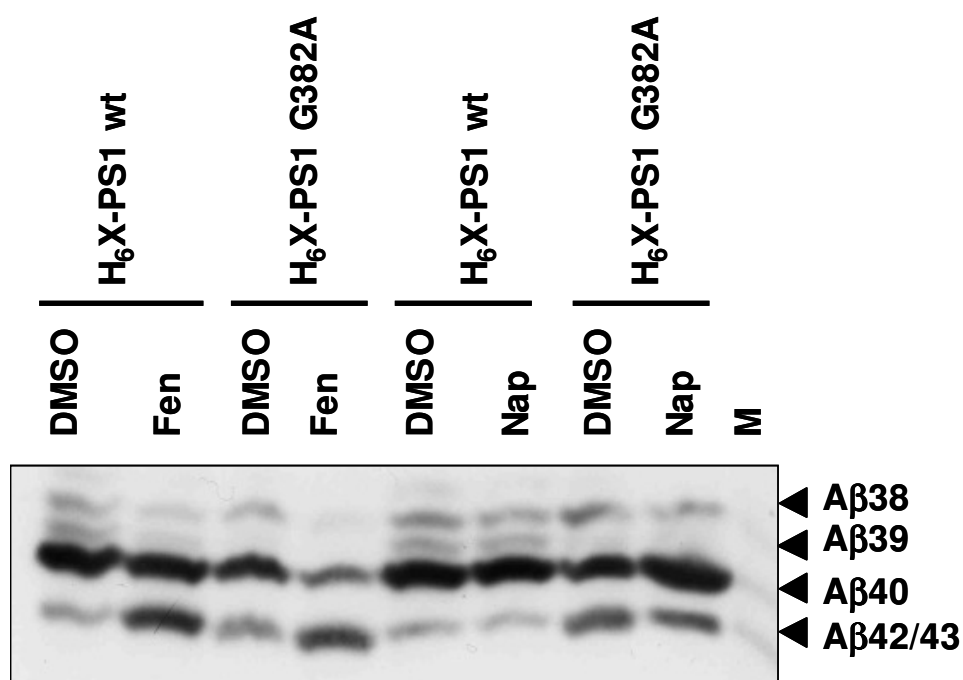


Figure 25. HEK/sw cells expressing the indicated PS1 constructs were treated with Fen (100  $\mu$ M) and Nap (200  $\mu$ M) or left untreated (DMSO). After the treatment, conditioned media were recollected and subjected to immunoprecipitation for A $\beta$  with polyclonal antibody 3552. A $\beta$  species were separated on a Tris-bicine-urea gel system and identified by immunoblotting with monoclonal antibody 6E10. A $\beta$ 38, A $\beta$ 40 and A $\beta$ 42 standards were loaded in parallel (M)

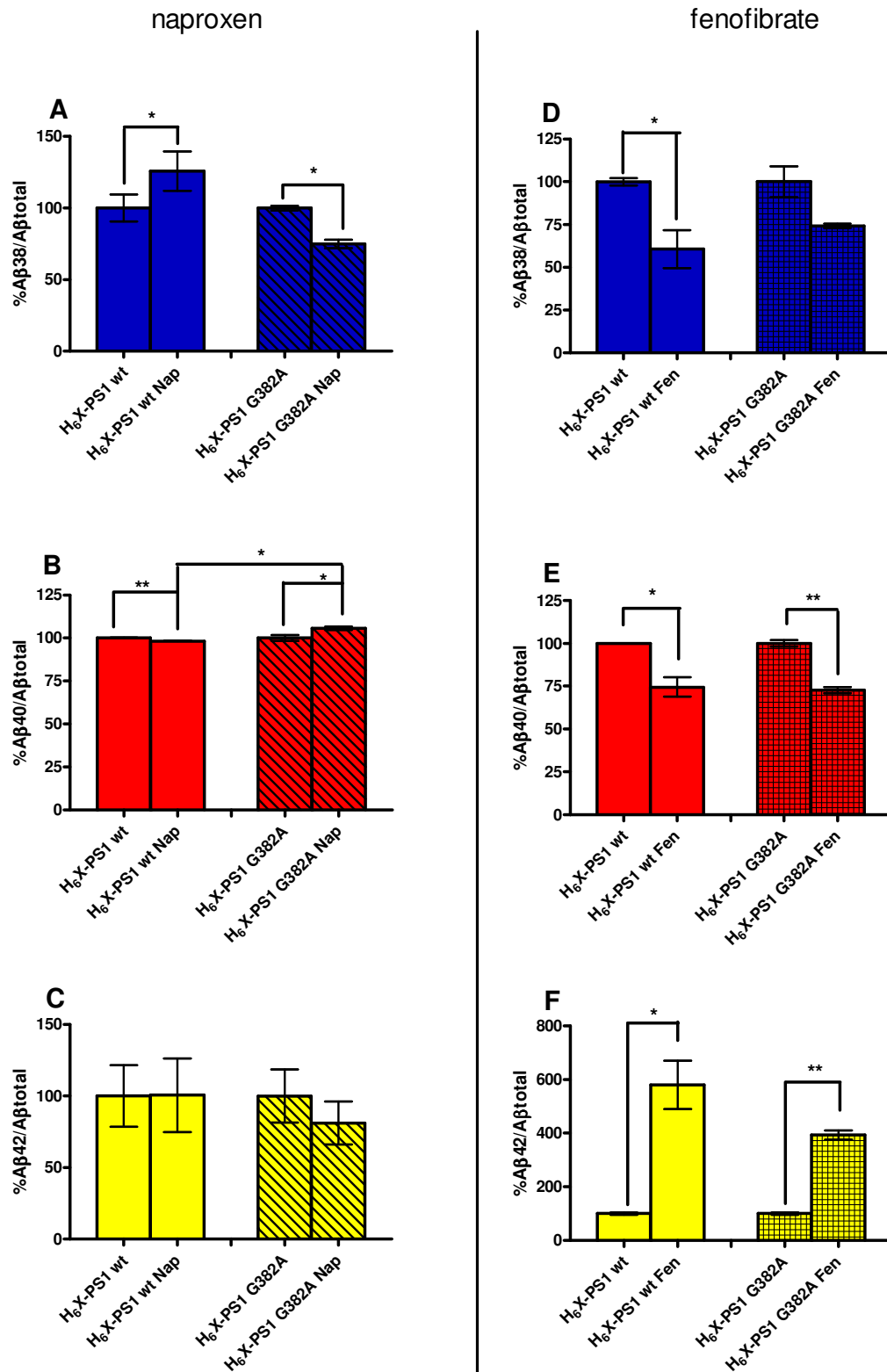


Figure 26. Effect of Nap (200  $\mu$ M) and Fen (100  $\mu$ M) treatment in HEK/sw cells expressing H<sub>6</sub>X-PS1 wt and H<sub>6</sub>X-PS1 G382A. Aβ38, Aβ40 and Aβ42 levels in conditioned media from HEK/sw cells stably expressing H<sub>6</sub>X-PS1 wt and H<sub>6</sub>X-PS1 G382A were measured by the Aβ sandwich immunoassay and the Aβ38/Aβtotal, Aβ40/Aβtotal, Aβ42/Aβtotal ratios were determined. Data were statistically analysed by paired two-tailed student's t test. (\* p<0.05; \*\* p<0.01; \*\*\* p< 0.001). The data are representative of three independent experiments (n=3).

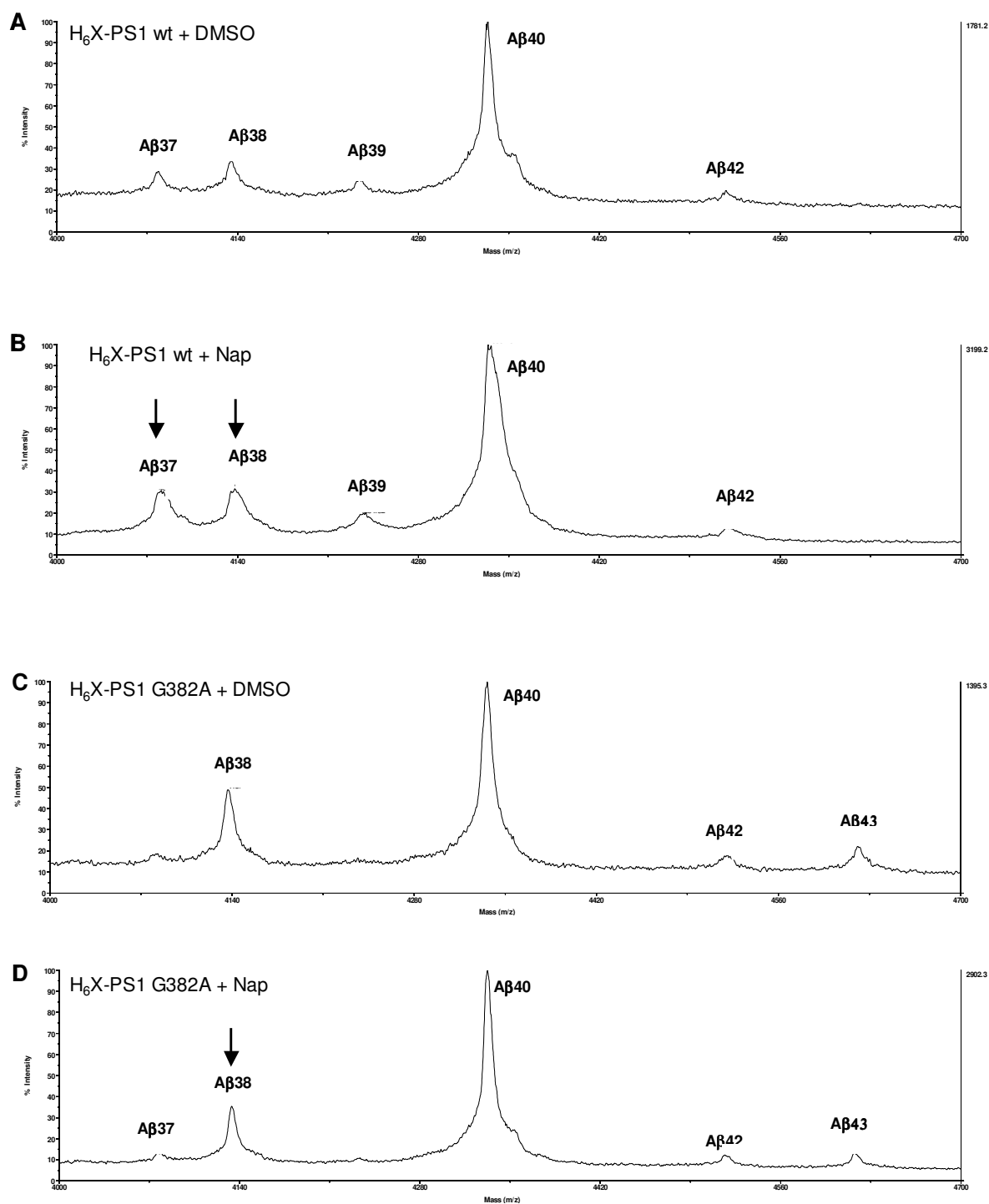


Figure 27. Representative MALDI-TOF MS of A $\beta$  peptides immunoprecipitated from conditioned media of HEK/sw cells expressing H<sub>6</sub>X-PS1 wt treated with DMSO (panel A) or Nap (Panel B), and cells expressing H<sub>6</sub>X-PS1 G382A treated with DMSO (panel C) and with Nap (panel D). Arrows indicate the major peak changes.

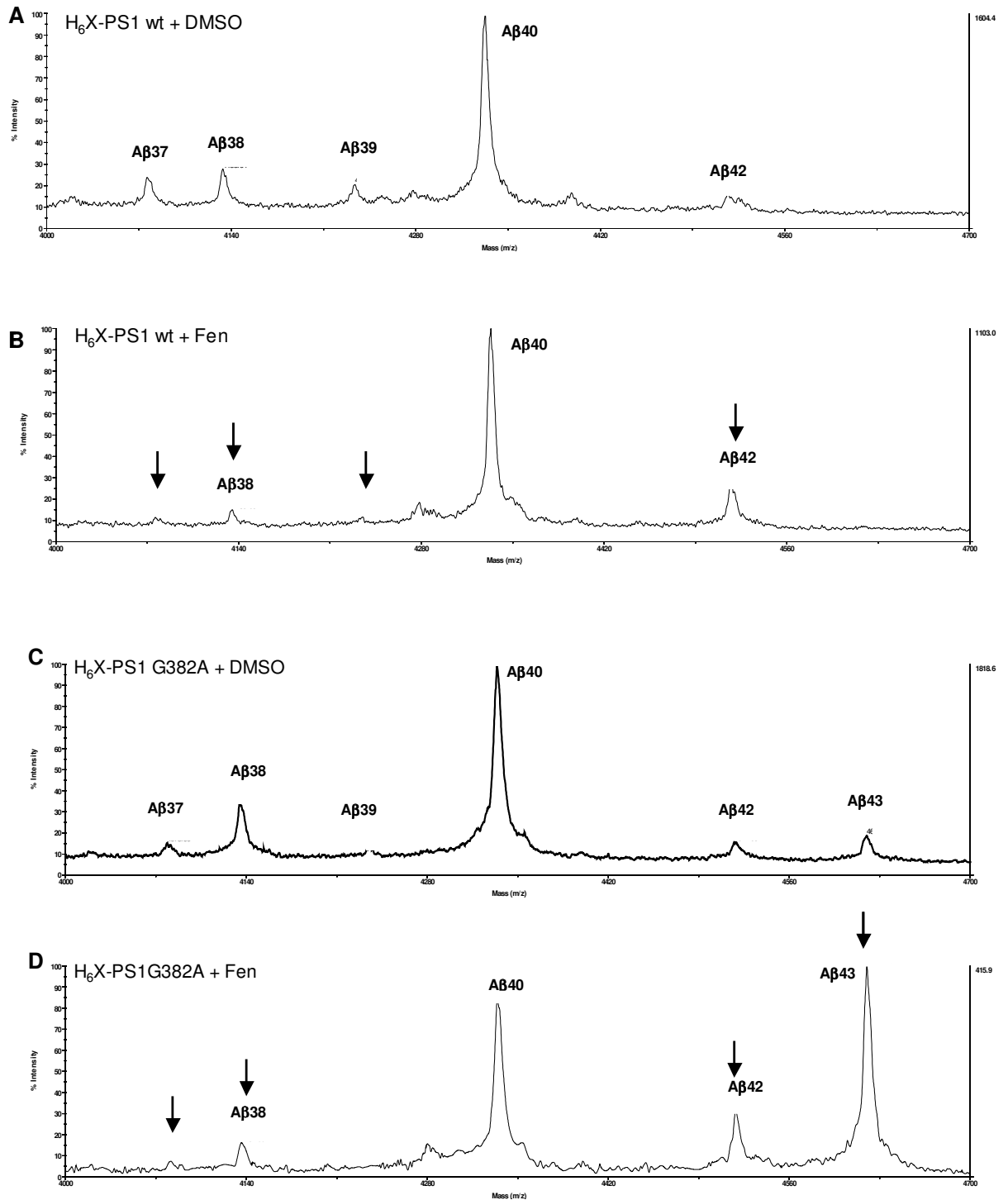


Figure 28. Representative MALDI-TOF MS of A $\beta$  peptides immunoprecipitated from media from HEK/sw cells expressing H<sub>6</sub>X-PS1 wt, treated with DMSO (panel A) and Fen (Panel B), and H<sub>6</sub>X-PS1 G382A treated with DMSO (panel C) and with Fen (panel D). Arrows indicate the major peak changes.

As shown in figure 26, both H<sub>6</sub>X-PS1 wt and H<sub>6</sub>X-PS1 G382A showed a decrease in the A $\beta$ 38/A $\beta$ total and A $\beta$ 40/A $\beta$ total ratios (figure 26 panels D and E) and both showed an increase in A $\beta$ 42/A $\beta$ total ratio (figure 26 panel F) in response to Fen treatment. On the other hand, Nap caused an increase in the A $\beta$ 38/A $\beta$ total ratio for H<sub>6</sub>X-PS1 wt whereas, H<sub>6</sub>X-PS1 G382A showed a decrease in the A $\beta$ 38/A $\beta$ total ratio and an increase in the A $\beta$ 40/A $\beta$ total ratio compared to H<sub>6</sub>X-PS1 wt. The A $\beta$ 42/A $\beta$ total ratio, however, did not significantly change for H<sub>6</sub>X-PS1 wt and H<sub>6</sub>X-PS1 G382A (figure 26 panels A, B and C).

These results were confirmed by MS analysis. Nap treatment caused a relative increase in shorter A $\beta$  species (A $\beta$ 37 and A $\beta$ 38) for H<sub>6</sub>X-PS1 wt (figure 27 panels A and B). In contrast, in response to Nap treatment a decrease in A $\beta$ 38 is observed in H<sub>6</sub>X-PS1 G382A (figure 27 panels C and D). As expected, Fen treatment increased long A $\beta$ 42 species decreasing the levels of A $\beta$ 38 for H<sub>6</sub>X-PS1 wt (figure 28 panels A and B). Strikingly, for H<sub>6</sub>X-PS1 G382A in addition to a relative increase in A $\beta$ 42 species in response to Fen treatment a large increase in A $\beta$ 43 species was observed (figure 28 panels C and D) suggesting a different behaviour between H<sub>6</sub>X-PS1 wt and H<sub>6</sub>X-PS1 G382A with regard to Fen treatment.

Taken together, these results suggest that the PS1 G382A mutant has an altered response to some GSMs on the generation of the A $\beta$  species than PS1 wt. The data further suggests that the production of A $\beta$ 38 and A $\beta$ 42 upon NSAID treatment is not coupled in PS1 mutants in agreement to the findings with PS1 FAD mutations (277).

### ***3.2 Impact of PS1 G382 mutants on the processing of other $\gamma$ -secretase substrates***

As shown in the previous experiments, APP processing is affected by the mutagenesis of the N-terminal glycine of the GxGD motif of PS1. When this glycine is changed to an amino acid with a large side chain, APP processing is generally impaired, whereas when the change is minor, processing can occur but with a lesser efficiency. It was then investigated whether the mutagenesis of this residue has also an impact on processing of other  $\gamma$ -secretase substrates. In order to address this question, mouse embryonic fibroblasts (MEF) cells derived from PS1/PS2 -/- knockout mice were used (268) where no



endogenous PS is present that could interfere with the result. Untagged PS1 G382 mutant cDNAs were transiently co-transfected in PS1/PS2  $-/-$  MEF cells with the cDNAs encoding for the substrate under investigation. The substrates used for this purpose were APP, Notch1, Notch2, Notch3, Notch4 and CD44 as these proteins have been previously shown to be processed by  $\gamma$ -secretase (191,192,204). cDNAs of PS1 wt, PS1 D385A as well as empty vector were generally co-transfected to serve as a positive and negative control respectively.

### **3.2.1 PS1 G382A supports processing of APPsw-6myc in PS1/PS2 $-/-$ MEF cells**

PS1/PS2  $-/-$  MEF cells have been shown to be a reliable system to study PS mutations in a PS free background (125,149,192,281). In order to first verify the results obtained in the HEK/sw background, cDNAs encoding the PS1 G382 mutants were transiently co-transfected with APPsw-6myc into PS1/PS2  $-/-$  MEF cells. APPsw-6myc is an APP molecule that harbors the Swedish mutation and is C-terminally tagged with 6myc epitopes (265).

Following transient transfection, total cell lysates were analysed by immunoblotting. NCT maturation was rescued upon expression of all PS1 proteins, indicating a normal  $\gamma$ -secretase complex formation (figure 29 panel A). As shown in figure 29, all transfected proteins were robustly expressed. PS1 wt and PS1 G382A were endoproteolysed to NTF and CTF whereas all other mutants remained as uncleaved holoprotein (Figure 29 panels B and C). This result is in agreement with the observations in the HEK/sw cells described above. To investigate the processing of APPsw-6myc, production of AICD and secretion of A $\beta$  peptide were examined. The 6myc-tagged AICD can be analysed in this experimental setting because it is more stable than the untagged AICD (265). AICD was only generated when APPsw-6myc is co-transfected with PS1 wt and PS1 G382A (figure 29 panels D and E and figure 30). In addition, PS1 wt expression strongly reduced the accumulation of APP<sub>CTFs</sub>. In contrast, PS1 G382A was not able to rescue APP<sub>CTFs</sub> accumulation (figure 29 panel D) suggesting that PS1 G382A mutant is only partially active. A $\beta$  peptide was only secreted when PS1 wt and PS1 G382A were present (figure 29 panel E). These data fully confirm the observation made with the G382 mutant in the background of the HEK/sw system.

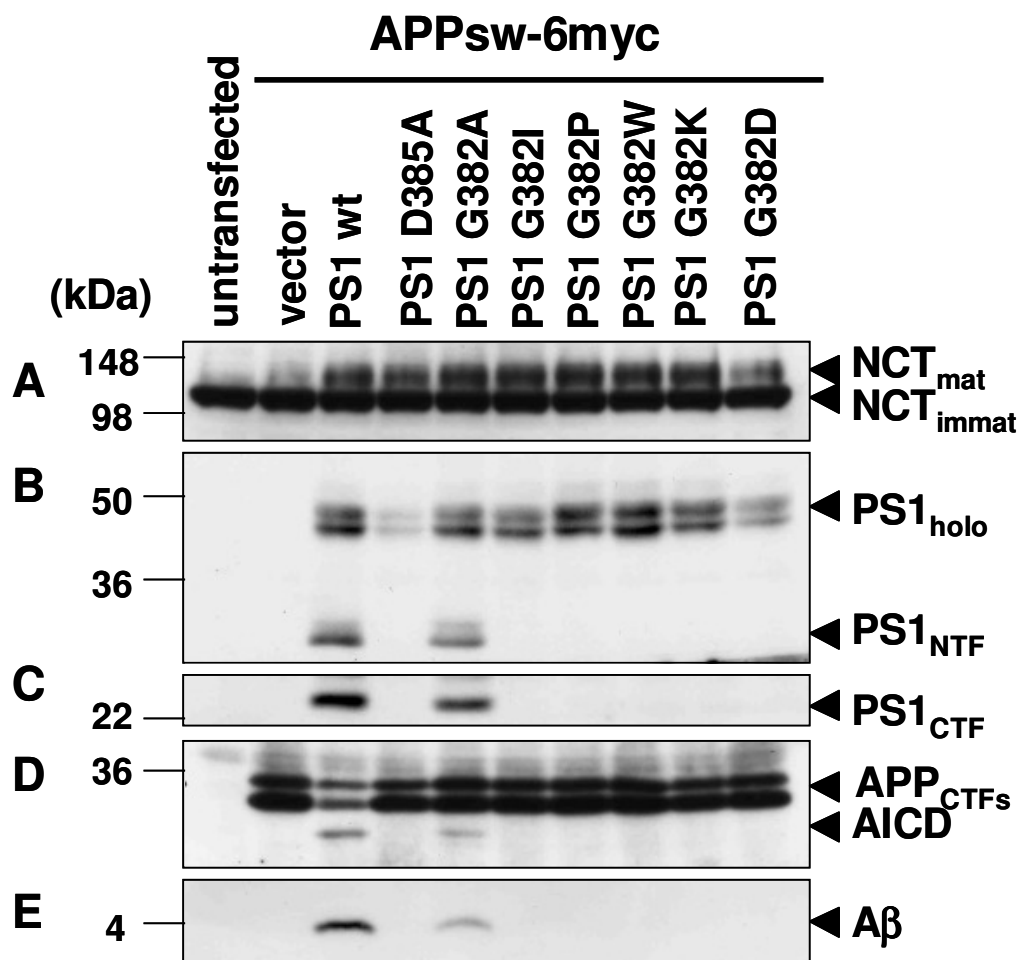


Figure 29. PS1 G382A mutants do not process APP<sup>sw</sup>-6myc with the exception of PS1 G382A. PS1/PS2<sup>-/-</sup> MEF cells were transiently transfected with the indicated PS1 constructs. Cell lysates were analysed for PS1 expression and  $\gamma$ -secretase complex formation (panel A) by immunoblotting using antibodies N1660 for the detection of NCT and PS1N and 3027 for the detection of PS1<sub>NTF</sub> and PS1<sub>CTF</sub> respectively (panels B and C). APP processing was analysed in panel D, AICD formation was detected with antibody 9E10 against the myc tag. Secreted A $\beta$  was analysed by combined immunoprecipitation/immunoblotting using polyclonal and monoclonal anti-A $\beta$  with antibodies 3552/6E10.  $\gamma$ -Secretase components and AICD were separated by 10% Tris-glycine-urea SDS-PAGE. A $\beta$  was separated in a 10-20% Tris-tricine SDS-PAGE.

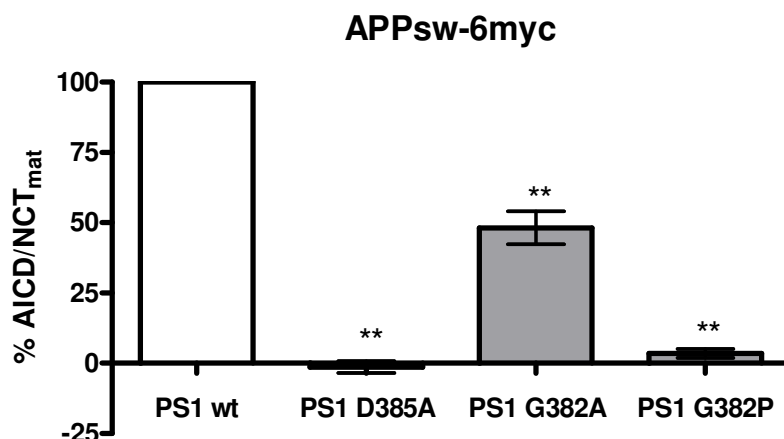


Figure 30: Signal intensity of AICD produced by PS1 G382A in PS1/PS2 <sup>-/-</sup> MEF cells. The intensity of the AICD bands were quantified and normalised by NCT<sub>mat</sub> protein levels. The normalised AICD produced by PS1 wt were set to 100%. %. Data were statistically analysed by one-way ANOVA with Dunnet's post correction test for comparison of multiple samples to a control (PS1 wt) (\*\* p<0.01). The data are representative of three independent experiments (n=3).

### 3.2.2 PS1 G382A supports processing of Notch1 in PS1/PS2 <sup>-/-</sup> MEF cells

Next, the PS1 G382 mutants were tested for their capability to process the most important physiological  $\gamma$ -secretase substrate, Notch1. PS1/PS2 <sup>-/-</sup> MEF cells were transiently co-transfected with cDNAs encoding the PS1 G382 mutants and with cDNA encoding F-NEXT, an extracellular truncated version of Notch1 tagged N-terminally with a Flag-epitope and C-terminally with a 6myc epitope to facilitate the analysis of the cleavage products (267). As described before, total cell lysates were analysed by immunoblotting. All transfected proteins were strongly expressed and NCT maturation was rescued upon PS1 expression (figure 31 panel A). PS1 wt and PS1 G382A mutants were endoproteolysed whereas other PS1 mutants remained as uncleaved holoprotein (figure 31 panels B and C). As seen in the vector-transfected lane (figure 31), F-NEXT was not processed due to the absence of a fully  $\gamma$ -secretase complex in these cells but upon expression of PS1 wt and PS1 G382A NICD was produced and N $\beta$  peptide was secreted to the media (figure 31 panels D, E, F and figure 32) although no reduction in the substrate levels is observed. This lack of reduction in the substrate levels observed in the PS1 wt lane is probably due to an excess of the substrate present in the cells that cannot be completely processed. As observed for APP, the other PS1 G382 mutants did not support F-NEXT processing. Thus, similar as for APP processing, only subtle changes in the GxGD motif are partially accepted for F-NEXT processing.

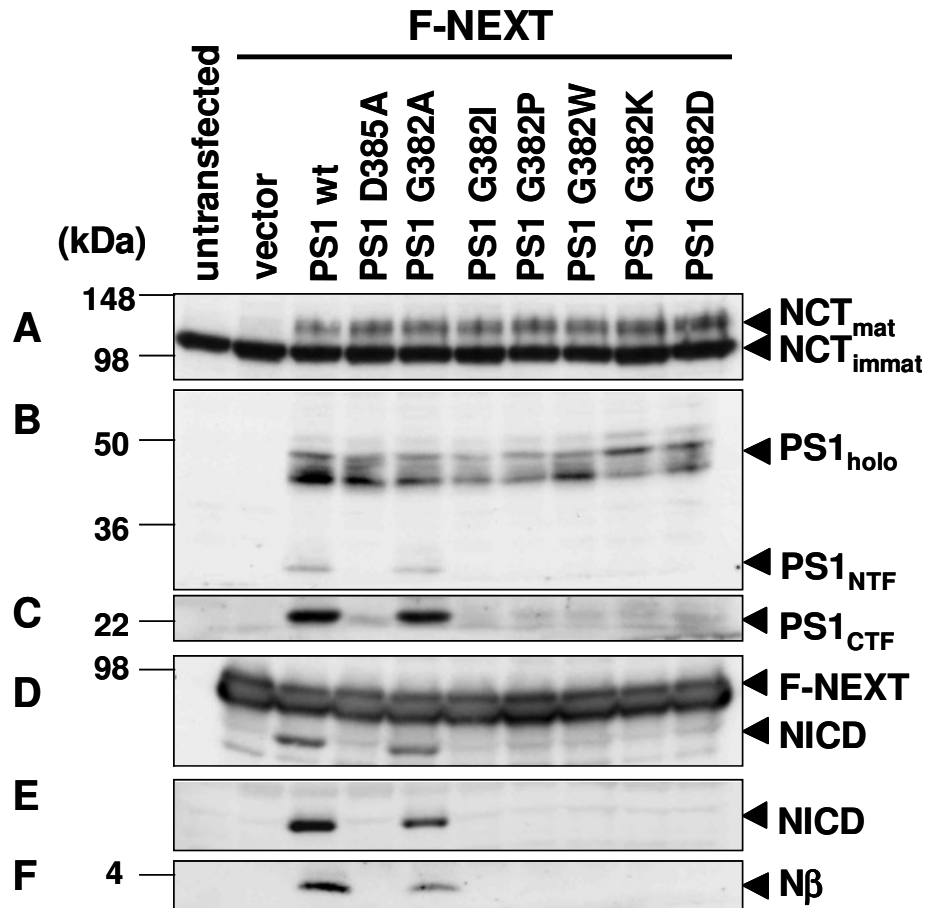


Figure 31. PS1 G382A mutants do not process F-NEXT with the exception of PS1 G382A. Panels A, B and C, lysates from cells transiently expressing the above PS1 constructs were analysed by immunoblotting for  $\gamma$ -secretase complex formation and PS1 endoproteolysis using N1660, PS1N and 3027 antibody. In Panel D, processing of F-NEXT was analysed by immunoblotting with antibody 9E10. Panel E, NICD was immunoblotted with cleaved Notch1 antibody, specific for NICD. Panel F, secreted N $\beta$  peptide was analysed by immunoprecipitation with Flag M2 agarose and immunoblotting with Flag-M2 antibody.  $\gamma$ -Secretase components were separated by 10% Tris-glycine-urea SDS-PAGE. NICD and F-NEXT were separated by 7% Tris-glycine SDS-PAGE. N $\beta$  was separated by 10%-20% Tris-tricine SDS-PAGE.

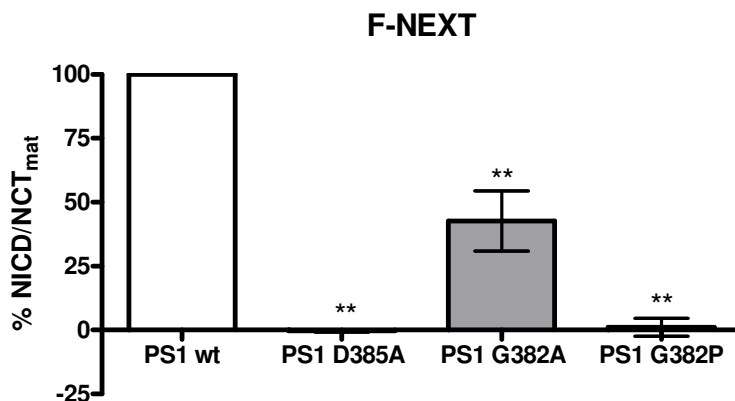


Figure 32: Signal intensity of NICD produced by PS1 G382A in PS1/PS2  $-/-$  MEF cells. The intensity of the NICD bands were quantified and normalized by NCT<sub>mat</sub> protein levels. The normalized NICD levels produced by PS1 wt were set to 100%. Data were statistically analysed by one-way ANOVA with Dunnet's post correction test for comparison of multiple samples to a control (PS1 wt) (\*\*  $p < 0.01$ ). The data are representative of three independent experiments ( $n=3$ ).

### 3.2.3 PS1 G382A supports Notch2 processing in PS1/PS2 -/- MEF cells

Next it was investigated whether PS1 G382 mutants can process homologues of Notch1 (see section 1.3.3.3.1). Notch2 was investigated first. PS1/PS2 -/- MEF were transiently co-transfected with cDNAs encoding the PS1 G382A mutant and PS1 G382P and PS1 G382K as strong mutations, with cDNA encoding for mouse Notch2 $\Delta$ E. mNotch2 $\Delta$ E is the extracellular truncated version of mouse Notch2 tagged at the C-terminus with a 6myc epitope. Following transfection, total cell lysates were analysed as before. As expected, NCT maturation was rescued upon PS expression and PS1 wt and PS1 G382A underwent endoproteolysis, while the other two mutants did not (figure 33 panels A, B and C). As expected in the vector-transfected lane processing of mNotch2 $\Delta$ E was not observed, since no functional  $\gamma$ -secretase complex was present. This was reverted when PS1 wt and PS1 G382A mutant were present as NICD was produced (figure 33 panel D and figure 34). However, as for Notch1, neither PS1 G382P nor PS1 G382K rescued the processing of mNotch2 $\Delta$ E. Thus, only subtle changes, from a glycine to an alanine within the GxGD motif are accepted for mNotch2 $\Delta$ E processing.

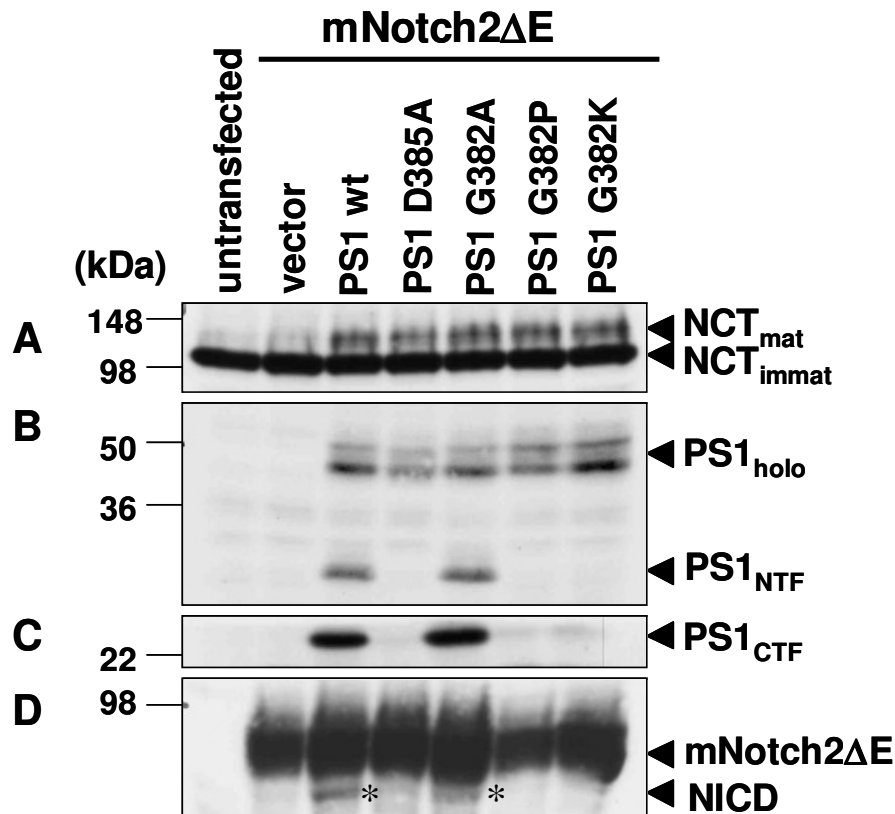


Figure 33. PS1 G382A mutants do not process mNotch2ΔE with the exception of PS1 G382A. Panels A, B and C, lysates from cells transiently expressing the PS1 constructs were analysed by immunoblotting for  $\gamma$ -secretase components using N1660, PS1N and 3027 antibodies. In Panel D, processing of mNotch2ΔE was analysed by immunoblotting with antibody 9E10. Asterisks denote the cleaved Notch2 fragment.  $\gamma$ -Secretase components were separated by 10% Tris-glycine-urea SDS-PAGE. NICD and mNotch2ΔE were separated by 7% Tris-glycine SDS-PAGE.

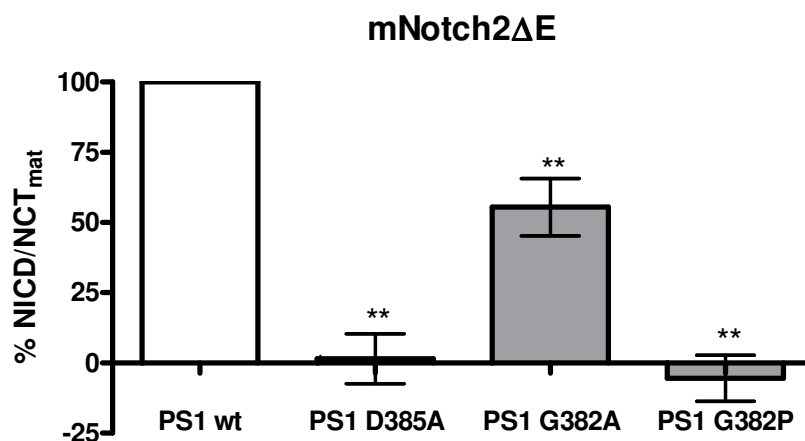


Figure 34: Signal intensity of NICD produced by PS1 G382A in PS1/PS2<sup>-/-</sup> MEF cells. The NICD bands intensity were quantified and normalised by NCT<sub>mat</sub> protein levels. The normalised NICD levels produced by PS1 wt were set to 100%. Data were statistically analysed by one-way ANOVA with Dunnet's post correction test for comparison of multiple samples to a control (PS1 wt) (\*\*  $p < 0.01$ ). The data are representative of three independent experiments ( $n=3$ ).

### 3.2.4 PS1 G382A mutant supports processing of Notch3 in PS1/PS2 -/- MEF cells

The capacity of the PS1 G382 mutants in processing of Notch3, another Notch1 homologue, was investigated next. PS1/PS2 -/- MEF cells were transiently co-transfected with the same set of PS1 cDNAs as before and with the cDNA encoding the mouse mNotch3 $\Delta$ E, an extracellular truncated mouse version of Notch3 tagged at the C-terminus with a 6myc epitope (191). Following transfection, total cell lysates were analysed as before. All transfected proteins were robustly expressed. PS1 wt and PS1 G382A underwent endoproteolysis as expected and NCT maturation was rescued by the presence of PS1 (figure 35 panels A, B and C). In the vector-transfected lane due to the absence of an active  $\gamma$ -secretase complex no process of mNotch3 $\Delta$ E was observed. When PS1 wt and PS1 G382A were present this was reverted and NICD was produced (figure 35 panel D and figure 36). Thus again, only a minor change in the position 382 of presenilin from glycine to alanine allows processing to some extent. More drastic changes, like proline or lysine, interfere with processing.

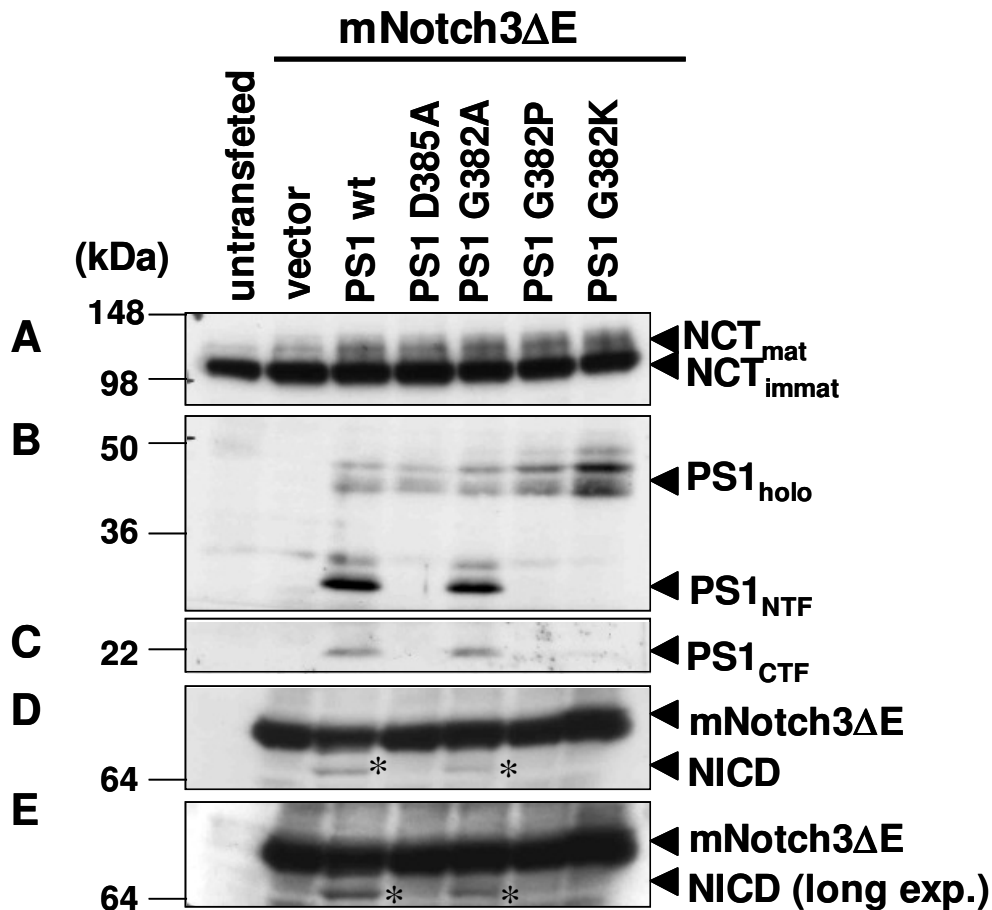


Figure 35. PS1 G382A mutants do not process mNotch3ΔE with the exception of PS1 G382A. In panels A, B and C, lysates from cells transiently expressing the above PS1 constructs were analysed by immunoblotting for  $\gamma$ -secretase components using N1660, PS1N and 3027 antibodies. In Panel D, processing of mNotch3ΔE was analysed by immunoblotting with antibody 9E10. Asterisks denote the cleaved notch3 fragment.  $\gamma$ -Secretase components were separated by 10% Tris-glycine-urea SDS-PAGE. NICD and mNotch3ΔE were separated by 7% Tris-glycine SDS-PAGE.

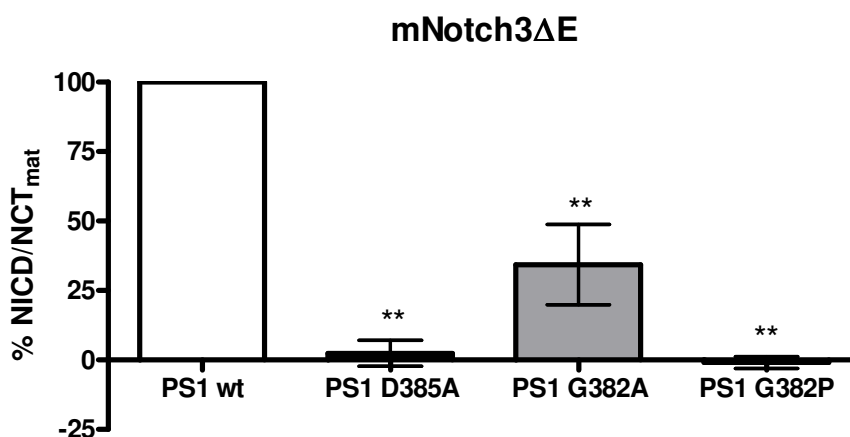


Figure 36: Signal intensity of NICD produced by PS1 G382A in PS1/PS2<sup>-/-</sup> MEF cells. The NICD band intensities were quantified and normalized to NCT<sub>mat</sub> protein levels. The normalized NICD levels produced by PS1 wt were set to 100%. Data were statistically analysed by one-way ANOVA with Dunnet's post correction test for comparison of multiple samples to a control (PS1 wt) (\*\*  $p < 0.01$ ). The data are representative of three independent experiments (n=3).



### **3.2.5 PS1 G382 mutants do not support Notch4 processing in PS1/PS2<sup>-/-</sup> MEF cells**

The last Notch homologue to be investigated was Notch4. As before PS1/PS2<sup>-/-</sup> MEF cells were transiently co-transfected with the cDNAs encoding for the PS1 G382 mutants, and with cDNA encoding for mouse Notch4 $\Delta$ E, which is an extracellular truncated mouse version of Notch4 tagged at the C-terminus with 6myc epitopes (191). Following transfection, total cell lysates were analysed as before. As shown in figure 32 all transfected proteins were robustly expressed. As expected, the presence of PS1 restored NCT maturation suggesting normal  $\gamma$ -secretase complex formation. PS1 wt and PS1 G382A, as before, were endoproteolysed (figure 37, panels A, B and C). Strikingly, only cells expressing PS1 wt allowed the generation of NICD, whereas cells expressing PS1 G382A did not produce any NICD (figure 37, panels D, E and figure 38). This result suggests that G382 is indeed important for mNotch4 $\Delta$ E processing, since not even a minor change in this region of the GxGD motif allows the processing of this substrate.

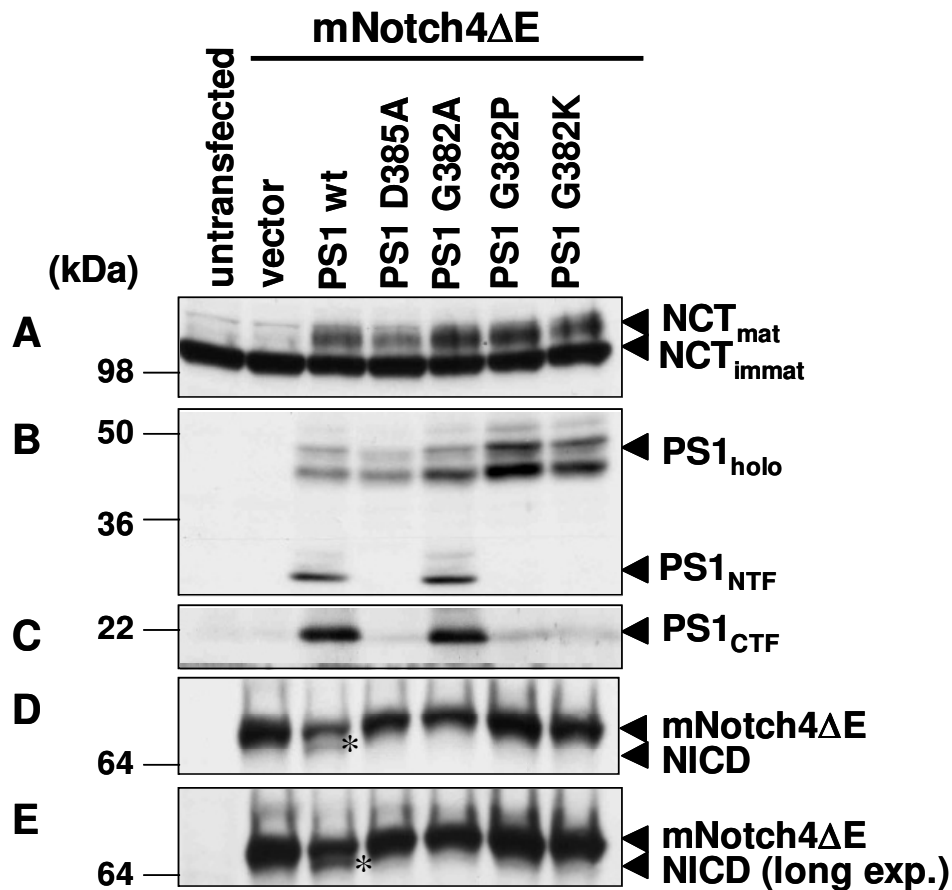


Figure 37. PS1 G382A mutant does not process mNotch4ΔE. Panels A, B and C, lysates from cells transiently expressing the above PS1 constructs were analysed by immunoblotting for  $\gamma$ -secretase components using N1660, PS1N and 3027 antibodies. In Panel D, processing of mNotch4ΔE was analysed by immunoblotting with antibody 9E10. Asterisk denotes the cleaved Notch4 fragment.  $\gamma$ -Secretase components were separated by 10% Tris-glycine-urea SDS-PAGE. NICD and mNotch4ΔE were separated by 7% Tris-glycine SDS-PAGE.

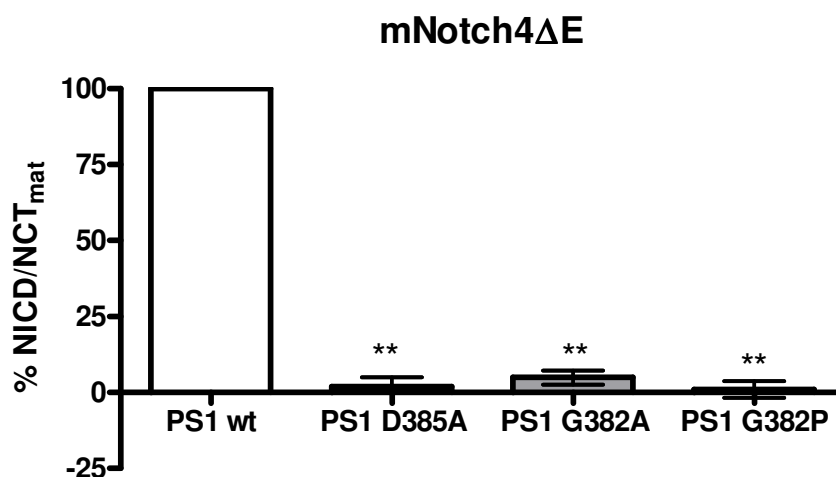


Figure 38: Signal intensity of NICD produced by PS1 G382A in PS1/PS2<sup>-/-</sup> MEF cells. The NICD band intensities were quantified and normalised by  $NCT_{mat}$  protein levels. The normalised NICD levels produced by PS1 wt were set to 100%. Data were statistically analysed by one-way ANOVA with Dunnet's post correction test for comparison of multiple samples to a control (PS1 wt) (\*\*  $p < 0.01$ ). The data are representative of three independent experiments (n=3).

### 3.2.6 PS1 G382 mutants do not support processing of CD44 in PS1/PS2<sup>-/-</sup> MEF cells

Finally, it was investigated whether PS1 G382 mutants can process CD44. The cDNA of this construct encodes for an extracellular truncated version of CD44 with a Flag epitope at the N-terminus, which allows the analysis of the secreted CD44 $\beta$  peptide, and a 6myc epitope at the C-terminus to allow analysis of the CD44-ICD formation (192). This cDNA construct was co-transfected with the cDNAs encoding for the PS1 G382 mutants. As shown above, PS1 wt and PS1 D385A cDNAs as well as vector alone were co-transfected as controls. Following transfection, total cell lysates were analysed as before. As expected, endoproteolysis occurred in PS1 wt and PS1 G382A and the presence of the PS1 rescued the maturation of NCT suggesting normal  $\gamma$ -secretase complex formation (figure 39 panels A, B and C). In the vector-transfected lane, consistent with the absence of an active  $\gamma$ -secretase in PS1/PS2<sup>-/-</sup> MEF cells, no CD44-ICD was observed and no CD44 $\beta$  was detected in the conditioned media. Only when PS1 wt was present this situation was reverted as CD44-ICD was produced and CD44 $\beta$  peptide was detected in the conditioned media (figure 39 panels E and F). Due to the weak intensity of the CD44-ICD band, CD44 $\beta$  was used instead for quantitation. Quantitation of the experiment shows a reduction of CD44 $\beta$  peptide produced by PS1 G382A (figure 40). In contrast, all the PS1 G382 mutants were inactive, suggesting that as also observed for mNotch4 $\Delta$ E, this glycine in position 382 of the GxGD motif is also crucial for CD44 $\Delta$ E-Flag processing. Thus, not even a subtle change of G382 to alanine allows the processing of this substrate.

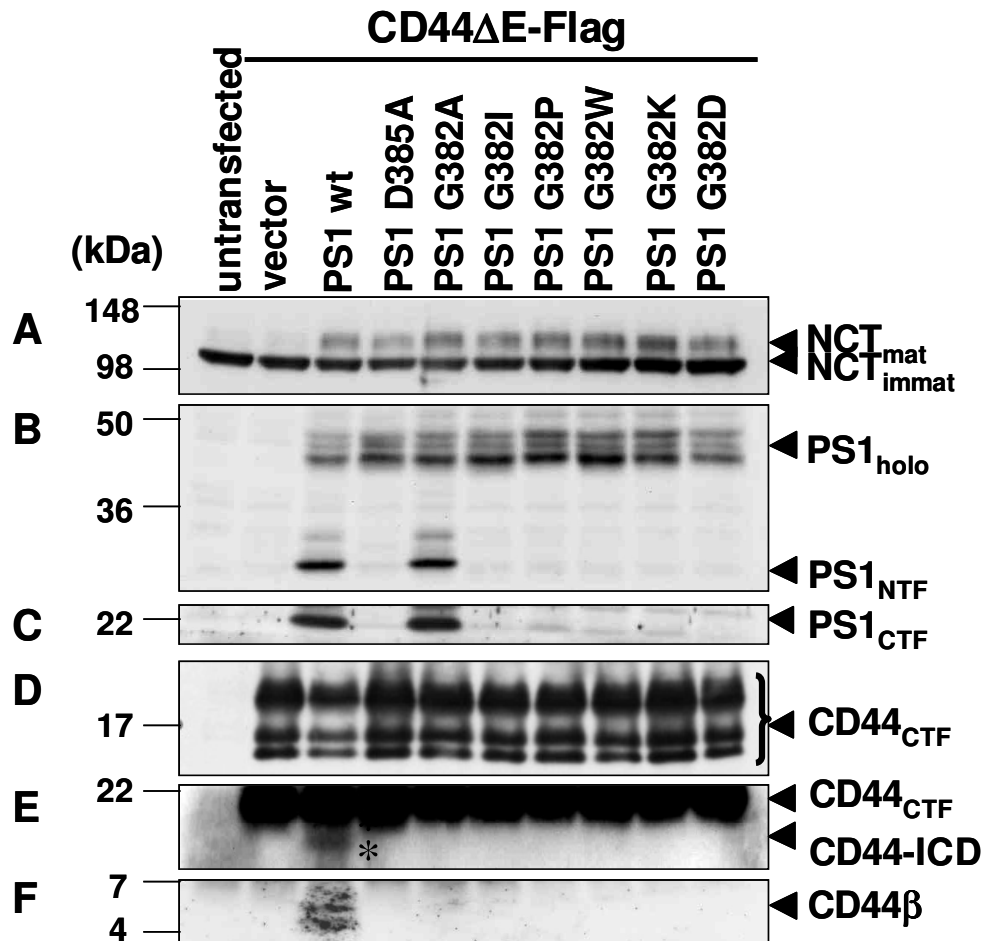


Figure 39. PS1 G382A mutant does not process CD44 $\Delta$ E-Flag. Panels A, B and C lysates from cells transiently expressing the indicated PS1 constructs were analysed by immunoblotting for  $\gamma$ -secretase components using N1660, PS1N and 3027 antibody. In Panel D, processing of CD44 $\Delta$ E-Flag was analysed by immunoblotting with antibody 9E10. Panel E, CD44-ICD was detected by immunoprecipitation with anti c-myc agarose and immunoblotting with 9E10 antibody. Asterisk denotes CD44-ICD fragment. Panel F, secreted CD44 $\beta$  peptide was analysed by immunoprecipitation with Flag M2 agarose and immunoblotted with Flag M2 antibody.  $\gamma$ -Secretase components were separated by 10% Tris-glycine-urea SDS-PAGE. CD44<sup>CTFs</sup> and CD44-ICD were separated by 12% Tris-glycine SDS-PAGE. N $\beta$  was separated by 10%-20% Tris-tricine SDS-PAGE.

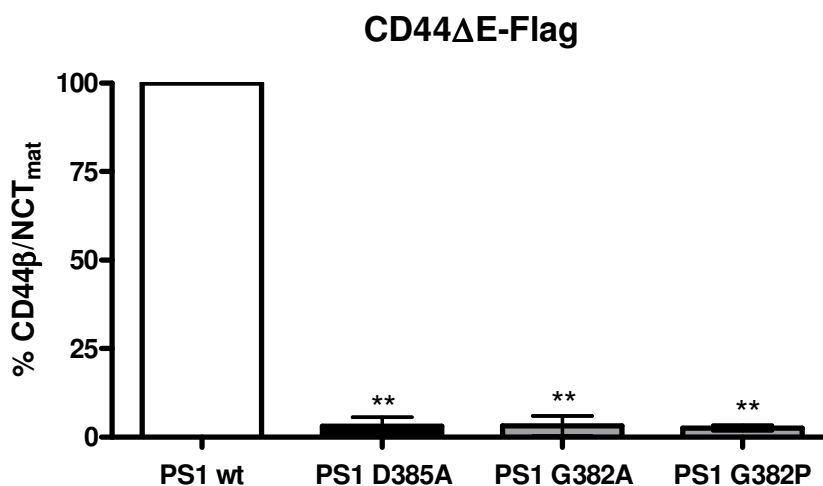


Figure 40: Signal intensity of CD44 $\beta$  produced by PS1 G382A in PS1/PS2  $-/-$  MEF cells. The CD44 $\beta$  band intensities were quantified and normalised by NCT<sub>mat</sub> protein levels. The normalised NICD levels produced by PS1 wt were set to 100%. Data were statistically analysed by one-way ANOVA with Dunnet's post correction test for comparison of multiple samples to a control (PS1 wt) (\*\*  $p < 0.01$ ). The data are representative of three independent experiments ( $n=3$ ).

### ***3.3 Proteasomal turn over of NICD generated by PS1 wt, PS1 G382A and PS1 L383F is similar***

As shown in figure 31 and 32, PS1 G382A supports F-NEXT processing as it produces NICD, but the levels produced by the PS1 G382A mutant are reduced compared to the levels produced by PS1 wt. A much stronger processing reduction was observed for the PS1 L383F mutant where F-NEXT processing was strongly impaired (149). While it is plausible that the mutations reduce the cleavage efficiency of the enzyme, therefore the cleavage product obtained is reduced, another explanation could be that the mutations do not alter the efficiency of the enzyme but rather alter the cleavage site. If that is the case it is possible that the new N-terminal residue is a de-stabilizing residue targeting the resultant cleavage product to the proteasome for degradation according to the "N-end rule" (282) (figure 41). NICD itself is a target for the proteasome (204,283,284). Substitutions at the S3 site of Notch1, such as Notch1 V1744L and Notch1 V1744G were reported to decrease Notch processing and to affect NICD stability by increasing its rate of degradation (285). However, a careful re-examination showed that these mutants have the same rate of degradation as the wild type protein, while the processing rates of these mutants were still significantly lower as those of the wild type protein (286).

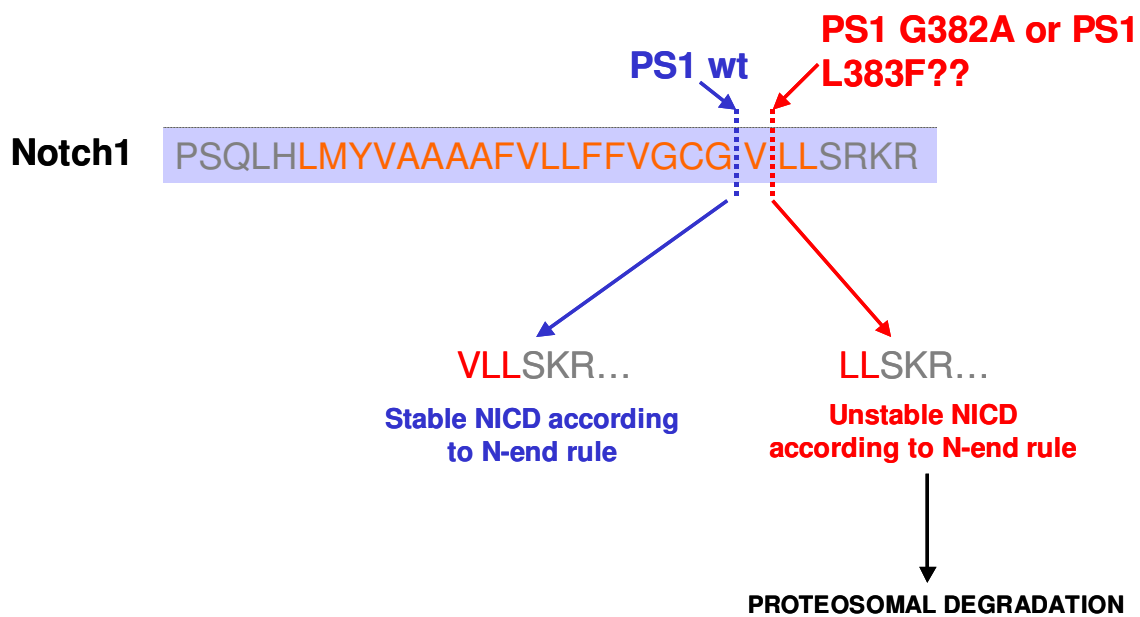


Figure 41: Schematic depiction of an hypothetical alteration of the cleavage site in Notch1 produced by PS1 G382A and PS1 L383F. The amino acids of the TMD of Notch are depicted in orange. PS1 wt site of processing is depicted in blue whereas the hypothetical site of processing of the mutants is depicted in red.

To investigate the possibility whether the NICD produced by the PS1 G382A and PS1 L383F mutants are differently turned over by the proteasome than the NICD produced by PS1 wt, PS1/PS2  $-/-$  MEF cells were transiently co-transfected with the cDNA encoding for F-NEXT and with the cDNAs encoding for PS1 wt, PS1 G382A, PS1 D385A and vector alone (figure 42) as well as with the H<sub>6</sub>X-tag versions of PS1 wt, PS1 D385A and PS1 L383F (figure 43). Cells were treated with lactacystin, a well-characterized proteasome inhibitor (269) for 5 hours. Following transfection and inhibitor treatment, total cell lysates were analysed as before.  $\beta$ -Catenin was immunoblotted as independent control to monitor the increase in levels of  $\beta$ -catenin upon proteasome inhibitor treatment (figure 42 and figure 43, panel F) (287). All proteins were robustly expressed. As before, PS1 were endoproteolysed except for the PS1 D385A mutant and maturation of NCT was observed demonstrating correct  $\gamma$ -secretase complex formation (figure 42 and figure 43, panels A, B and C). As expected, PS1 wt, PS1 G382A and PS1 L383F mutants processed F-NEXT to NICD with significant difference in efficiency (figure 42 and figure 43 panels D and E). When PS1 wt, PS1 G382A and PS1 L383F were treated with the proteasome inhibitor, an increase in the holoprotein was observed (137) but not in the PS1<sub>NTF</sub> and PS1<sub>CTF</sub> as they form part of a stable and active  $\gamma$ -secretase complex (figure 42 and figure 43 panels B and C) (137). Upon proteasome inhibitor treatment, NICD levels were increased in PS1 wt, PS1 G382A and PS1 L383F mutants. The increase of NICD observed in PS1 G382A and PS1 L383F is, however, similar as the one observed for PS1 wt, suggesting that the

NICDs generated by the mutants are similarly degraded as PS1 wt (figure 42 and figure 43, panels D and E). Therefore the reduced amount of NICD produced in the PS1 G382A and PS1 L383F mutants is most probably due to a reduced activity of the enzyme.

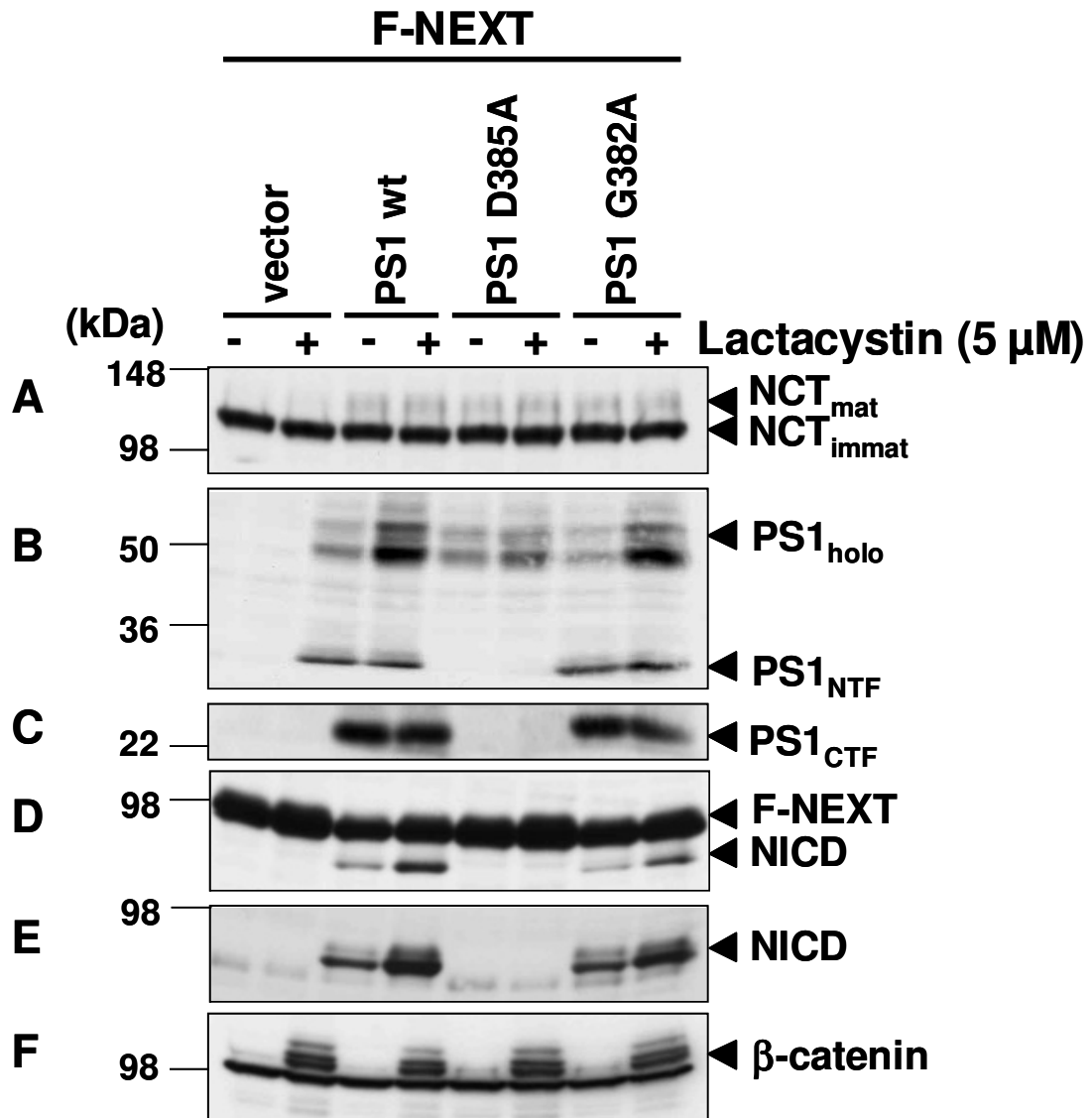


Figure 42. PS1 G382A mutant does not miscleave the substrate. In panels A, B and C, lysates from cells transiently expressing the above PS constructs and F-NEXT as substrate were analysed by immunoblotting for  $\gamma$ -secretase components using N1660, PS1N and 3027 antibody. In Panel D, processing of F-NEXT was analysed by immunoblotting with antibody 9E10. Panel E, NICD was detected by cleaved Notch1 antibody. Panel F,  $\beta$ -catenin was analysed by anti- $\beta$ -catenin antibody.  $\gamma$ -Secretase components were separated by 10% Tris-glycine-urea SDS-PAGE. F-NEXT and NICD were separated by 7% Tris-glycine SDS-PAGE as well as  $\beta$ -catenin.

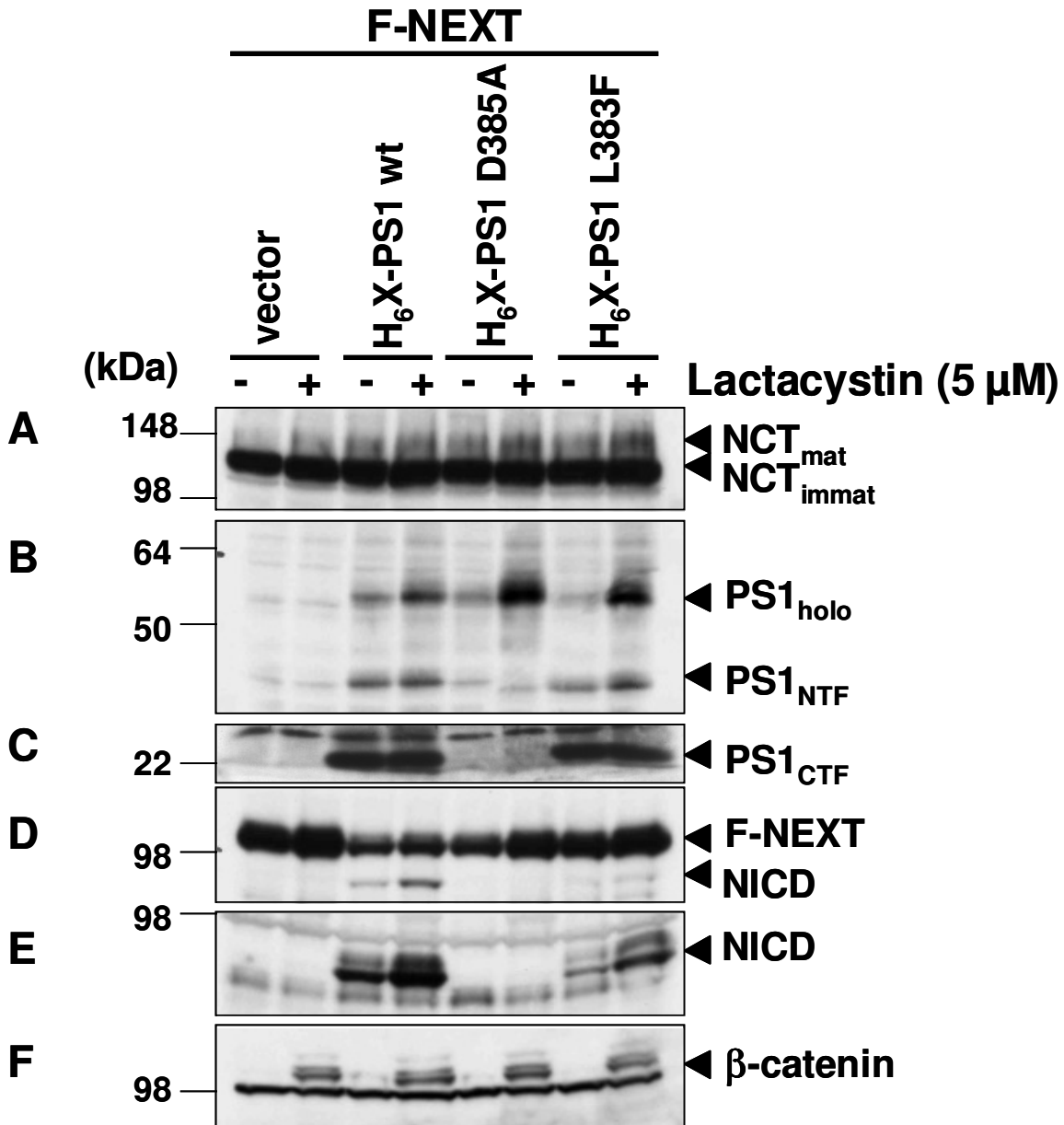


Figure 43. PS1 L383F does not miscleave F-NEXT. Panels A, B and C, lysates from cells transiently expressing the indicated PS1 constructs and F-NEXT as substrate were analysed by immunoblotting for  $\gamma$ -secretase components, using N1660, PS1N and 3027 antibody. In Panel D, processing of F-NEXT was analysed by immunoblotting with antibody 9E10. Panel E, NICD was detected by cleaved Notch1 antibody. Panel F,  $\beta$ -catenin was analysed by anti- $\beta$ -catenin antibody.  $\gamma$ -Secretase components were separated by 10% Tris-glycine-urea SDS-PAGE. F-NEXT and NICD were separated by 7% Tris-glycine SDS-PAGE as well as  $\beta$ -catenin.



## 4 Discussion

In order to study the role of the N-terminal glycine of the GxGD motif in PS1 a mutagenesis approach was used. The N-terminal glycine was mutated to alanine, isoleucine, proline, tryptophan, lysine, and aspartate to cover a wide range of diverse side chains. Once the mutants were created the role of PS1 G382 in  $\gamma$ -secretase assembly and activity was studied.

### ***4.1 Most of the PS1 G382 mutants inhibit PS1 endoproteolysis***

As judged from the normal NCT maturation,  $\gamma$ -secretase complex assembly was found to be normal for all PS1 G382 mutants. Maturation of NCT only takes place when the  $\gamma$ -secretase components are correctly assembled, allowing the complex to leave the ER and to traffic to the Golgi apparatus where NCT becomes fully mature by complex glycosylation (figure 15) (154,289-291). These data demonstrate that PS1 G382 mutants do not disturb  $\gamma$ -secretase assembly. Surprisingly, however, none of the PS1 G382 mutants supports PS1 endoproteolysis with the exception of PS1 G382A (figure 15). Clearly, the impaired endoproteolysis is not due to an incorrect  $\gamma$ -secretase complex formation. Rather it is more likely that PS1 G382 mutants do not go endoproteolysis due to a structural change in the molecule that affects this autocatalytic mechanism. Similar observations have been made previously for other mutations in the GxGD motif like PS1 G384K and PS1 G384D, in the PALP motif, in the TMD1 of PS, and in the C-terminus of PS which have been reported to impair this autocatalytic activity probably by distorting PS conformation (292-294). This result suggests that PS1 G382 is an important determinant for PS endoproteolysis. Only minor changes of this residue from glycine to alanine are accepted for PS endoproteolysis.

## **4.2 PS1 G382A has reduced $\gamma$ -secretase activity possibly due to a distorted docking site**

### **4.2.1 PS1 G382 mutants are inactive regarding APP processing except PS1 G382A mutant**

Most PS1 G382 mutants do not support  $\gamma$ -secretase activity in APP processing. The only exception found was PS1 G382A, in both HEK/sw cells and in *in vitro* assays (figure 15 and 17). The PS1 G382A mutant rescues the accumulation of APP<sub>CTFs</sub> observed in the aspartate mutant and can secrete A $\beta$  to the conditioned media. Nevertheless its activity is lower in comparison to PS1 wt (figure 15). Similar results were observed *in vitro* where no endogenous  $\gamma$ -secretase complex could interfere with the results as PS1 G382  $\gamma$ -secretase mutant complexes were isolated by immunoprecipitation against the Xpress epitope (figure 17) and in PS1/PS2  $-/-$  MEF cells where PS1 G382A is able to process APP (figure 29). These results suggest that a minor change within this motif is accepted for APP processing.

Because the PS1 G384A mutant alters the specificity of the  $\gamma$ -cleavage increasing A $\beta$ 42 levels (148), it was investigated if the PS1 G382A mutant also alters the specificity of the  $\gamma$ -cleavage. Indeed, PS1 G382A increased A $\beta$ 38 and slightly A $\beta$ 42 production and produced a longer A $\beta$  species, A $\beta$ 43 (figure 18 and figure 20). This suggests that the PS1 G382A mutation may cause a conformational alteration in PS1, which effects an alteration of the specificity of the  $\gamma$ -cleavage.

### **4.2.2 PS1 G382A has an altered response to NSAIDs**

It has been widely assumed that A $\beta$ 38 and A $\beta$ 42 production by  $\gamma$ -secretase are coupled since NSAIDs effect a decrease in A $\beta$ 42 and a concomitant increase in A $\beta$ 38 and vice versa (233,270). The PS1 G382A mutant can be regarded as an artificial FAD mutation as A $\beta$ 42 and A $\beta$ 43 levels are elevated in comparison to PS1 wt (figure 18 and 19). Surprisingly, from the three NSAIDs tested (sulindac sulfide, flurbiprofen and naproxen) and the lipid-regulating drug fenofibrate, only with sulindac sulfide and fenofibrate PS1 G382A had a similar response as PS1 wt (figure 22 and 26). Interestingly, fenofibrate

markedly increased A $\beta$ 43 species production in PS1 G382A (figure 25 and figure 28). On the other hand, PS1 G382A had an altered response to flurbiprofen and naproxen compared to PS1 wt. For both NSAIDs, PS1 G382A can cause a decrease in A $\beta$ 38 and A $\beta$ 42 levels with a concomitant increase in A $\beta$ 40 levels (figure 22 and 26). Interestingly, naproxen, which was believed to be an inactive  $\gamma$ -secretase modulator (233), can cause a slightly increase in A $\beta$ 38 and A $\beta$ 37 levels in PS1 wt overexpressing cells (figure 26 and figure 27). This suggests that naproxen is a GSM only modulating the production of short species. Taken together, these data show that A $\beta$ 38 and A $\beta$ 42 production are not coupled.

This uncoupled production has recently been also observed in FAD mutants of PS1 and for the PS2 FAD mutation N141I (277-279). Both studies showed that strong FAD mutations are partially insensitive to  $\gamma$ -secretase inhibitors and unresponsive to the A $\beta$ 42 modulatory effect of NSAIDs (279,295,296). However, they still responded to the A $\beta$ 38 modulatory effect of the NSAID investigated (277,278).

Fluorescence resonance energy transfer (FRET) experiments have suggested that NSAIDs affect the conformation of PS and the proximity of APP and PS (237). In addition, FAD mutations have also been shown to alter the structure of the active site by changing the proximity of the PS<sub>NTF</sub> and PS<sub>CTF</sub> (237). It is then plausible that PS1 G382A mutant alters the PS conformation causing an alteration in the cleavage specificity of  $\gamma$ -secretase, thereby increasing the amount of A $\beta$ 38 A $\beta$ 42 and A $\beta$ 43 (Figures 18–20). This conformational change thereby may also affect the binding and modulation of  $\gamma$ -secretase by NSAIDs. Some NSAIDs modulate the  $\gamma$ -secretase activity of PS1 G382A but less efficient as in the wild type situation (sulindac sulfide and the lipid-regulating drug fenofibrate) whereas some other NSAIDs (flurbiprofen and naproxen) modulate the PS1 G382A  $\gamma$ -secretase activity in a completely different way as for PS1 wt.

The molecular mechanism of GSMs action on  $\gamma$ -secretase has not been elucidated yet. One possible mode of action can be that the GSMs slightly misplace the substrate in the catalytic center by changing PS conformation thus causing changes in the cleavage specificity of  $\gamma$ -secretase (see figure 44 panel B). In PS1 mutants, the substrate is likely already misplaced due to a distorted PS conformation (see figure 45 panel A). GSM treatment of PS1 mutants could further distort the conformation, depending on the particular GSM and the particular PS1 mutant present and gives rise to an additional

alteration of the cleavage specificity of the enzyme for the substrate (see figure 47 panel B).



Figure 44. Schematic depiction of potential conformational changes of PS wt upon GSMs treatment. In green are the TMD carrying the critical aspartates. The substrate is depicted in orange. The normal placement of the substrate in the protease is shown (A). In response to GSMs, PS wt changes its conformation causing misplacement of the substrate (B).



Figure 45. Schematic depiction of potential conformational changes of PS mutant in response to GSMs treatment. In green are the TMD carrying the critical aspartates. The substrate is depicted in orange. In A, in PS1 mutants the conformation of the protease is changed misplacing the substrate. In response to GSMs, PS mutants change their conformation further misplacing the substrate (B).

#### 4.2.3 PS1 G382A processes APP and Notch1-3 homologues but not Notch4 and CD44

Because it was found that all PS1 G382 mutants (except PS1 G382A) did not allow APP processing, it was next investigated whether other substrates behaved similarly. PS1/PS2  $-/-$  MEF cells were used to further confirm the results obtained in section 3.1.1. In addition, PS1 G382 mutants undergo normal  $\gamma$ -secretase complex formation in PS1/PS2  $-/-$  MEF cells as NCT maturation was observed. Again, however, except for the PS1 G382A mutant, no endoproteolysis was observed (figures 29,31,33,35,37 and 39) confirming the results obtained in HEK/sw cells (figure 15). In terms of  $\gamma$ -secretase activity PS1 G382A

mutant is able to cleave APP and Notch1-3 homologues although less efficient as PS1 wt (figures 29-36). On the other hand, strikingly, PS1 G382A was unable to process Notch4 and CD44 (figures 37-40) suggesting that for some substrates, a small side chain is accepted and their processing can occur (APP and Notch1-3). For some other substrates, however, (Notch4 and CD44), a glycine in position 382 is indispensable for their processing and not even a minor side chain change is accepted. These results point to a necessity to provide as less steric hindrance as possible in this region and suggests that this residue must be as small as possible to allow the accommodation of the many PS substrates, which all differ in their transmembrane domains, at the active site region. Because glycine does not have any lateral side chain, this amino acid minimizes possible steric hindrance effects allowing that all  $\gamma$ -secretase substrates can be efficiently bound and processed.

#### **4.2.4 NICD generated by PS1 G382A and PS1 L383F mutants have a similar proteasomal turn over**

The subtle change in the protein conformation due to the PS1 G382A mutation may affect the velocity of the enzyme causing a slow turn over of the substrate. In fact, this is the case as the processing of APP and Notch1-3 is somewhat diminished in the PS1 G382A mutant (see figure 17 and figures 29-36). Another mutation within the GxGD motif, the PS1 L383F mutant has been shown to strongly impair Notch processing (149). Because NICD is a substrate for proteasomal degradation, the observed reduction in both mutants could potentially be due to a miscleavage of the substrate at S3 exposing a new destabilizing N-terminal residue of the NICD (figure 41). According to the N-end rule, the half-life of a protein is determined by the nature of its N-terminal amino acid, as a destabilizing N-terminal residue will affect the rate of proteasomal degradation of the peptide (282). As observed in figure 42 and figure 43 an increase of NICD is detected upon lactacystin treatment in PS1 wt, PS1 G382A and PS1 L383F. The increase of NICD observed in the mutants is similar as the one observed for PS1 wt suggesting that the NICDs produced by these two PS1 mutants have a similar proteasomal turn over as the NICD produced by PS1 wt. This suggests that PS1 G382A and PS1 L383F do not miscleave the substrate in the S3-site but rather in the  $\gamma$ -site as both mutants changes the ratio of A $\beta$ 43/A $\beta$ 42 to A $\beta$ 40 (figure 18-20 and Yamasaki *et al*, unpublished observations). These results suggest that the reduction in the catalysis of the  $\gamma$ -secretase substrates observed in these two mutants of the GxGD motif is due to a reduced activity of the

enzyme. This reduced activity could be because the mutations influence the active site conformation thus slowing the catalysis.

#### **4.2.5 PS1 G382 may form part of the $\gamma$ -secretase substrate docking site**

The slow turnover of the substrate by the PS1 G382 mutant may be also because the mutation affects the docking site thereby reducing the affinity of the enzyme for its substrate. Preliminary co-immunoprecipitation experiments, inactive PS1 G382 mutants have less substrate associated to the enzyme in comparison to an active site mutant (PS1 D385A) (data not shown). It is very unlikely, however, that PS1 G382  $\gamma$ -secretase mutants have an impact on the ability of NCT to bind the substrates because NCT (figure 46 blue) does only recognize the free amino terminal residue from shedded substrates (e.g. the APP CTFs) as first recognition step (figure 46 panel B) (165). The shedded substrate is then transferred to the docking site in PS (2) (depicted in yellow) where it binds before the substrate translocates to the active site (depicted in red) where it is processed (4). Helical ten amino acid peptide inhibitors based on the TMD of APP were shown to inhibit  $\gamma$ -secretase apparently by binding to its docking site (224). Interestingly, an extension of three extra amino acids resulted in an inhibition of  $\gamma$ -secretase by binding to its docking and active site (224). This result suggests that the docking and active site are very close, within a distance of three amino acids, and partially overlapping (224). In the case of the PS1 G382 mutants (figure 46 panel B), NCT also recognizes the shedded substrate (1) and transfers it to a distorted docking site (2). If the PS1 G382 mutants distort the docking site, the affinity of the enzyme for its substrate will be impaired (figure 46 panel B). In the case of the PS1 G382A mutant, the docking site is not extremely altered, therefore the enzyme retains affinity for some substrates allowing to a considerable extent their processing (APP, Notch1-3). For other substrates, the enzyme would not retain any affinity so they will dissociate from the enzyme and thus not being processed (Notch4 and CD44) (figure 46 panel B). The reason why for some substrates the PS1 G382A retain some affinity and not to some others is currently unclear and will need further studies to be solved.

Recent evidence suggests that the GxGD motif has a dual role in PS. This motif contributes on one side to the catalytic function of the enzyme by the active site aspartate and the glycine preceding it (143-145)(148), and on the other side to substrate discrimination by the amino acid in position x (149). These two functions are probably

overlapping (149). Preliminary results suggest that this motif contributes to the substrate docking site. Changes within this motif will affect the proposed roles of the GxGD motif. PS has a variety of substrates with different transmembrane domains. In order to accommodate all of them at the active site region, the docking site must have certain sequence requirements. Since glycine's side chain is a hydrogen atom, it is the optimal amino acid to minimize possible steric hindrance effects enabling that all  $\gamma$ -secretase substrates are effectively bound prior to their processing.

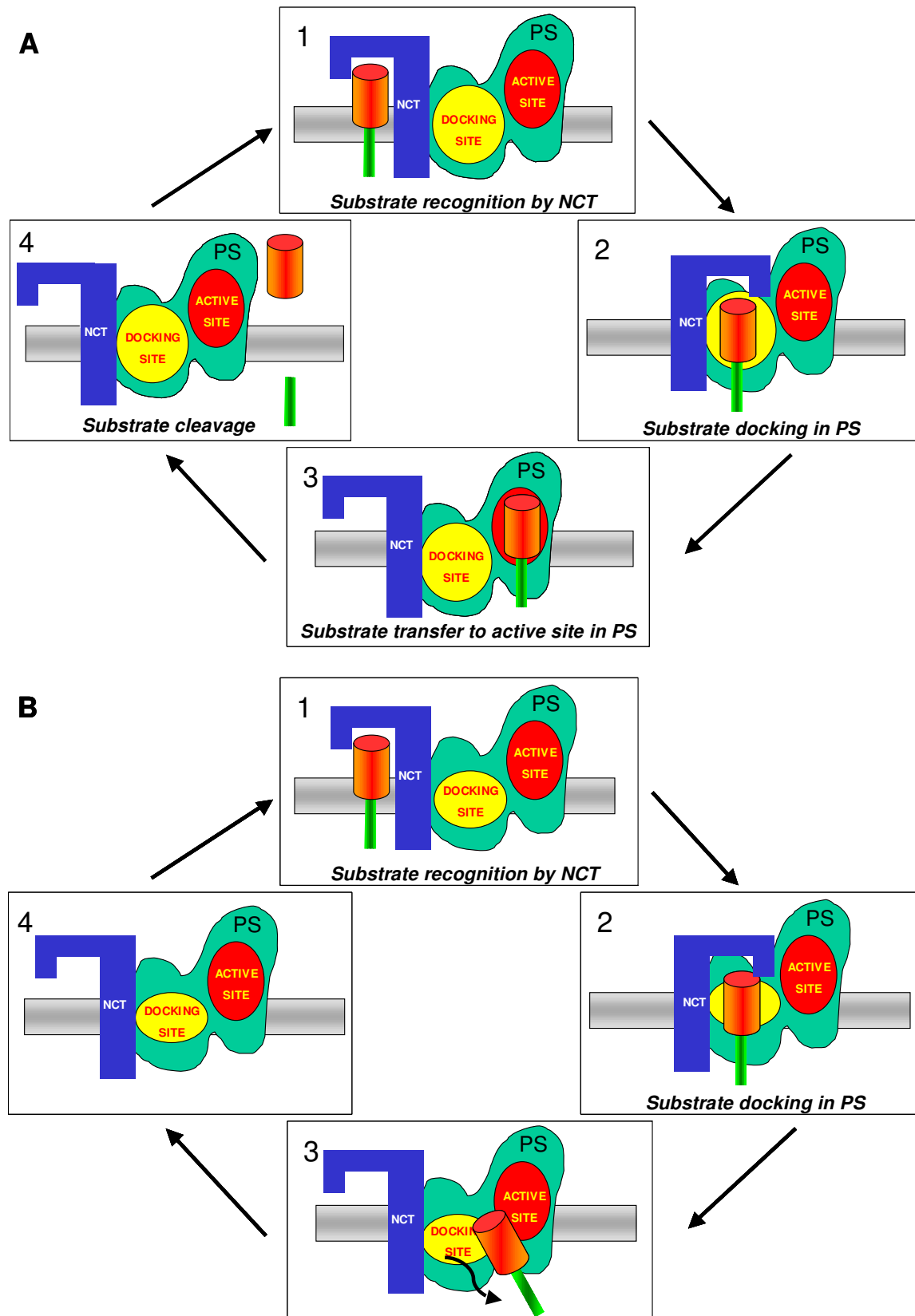


Figure 46. Schematic representation of the hypothetical substrate binding and processing in PS1 wt (panel A) and in PS1 G382 mutants (panel B).



### 4.3 Putative structural placement of PS1 G382

Recently, the crystal structures of two intramembrane proteases have been elucidated, the rhomboid structure (297-301) and the S2P structure (302). These structures have shown that the substrate entry mechanism may be conserved in these intramembrane proteases.

Rhomboid is an intramembrane serine protease (303) whose structure has been revealed to be a horseshoe structure (304) that allows the substrate to enter laterally to the active site for its processing. The active site is formed by  $\alpha$ -helix 6 and  $\alpha$ -helix 4.  $\alpha$ -Helix 4 carries the critical serine residue and is tilted inside within the membrane (297-301). For S2P, a horseshoe structure has been also observed allowing the substrate to enter laterally. The active site in S2P is formed by three  $\alpha$ -helices, which are also tilted within the membrane. Interestingly, in  $\alpha$ -helix 3 a putative dimerization motif is observed (AG/xxxN/S/G) which may help to stack these three helices together. This motif is also believed to form part of the active site as mutagenesis of the N-terminal glycine is predicted to perturb the conformation of the active site due to steric hindrance (302).

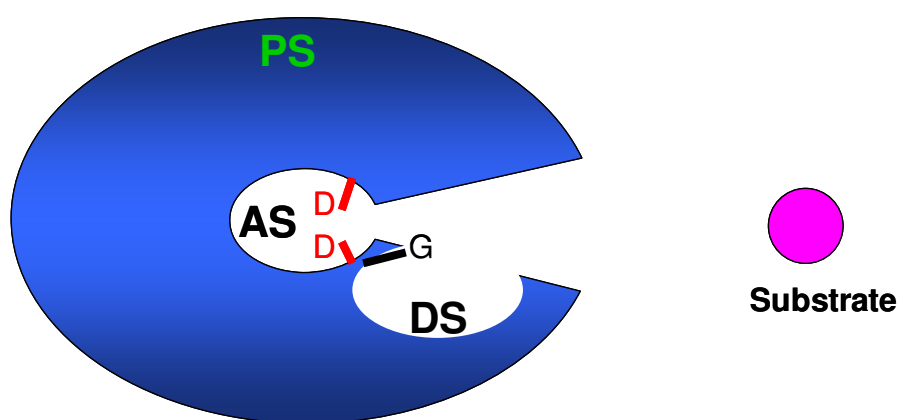


Figure 47. Schematic model of a hypothetical horseshoe-like structure of PS (top view). The substrate (pink) will first bind to the docking site (DS) to which G382 (depicted in black) might contribute. From there, the substrate may enter laterally to the active site of PS (AS) where the critical aspartes (depicted in red) are located.

It is possible and likely that the intramembrane proteases have a common substrate entry mechanism. Therefore, the substrates for PS can also enter laterally as the substrates for Rhomboid and S2P do (see figure 47). For being processed, the substrates must enter laterally, binding first to the docking site and then move to the active site. If PS1 G382 of the GxGD motif in PS plays a role in the docking site, the TMD7 is unlikely to be in a perfect helix conformation spanning the membrane, but more tilted inside the membrane.

If TMD7 is tilted inside the membrane, then glycine 382 of the PS1 GxGD motif is exposed more outside (see figure 48) being the first amino acid of the GxGD motif to have a contact with the substrate. This event will allow PS1 G382 to take part in the formation of the docking site for the substrate. If PS1 G382 forms part of the substrate docking site, it may allow conformational flexibility of the docking pocket and less steric impediments for the different TMDs of the many  $\gamma$ -secretase substrates due to the presence of the smallest possible side group: the hydrogen atom. Changes in this region, even subtle ones, will restrict the flexibility of the docking pocket and will provoke more steric hindrances for the substrates. These steric hindrances may affect the affinity of the enzyme for the substrate close to the active site such that some substrates can be processed while others not (see figure 46 panel B). Nevertheless, the internal structure of  $\gamma$ -secretase still has not been elucidated so it is not known whether the TMD7 of PS is indeed tilted inside the membrane or whether it has a funnel-like structure as it has been suggested by others (130).

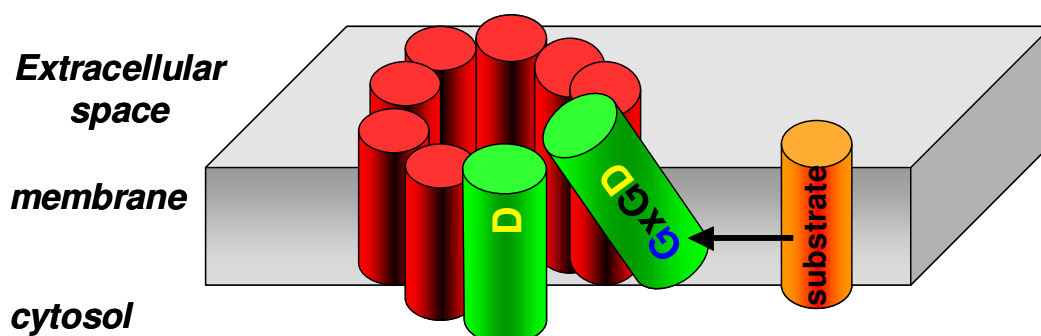


Figure 48. Schematic depiction of PS with TMD7 tilted inside the membrane. TMDs of PS molecule are depicted in red. TMD6 and TMD7 are depicted in green. Critical aspartates are shown in yellow. Substrate is depicted in orange.

The N-terminal glycine of the GxGD motif is conserved in all GxGD aspartyl protease families and is also suggested in this study to be functionally conserved in SPP as its mutation significantly reduces the activity of the protease (data not shown). However, whether the N-terminal glycine mutations distort the active site enabling the activity or enabling the putative similar substrate docking site in SPP may need deeper studies.

There are some exceptions found in the conserved GxGD motif within the TFPP family, in the bundle-forming prepilin peptidase (BfpP) from *E.coli* (248) and in the Archaea

*Methanosphaera stadtmanae*, *Methanothermobacter thermautotrophicus*, *Pyrococcus abyssi*, *Pyrococcus furiosus*, *Pyrococcus horikoshii* and *Thermococcus kodakarensis* (305). However, in these cases, the N-terminal amino acid found in the GxGD motif is an alanine again implying the importance for this region to have the less steric hindrance and is consistent with the findings reported here. As shown in this study, the side chain of alanine is a methyl group and the length of this methyl group is the maximal length tolerated for this residue. All of the larger side chains cause an inactivation of the enzyme.

#### **4.4 PS1 G382 may form part of a putative helix-packing motif**

Glycines residues that are present in the membrane-spanning helices usually do not disrupt the secondary structure and are known to support efficiently helix-packing in polytopic membrane proteins (306,307). Interestingly, PS1 and PS2 have a conserved helix-packing motif GxxxG in TMD7, of which PS1 G382 is the C-terminal residue. The GxxxG motif has been shown to promote helix-packing in polytopic membrane proteins as well as to promote dimerization (308). In general, a helix-packing motif requires a small side chain amino acid (glycine, alanine, serine, threonine or proline) followed by three aliphatic amino acids and finally another small side chain amino acid (309,310). This GxxxG motif has also been found in APP suggesting that APP can form a dimer. Interestingly, the replacement of the glycines in this motif lead to an attenuation of APP dimerization altering the  $\gamma$ -cleavage by reducing the levels of A $\beta$ 40 and A $\beta$ 42 but without altering the  $\epsilon$ -cleavage (311,312). APH-1 also carries a GxxxG motif, which has been shown to be important for the stable association of APH-1 in the  $\gamma$ -secretase complex (313-316).

It is maybe possible that PS1 G382 contributes to packing of TMD7. Alanine also supports the close packing of helical proteins (307), explaining why the alanine is tolerated in this position. The introduction of an alanine will thus create a GxxxA, which is a GxxxG-like motif, compatible with TMD packing (317). The close packing of two helices in polytopic membrane proteins opens up interhelical regions that become more loosely packed. These regions can contain polar residues and can provide the binding sites for substrates and ligands (307). So it might be, that due to the packing motif to which G382 might take part, a cavity or pocket is formed in which the substrates are pre-bound prior to its processing.

One has to note, however, that this GxxxG motif of TMD7 is not found in all the members of the PS family. In *C.elegans*, the PS homologues HOP-1 (homologue of PS 1) and SPE-4 (spermatogenesis defective) do not have the GxxxG motif, whereas it is found in Sel-12 (Suppressor/Enhancer of Lin-12) another *C.elegans* homologue. HOP-1 has a TxxxG motif, which is sometimes found in helix-packing motifs in a variety of proteins like receptor Erb-3 (318) and in EGFR and Ros (309). Furthermore, no helix-packing motif is found in SPP family members as they have a FxxxG (SPP, SPPL2b and SPPL3) or VxxxG motif (SPPL2a). SPP family members are believed to be active without any additional proteins (246). It might be, thus, that this motif is only present in proteins that form complexes with other proteins. This motif would be then needed for interaction the substrate APP that also has a GxxxG motif (312) or maybe is important for the complex association with APH-1 (313). On the other hand, proteins that are in a complex might need to be closer packed than proteins that work as monomer and are not part of a complex. Regarding PS, the insertion of a big side amino acid in this motif may avoid the close packing, disrupting the self-catalysis of PS and the active conformation, however, this would cause disrupt complex formation, which is not observed.

#### **4.5 The GxGD and PALP motif may be located close together in PS**

Apart from the conserved motif GxGD, PS has another conserved motif, the PALP motif in TMD9 (see figure 49). This motif comprises amino acid 433-436 of PS1. Interestingly, this motif is also found in all other GxGD-type aspartyl proteases, such as the SPP/SPPL and TFPP families, where a PxL motif is conserved (244,246). In PS1, mutations in the PALP motif impair the endoproteolysis and depending of the mutation inhibit  $\gamma$ -secretase activity (294). The PALP motif has been suggested to contribute to a stable active site conformation of PS because mutations in this motif do not allow the binding of a transition state analogue inhibitor (294).

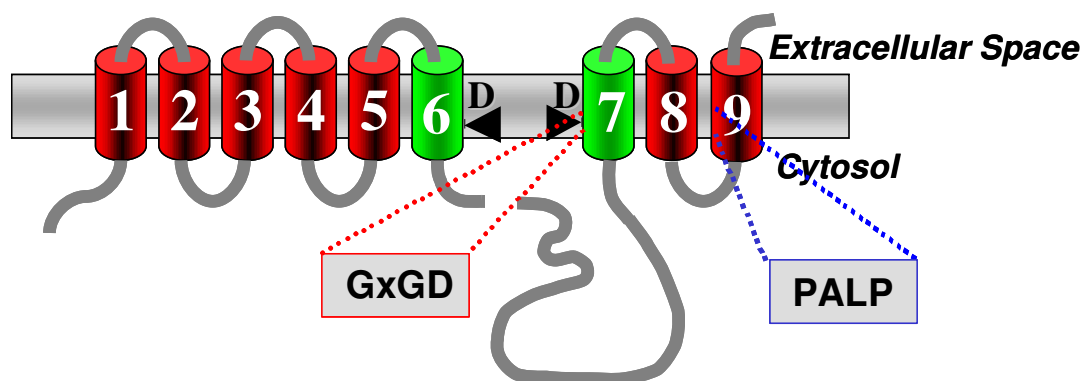


Figure 49: Schematic depiction of the PS molecule showing the conserved GxGD and PALP motifs.

Changes in the N-terminal proline (P433) of the PALP motif, result in an impairment of PS1 endoproteolysis (294) except for the PS1 P433A mutation. Interestingly, this mutant can also support APP and Notch1 processing (294). These observations are similar to PS1 G382A and PS1 P433A where only a small side chain of amino acid is tolerated for endoproteolysis and activity, suggesting that in both positions a very small side chain is required. Furthermore, both mutants behave similar to NSAIDs. PS1 433A and PS1 G382A have a typical NSAID response to sulindac sulfide, whereas flurbiprofen decreases A $\beta$ 42 to the same extent as PS1 wt but strongly decreases A $\beta$ 38 levels (Tomioka *et al*, unpublished observation).

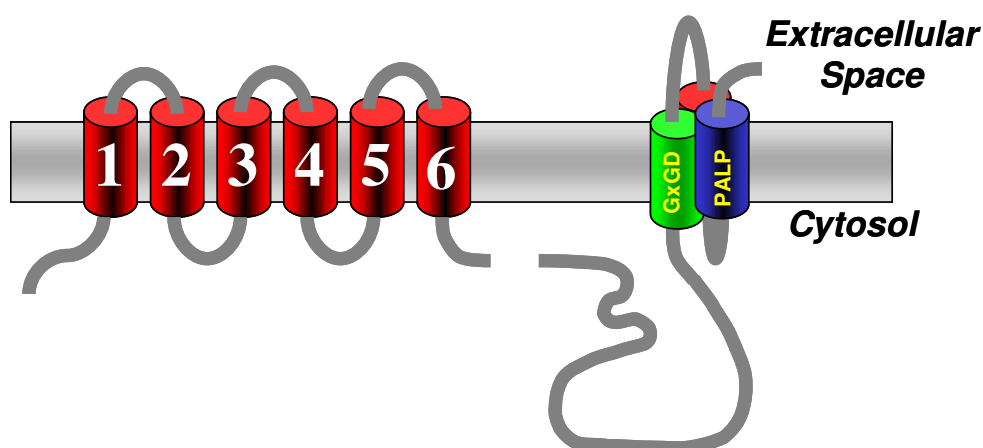


Figure 50. Schematic depiction of the PS with a hypothetical structure of the last three transmembrane domains. TMD7 containing the GxGD motif is in green and TMD9 with its PALP motif is in blue.

Although this PALP motif is found distant from the GxGD motif in the primary sequence, it might be close to the GxGD motif in the tertiary structure of PS (see figure 50). This would

be supported by the similar behaviours upon mutation of the motifs (294). This would suggest that both PALP and GxGD motifs are very close together. Furthermore, the PS1 A431 of the PALP motif might form part of the helix-packing motif AxxxSxxxG (319). Thus, it is possible that due to the both helix-packing motifs found in TMD7 and TMD9 these two TMD are close together taking both part of the active site conformation of the complex. Changes in one of these two motifs might affect the conformation of the other, and vice versa distorting the active site conformation of PS in a similar way.

Interestingly, a recent work has reported new results indicating that the GxGD motif and the PALP motif might be indeed close together, both forming part of the catalytic pore (320).

## **4.6 Outlook**

Taken together, the mutational analysis data of the G382 residue in PS1 presented in this thesis, demonstrate the crucial importance of this glycine for the activity of  $\gamma$ -secretase. Preliminary results suggest this residue as a possible element of the substrate docking site. To further confirm that G382 forms part of the docking site of the protease, Co-IP experiments with substrates that are not cleaved in the PS1 G382A mutant could be performed in order to confirm whether these substrates are bound to the complex or not. It will be also very helpful to investigate the binding capacity of helical-peptide inhibitors that are believed to bind to the docking site of the substrate (224). If PS1 G382 is involved in the docking site formation, the binding of these helical-peptide inhibitors is expected to be altered.

To further address the question why PS1 G382A mutant retains some affinity to certain  $\gamma$ -secretase substrates and not to others, additional substrates should be analysed. This may also give information about the sequence requirements of the TMD of the different substrates to be able to be cleaved by the protease.

Fluorescence resonance energy transfer experiments can be performed in order to investigate whether PS1 G382 mutants change the PS conformation by altering the distance between PS1<sub>CTF</sub> and PS1<sub>NTF</sub> as observed previously for FAD mutants.

To prove the slower rate of the mutant enzyme a kinetic study of the mutant enzyme should be performed. For these studies, purified  $\gamma$ -secretase and substrate are required.

Finally, to further evaluate whether PS1 G382 also forms part of a helix-packing motif a mutagenesis approach should be used mutagenizing both glycines of the GxxxG motif to investigate if  $\gamma$ -secretase assembly is impaired or if an alteration of PS conformation is observed which might have repercussions in the catalytic activity of the enzyme.

## 5 Summary

$\gamma$ -Secretase catalyses the final processing step of the  $\beta$ -amyloid precursor protein (APP) and thereby generates the AD-causing amyloid  $\beta$ -peptide ( $A\beta$ ) as well as the APP intracellular domain (AICD). Apart from APP,  $\gamma$ -secretase has more than 20 known substrates. These are type I membrane proteins that undergo ectodomain shedding to become a  $\gamma$ -secretase substrate.  $\gamma$ -Secretase is a multimeric complex formed of four essential subunits, presenilin (PS), nicastrin (NCT), anterior pharynx defective 1 (APH-1) and presenilin enhancer 2 (PEN-2). PS1 and PS2 are the catalytic subunit of  $\gamma$ -secretase and provide the catalytically active aspartates located in transmembrane domains (TMD) 6 and 7. NCT has been shown to act as a  $\gamma$ -secretase substrate receptor by recognizing the free amino terminus of the shedded substrate. Following NCT binding, the substrate is believed to translocate to the postulated docking site that has been shown in PS1 to be within three amino acid distance to the critical aspartate in PS1 TMD7. PS is an unusual aspartyl protease, with a novel GxGD active site motif, which is also found in other aspartyl proteases such as SPP and TFPP. The functional characterization of the GxGD motif has only been partially addressed so far. Mutational analysis of the glycine neighbouring the critical aspartate and the amino acid in position x in PS1 have shown that this motif is important for the activity of the enzyme as well as for substrate (APP/Notch) selectivity. To further characterize this conserved motif an extensive mutational analysis of the N-terminal glycine was performed in PS1.

The following results were obtained: 1) PS1 G382 is not critical for  $\gamma$ -secretase complex formation. All the PS1 G382 mutants investigated support normal  $\gamma$ -secretase complex formation as judged from the normal maturation of NCT that is observed for all PS1 G382 mutants. Surprisingly, none of the PS1 G382 mutants could support endoproteolysis of PS1 except the PS1 G382A mutant. This shows that PS1 G382 is important for endoproteolysis of PS and that PS endoproteolysis requires a small side chain amino acid in this region of the enzyme.

2) PS1 G382 mutants do not support APP cleavage with the exception of the PS1 G382A mutant, which is partially active and is capable of generating  $A\beta$  and AICD. Furthermore, PS1 G382A increases the generation of  $A\beta_{43}$  and is expected to be a FAD mutation if it occurs in humans. Interestingly, however, also  $A\beta_{38}$  generation is increased. This suggests that PS1 G382A changes the PS conformation altering its cleavage specificity.



3) PS1 G382A has an altered response to NSAID treatment (non-steroidal anti-inflammatory drugs), which have been shown to modulate  $\gamma$ -secretase activity by lowering A $\beta$ 42 species and increasing A $\beta$ 38 species. For some  $\gamma$ -secretase modulators (GSMs) PS1 G382A responds similar to PS1 wt regarding A $\beta$ 38 and A $\beta$ 42 modulation (sulindac sulfide and fenofibrate) whereas for other GSMs (flurbiprofen and naproxen), PS1 G382A has an altered response regarding A $\beta$ 38 and A $\beta$ 42 modulation. Furthermore, A $\beta$ 40 levels are increased by PS1 G382A when treated with flurbiprofen and naproxen. This implies that modulation of A $\beta$ 38 and A $\beta$ 42 generation by GSMs is not coupled as it was initially thought.

4) PS1 G382 mutations have a strong impact on the processing of a number of  $\gamma$ -secretase substrates. Notch1, Notch2 and Notch3 were partially processed by the PS1 G382A mutant. Surprisingly, PS1 G382A did not support the processing of CD44 and Notch4 implicating that changes in this region are accepted for the processing of some but not for all the  $\gamma$ -secretase substrates.

Taken together, the findings in this thesis demonstrate the importance of the GxGD motif in PS1. The conservation of the glycines in the motif in different intramembrane proteases might fulfil the role to restrain the steric hindrance close to the active site in order to allow catalysis of the different substrates.

## 6 References

1. Wancata, J., Musalek, M., Alexandrowicz, R., and Krautgartner, M. (2003) *Eur Psychiatry* 18(6), 306-313
2. Alzheimer, A. (1907) *Allg. Z. Psychiatrie Psychisch-Gerichtl. Med.* 64, 146-148
3. Bertoni-Freddari, C., Fattoretti, P., Casoli, T., Caselli, U., and Meier-Ruge, W. (1996) *Anal Quant Cytol Histol* 18(3), 209-213
4. Scheff, S. W., DeKosky, S. T., and Price, D. A. (1990) *Neurobiol Aging* 11(1), 29-37
5. Grundke-Iqbal, I., Iqbal, K., Tung, Y. C., Quinlan, M., Wisniewski, H. M., and Binder, L. I. (1986) *Proc Natl Acad Sci U S A* 83(13), 4913-4917
6. Al-Bassam, Ozer, R., Safer, D., Halpain, S., and Milligan, R. (2002) *JCB* 157, 1187-1196
7. Drubin, D., and Kirschner, M. (1986) *JCB* 103(December), 2739-2746
8. Goedert, M., Spillantini, M. G., Cairns, N. J., and Crowther, R. A. (1992) *Neuron* 8(1), 159-168
9. Dickson, D. (1997) *J Neuropathol exp Neurol* 56, 321-339
10. Masters, C. L., Simms, G., Weinman, N. A., Multhaup, G., McDonald, B. L., and Beyreuther, K. (1985) *Proc Natl Acad Sci U S A* 82(12), 4245-4249
11. Selkoe, D. J., Abraham, C. R., Podlisny, M. B., and Duffy, L. K. (1986) *J Neurochem* 46(6), 1820-1834
12. Pike, C., Cummings, B., Monzavi, R., and Cotman, C. (1994) *Neuroscience* 63(2), 517-531
13. Goldgaber, D., Lerman, M. I., McBride, O. W., Saffiotti, U., and Gajdusek, D. C. (1987) *Science* 235(4791), 877-880
14. Tanzi, R. E., Gusella, J. F., Watkins, P. C., Bruns, G. A., St George-Hyslop, P., Van Keuren, M. L., Patterson, D., Pagan, S., Kurnit, D. M., and Neve, R. L. (1987) *Science* 235(4791), 880-884
15. Iwatsubo, T., Odaka, A., Suzuki, N., Mizusawa, H., Nukina, N., and Ihara, Y. (1994) *Neuron* 13(1), 45-53
16. Roher, A. E., Lowenson, J. D., Clarke, S., Woods, A. S., Cotter, R. J., Gowing, E., and Ball, M. J. (1993) *Proc Natl Acad Sci U S A* 90(22), 10836-10840
17. Wang, R., Sweeney, D., Gandy, S. E., and Sisodia, S. S. (1996) *J. Biol. Chem.* 271(50), 31894-31902
18. Tsai, J., Grutzendler, J., Duff, K., and Gan, W. B. (2004) *Nature Neurosci.* 7, 1181-1183
19. Walsh, D. M., Klyubin, I., Fadeeva, J. V., Cullen, W. K., Anwyl, R., Wolfe, M. S., Rowan, M. J., and Selkoe, D. J. (2002) *Nature* 416(6880), 535-539.
20. Cleary, J. P., Walsh, D. M., Hofmeister, J. J., Shankar, G. M., Kuskowski, M. A., Selkoe, D. J., and Ashe, K. H. (2005) *Nat Neurosci* 8(1), 79-84
21. Shankar, G. M., Bloodgood, B. L., Townsend, M., Walsh, D. M., Selkoe, D. J., and Sabatini, B. L. (2007) *J Neurosci* 27(11), 2866-2875
22. Arrasate, M., Mitra, S., Schweitzer, E. S., Segal, M. R., and Finkbeiner, S. (2004) *Nature* 431(7010), 805-810
23. Lassmann, H., Weiler, R., Fischer, P., Bancher, C., Jellinger, K., Floor, E., Danielczyk, W., Seitelberger, F., and Winkler, H. (1992) *Neuroscience* 46(1), 1-8
24. Terry, R. D., Masliah, E., Salmon, D. P., Butters, N., DeTeresa, R., Hill, R., Hansen, L. A., and Katzman, R. (1991) *Ann Neurol* 30(4), 572-580
25. Farris, W., Mansourian, S., Chang, Y., Lindsley, L., Eckman, E. A., Frosch, M. P., Eckman, C. B., Tanzi, R. E., Selkoe, D. J., and Guenette, S. (2003) *Proc Natl Acad Sci U S A* 100(7), 4162-4167
26. Iwata, N., Tsubuki, S., Takaki, Y., Shirotani, K., Lu, B., Gerard, N. P., Gerard, C., Hama, E., Lee, H. J., and Saido, T. C. (2001) *Science* 292(5521), 1550-1552

27. Yang, L., Lindholm, K., Yan, R., Citron, M., Xia, W., Yang, X., Beach, T., Sue, L., Wong, P., Price, D. L., Li, R., and Shen, Y. (2003) *Nat Med* 9(1), 3-4
28. Selkoe, D. J. (2001) *Physiol. Rev.* 81(2), 741-766
29. Goate, A., Chartier-Harlin, M. C., Mullan, M., Brown, J., Crawford, F., Fidani, L., Giuffra, L., Haynes, A., Irving, N., James, L., and et al. (1991) *Nature* 349(6311), 704-706
30. Levy-Lahad, E., Wasco, W., Poorkaj, P., Romano, D. M., Oshima, J., Pettingell, W. H., Yu, C. E., Jondro, P. D., Schmidt, S. D., Wang, K., and et al. (1995) *Science* 269(5226), 973-977.
31. Schellenberg, G. D., Bird, T. D., Wijsman, E. M., Orr, H. T., Anderson, L., Nemens, E., White, J. A., Bonnycastle, L., Weber, J. L., Alonso, M. E., and et al. (1992) *Science* 258(5082), 668-671
32. Sherrington, R., Rogaev, E. I., Liang, Y., Rogaeva, E. A., Levesque, G., Ikeda, M., Chi, H., Lin, C., Li, G., Holman, K., and et al. (1995) *Nature* 375(6534), 754-760
33. Jarrett, J. T., Berger, E. P., and Lansbury, P. T., Jr. (1993) *Biochemistry* 32(18), 4693-4697.
34. Selkoe, D. J. (1997) *Science* 275(5300), 630-631
35. Suzuki, N., Cheung, T. T., Cai, X. D., Odaka, A., Otvos, L., Jr., Eckman, C., Golde, T. E., and Younkin, S. G. (1994) *Science* 264(5163), 1336-1340
36. Citron, M., Oltersdorf, T., Haass, C., McConlogue, L., Hung, A. Y., Seubert, P., Vigo-Pelfrey, C., Lieberburg, I., and Selkoe, D. J. (1992) *Nature* 360(6405), 672-674
37. Cai, X. D., Golde, T. E., and Younkin, S. G. (1993) *Science* 259(5094), 514-516
38. Wisniewski, T., Ghiso, J., and Frangione, B. (1991) *Biochem Biophys Res Commun* 180(3), 1528
39. Kang, J., Lemaire, H. G., Unterbeck, A., Salbaum, J. M., Masters, C. L., Grzeschik, K. H., Multhaup, G., Beyreuther, K., and Muller-Hill, B. (1987) *Nature* 325(6106), 733-736
40. Robakis, N. K., Ramakrishna, N., Wolfe, G., and Wisniewski, H. M. (1987) *Proc Natl Acad Sci U S A* 84(12), 4190-4194
41. Lemere, C. A., Blusztajn, J. K., Yamaguchi, H., Wisniewski, T., Saido, T. C., and Selkoe, D. J. (1996) *Neurobiol Dis* 3(1), 16-32
42. Mann, D. M., Pickering-Brown, S. M., Siddons, M. A., Iwatsubo, T., Ihara, Y., Asami-Odaka, A., and Suzuki, N. (1995) *Neurosci Lett* 196(1-2), 105-108
43. Rovelet-Lecrux, A., Hannequin, D., Raux, G., Le Meur, N., Laquerriere, A., Vital, A., Dumanchin, C., Feuillet, S., Brice, A., Vercelletto, M., Dubas, F., Frebourg, T., and Campion, D. (2006) *Nat Genet* 38(1), 24-26
44. Borchelt, D. R., Thinakaran, G., Eckman, C. B., Lee, M. K., Davenport, F., Ratovitsky, T., Prada, C. M., Kim, G., Seekins, S., Yager, D., Slunt, H. H., Wang, R., Seeger, M., Levey, A. I., Gandy, S. E., Copeland, N. G., Jenkins, N. A., Price, D. L., Younkin, S. G., and Sisodia, S. S. (1996) *Neuron* 17(5), 1005-1013
45. Borchelt, D. R., Ratovitski, T., van Lare, J., Lee, M. K., Gonzales, V., Jenkins, N. A., Copeland, N. G., Price, D. L., and Sisodia, S. S. (1997) *Neuron* 19(4), 939-945
46. Citron, M., Westaway, D., Xia, W., Carlson, G., Diehl, T., Levesque, G., Johnson-Wood, K., Lee, M., Seubert, P., Davis, A., Kholodenko, D., Motter, R., Sherrington, R., Perry, B., Yao, H., Strome, R., Lieberburg, I., Rommens, J., Kim, S., Schenk, D., Fraser, P., St George Hyslop, P., and Selkoe, D. J. (1997) *Nat. Med.* 3(1), 67-72
47. Duff, K., Eckman, C., Zehr, C., Yu, X., Prada, C. M., Perez-Tur, J., Hutton, M., Buee, L., Harigaya, Y., Yager, D., Morgan, D., Gordon, M. N., Holcomb, L., Refolo, L., Zenk, B., Hardy, J., and Younkin, S. (1996) *Nature* 383(6602), 710-713
48. Holcomb, L., Gordon, M. N., McGowan, E., Yu, X., Benkovic, S., Jantzen, P., Wright, K., Saad, I., Mueller, R., Morgan, D., Sanders, S., Zehr, C., O'Campo, K., Hardy, J., Prada, C. M., Eckman, C., Younkin, S., Hsiao, K., and Duff, K. (1998) *Nat Med* 4(1), 97-100

49. Scheuner, D., Eckman, C., Jensen, M., Song, X., Citron, M., Suzuki, N., Bird, T. D., Hardy, J., Hutton, M., Kukull, W., Larson, E., Levy-Lahad, E., Viitanen, M., Peskind, E., Poorkaj, P., Schellenberg, G., Tanzi, R., Wasco, W., Lannfelt, L., Selkoe, D., and Younkin, S. (1996) *Nat. Med.* 2(8), 864-870
50. Tomita, T., Maruyama, K., Saido, T. C., Kume, H., Shinozaki, K., Tokuhira, S., Capell, A., Walter, J., Grunberg, J., Haass, C., Iwatsubo, T., and Obata, K. (1997) *Proc. Natl. Acad. Sci. USA* 94(5), 2025-2030
51. Xia, W., Zhang, J., Kholodenko, D., Citron, M., Podlisny, M. B., Teplow, D. B., Haass, C., Seubert, P., Koo, E. H., and Selkoe, D. J. (1997) *J Biol Chem* 272(12), 7977-7982
52. Strittmatter, W. J., Saunders, A. M., Schmechel, D. E., Pericak-Vance, M., Enghild, J., Salvesen, G., and Roses, A. D. (1993) *PNAS* 90, 1977-1981
53. Jiang, Q., Lee, C. Y., Mandrekar, S., Wilkinson, B., Cramer, P., Zelcer, N., Mann, K., Lamb, B., Willson, T. M., Collins, J. L., Richardson, J. C., Smith, J. D., Comery, T. A., Riddell, D., Holtzman, D. M., Tontonoz, P., and Landreth, G. E. (2008) *Neuron* 58(5), 681-693
54. Daigle, I., and Li, C. (1993) *Proc Natl Acad Sci U S A* 90(24), 12045-12049
55. Rosen, D. R., Martin-Morris, L., Luo, L. Q., and White, K. (1989) *Proc Natl Acad Sci U S A* 86(7), 2478-2482
56. Coulson, E. J., Paliga, K., Beyreuther, K., and Masters, C. L. (2000) *Neurochem Int* 36(3), 175-184
57. Lorent, K., Overbergh, L., Moechars, D., De Strooper, B., Van Leuven, F., and Van den Berghe, H. (1995) *Neuroscience* 65(4), 1009-1025
58. Selkoe, D. J., Podlisny, M. B., Joachim, C. L., Vickers, E. A., Lee, G., Fritz, L. C., and Oltersdorf, T. (1988) *Proc Natl Acad Sci U S A* 85(19), 7341-7345
59. Kitaguchi, N., Takahashi, Y., Tokushima, Y., Shiojiri, S., and Ito, H. (1988) *Nature* 331(6156), 530-532
60. Tanzi, R. E., McClatchey, A. I., Lamperti, E. D., Villa-Komaroff, L., Gusella, J. F., and Neve, R. L. (1988) *Nature* 331(6156), 528-530
61. Sisodia, S. S., Koo, E. H., Hoffman, P. N., Perry, G., and Price, D. L. (1993) *J Neurosci* 13(7), 3136-3142
62. Zheng, H., Jiang, M., Trumbauer, M. E., Sirinathsinghji, D. J., Hopkins, R., Smith, D. W., Heavens, R. P., Dawson, G. R., Boyce, S., Conner, M. W., Stevens, K. A., Slunt, H. H., Sisodia, S. S., Chen, H. Y., and Van der Ploeg, L. H. (1995) *Cell* 81(4), 525-531
63. Phinney, A. L., Deller, T., Stalder, M., Calhoun, M. E., Frotscher, M., Sommer, B., Staufenbiel, M., and Jucker, M. (1999) *J Neurosci* 19(19), 8552-8559
64. von Koch, C. S., Zheng, H., Chen, H., Trumbauer, M., Thinakaran, G., van der Ploeg, L. H., Price, D. L., and Sisodia, S. S. (1997) *Neurobiol Aging* 18(6), 661-669
65. Heber, S., Herms, J., Gajic, V., Hainfellner, J., Aguzzi, A., Rulicke, T., von Kretschmar, H., von Koch, C., Sisodia, S., Tremml, P., Lipp, H. P., Wolfner, D. P., and Muller, U. (2000) *J Neurosci* 20(21), 7951-7963
66. Young-Pearse, T. L., Bai, J., Chang, R., Zheng, J. B., LoTurco, J. J., and Selkoe, D. J. (2007) *J Neurosci* 27(52), 14459-14469
67. Weidemann, A., Konig, G., Bunke, D., Fischer, P., Salbaum, J. M., Masters, C. L., and Beyreuther, K. (1989) *Cell* 57(1), 115-126
68. Seubert, P., Oltersdorf, T., Lee, M. G., Barbour, R., Blomquist, C., Davis, D. L., Bryant, K., Fritz, L. C., Galasko, D., Thal, L. J., and et al. (1993) *Nature* 361(6409), 260-263
69. Haass, C., Koo, E. H., Mellon, A., Hung, A. Y., and Selkoe, D. J. (1992) *Nature* 357(6378), 500-503
70. Shoji, M., Golde, T. E., Ghiso, J., Cheung, T. T., Estus, S., Shaffer, L. M., Cai, X. D., McKay, D. M., Tintner, R., Frangione, B., and et al. (1992) *Science* 258(5079), 126-129

71. Seubert, P., Vigo-Pelfrey, C., Esch, F., Lee, M., Dovey, H., Davis, D., Sinha, S., Schlossmacher, M., Whaley, J., Swindlehurst, C., and et al. (1992) *Nature* 359(6393), 325-327
72. Busciglio, J., Gabuzda, D. H., Matsudaira, P., and Yankner, B. A. (1993) *Proc. Natl. Acad. Sci. USA* 90(5), 2092-2096
73. Furukawa, K., Sopher, B., Rydel, R., Begley, J., Pham, D., Martin, G., Fox, M., and Mattson, M. (1996) *J Neurochem* 67, 1882-1896
74. Esch, F., Keim, P., Beattie, E., Blacher, R., Culwell, A., Oltersdorf, T., McClure, D., and Ward, P. (1990) *Science* 248, 1122-1124
75. Haass, C., Schlossmacher, M. G., Hung, A. Y., Vigo-Pelfrey, C., Mellon, A., Ostaszewski, B. L., Lieberburg, I., Koo, E. H., Schenk, D., Teplow, D. B., and Selkoe, D. J. (1992) *Nature* 359(6393), 322-325
76. Haass, C., Hung, A. Y., Schlossmacher, M. G., Teplow, D. B., and Selkoe, D. J. (1993) *J Biol Chem* 268(5), 3021-3024
77. Wolfe, M. S., Xia, W., Moore, C. L., Leatherwood, D. D., Ostaszewski, B., Rahmati, T., Donkor, I. O., and Selkoe, D. J. (1999) *Biochemistry* 38(15), 4720-4727
78. Yu, C., Kim, S. H., Ikeuchi, T., Xu, H., Gasparini, L., Wang, R., and Sisodia, S. S. (2001) *J. Biol. Chem.* 276, 43756-43760
79. Gu, Y., Misonou, H., Sato, T., Dohmae, N., Takio, K., and Ihara, Y. (2001) *J. Biol. Chem.* 276(38), 35235-35238.
80. Sastre, M., Steiner, H., Fuchs, K., Capell, A., Multhaup, G., Condrón, M. M., Teplow, D. B., and Haass, C. (2001) *EMBO Rep.* 2, 835-841
81. Weidemann, A., Eggert, S., Reinhard, F. B., Vogel, M., Paliga, K., Baier, G., Masters, C. L., Beyreuther, K., and Evin, G. (2002) *Biochemistry* 41(8), 2825-2835
82. Zhao, G., Mao, G., Tan, J., Dong, Y., Cui, M. Z., Kim, S. H., and Xu, X. (2004) *J Biol Chem* 279(49), 50647-50650
83. Zhao, G., Cui, M. Z., Mao, G., Dong, Y., Tan, J., Sun, L., and Xu, X. (2005) *J Biol Chem*
84. Qi-Takahara, Y., Morishima-Kawashima, M., Tanimura, Y., Dolios, G., Hirotani, N., Horikoshi, Y., Kametani, F., Maeda, M., Saido, T. C., Wang, R., and Ihara, Y. (2005) *J Neurosci* 25(2), 436-445
85. Funamoto, S., Morishima-Kawashima, M., Tanimura, Y., Hirotani, N., Saido, T. C., and Ihara, Y. (2004) *Biochemistry* 43(42), 13532-13540
86. Sato, T., Dohmae, N., Qi, Y., Kakuda, N., Misonou, H., Mitsumori, R., Maruyama, H., Koo, E. H., Haass, C., Takio, K., Morishima-Kawashima, M., Ishiura, S., and Ihara, Y. (2003) *J Biol Chem* 278(27), 24294-24301
87. Wolfsberg, T. G., Straight, P. D., Gerena, R. L., Huovila, A. P., Primakoff, P., Myles, D. G., and White, J. M. (1995) *Dev Biol* 169(1), 378-383
88. Blobel, C. P., Myles, D. G., Primakoff, P., and White, J. M. (1990) *J Cell Biol* 111(1), 69-78
89. Blobel, C. P., Wolfsberg, T. G., Turck, C. W., Myles, D. G., Primakoff, P., and White, J. M. (1992) *Nature* 356(6366), 248-252
90. Wolfsberg, T. G., Bazan, J. F., Blobel, C. P., Myles, D. G., Primakoff, P., and White, J. M. (1993) *Proc Natl Acad Sci U S A* 90(22), 10783-10787
91. Leighton, P. A., Mitchell, K. J., Goodrich, L. V., Lu, X., Pinson, K., Scherz, P., Skarnes, W. C., and Tessier-Lavigne, M. (2001) *Nature* 410(6825), 174-179
92. Zhou, H. M., Weskamp, G., Chesneau, V., Sahin, U., Vortkamp, A., Horiuchi, K., Chiusaroli, R., Hahn, R., Wilkes, D., Fisher, P., Baron, R., Manova, K., Basson, C. T., Hempstead, B., and Blobel, C. P. (2004) *Mol Cell Biol* 24(1), 96-104
93. Kurohara, K., Komatsu, K., Kurisaki, T., Masuda, A., Irie, N., Asano, M., Sudo, K., Nabeshima, Y., Iwakura, Y., and Sehara-Fujisawa, A. (2004) *Dev Biol* 267(1), 14-28
94. Sahin, U., Weskamp, G., Kelly, K., Zhou, H. M., Higashiyama, S., Peschon, J., Hartmann, D., Saftig, P., and Blobel, C. P. (2004) *J Cell Biol* 164(5), 769-779

95. Lammich, S., Kojro, E., Postina, R., Gilbert, S., Pfeiffer, R., Jasionowski, M., Haass, C., and Fahrenholz, F. (1999) *Proc. Natl. Acad. Sci. USA* 96(7), 3922-3927
96. Koike, H., Tomioka, S., Sorimachi, H., Saido, T. C., Maruyama, K., Okuyama, A., Fujisawa-Sehara, A., Ohno, S., Suzuki, K., and Ishiura, S. (1999) *Biochem. J.* 343, 371-375.
97. Buxbaum, J. D., Liu, K. N., Luo, Y., Slack, J. L., Stocking, K. L., Peschon, J. J., Johnson, R. S., Castner, B. J., Cerretti, D. P., and Black, R. A. (1998) *J. Biol. Chem.* 273(43), 27765-27767
98. Asai, M., Hattori, C., Szabó, B., Sasagawa, N., Maruyama, K., Tanuma, S., and Ishiura, S. (2003) *Biochem Biophys Res Commun* 391, 231-235
99. Hussain, I., Powell, D., Howlett, D. R., Tew, D. G., Meek, T. D., Chapman, C., Gloger, I. S., Murphy, K. E., Southan, C. D., Ryan, D. M., Smith, T. S., Simmons, D. L., Walsh, F. S., Dingwall, C., and Christie, G. (1999) *Mol. Cell. Neurosci.* 14(6), 419-427
100. Sinha, S., Anderson, J. P., Barbour, R., Basi, G. S., Caccavello, R., Davis, D., Doan, M., Dovey, H. F., Frigon, N., Hong, J., Jacobson-Croak, K., Jewett, N., Keim, P., Knops, J., Lieberburg, I., Power, M., Tan, H., Tatsuno, G., Tung, J., Schenk, D., Seubert, P., Suomensaaari, S. M., Wang, S., Walker, D., John, V., and et al. (1999) *Nature* 402(6761), 537-540
101. Vassar, R., Bennett, B. D., Babu-Khan, S., Kahn, S., Mendiaz, E. A., Denis, P., Teplow, D. B., Ross, S., Amarante, P., Loeloff, R., Luo, Y., Fisher, S., Fuller, J., Edenson, S., Lile, J., Jarosinski, M. A., Biere, A. L., Curran, E., Burgess, T., Louis, J. C., Collins, F., Treanor, J., Rogers, G., and Citron, M. (1999) *Science* 286(5440), 735-741
102. Yan, R., Bienkowski, M. J., Shuck, M. E., Miao, H., Tory, M. C., Pauley, A. M., Brashier, J. R., Stratman, N. C., Mathews, W. R., Buhl, A. E., Carter, D. B., Tomasselli, A. G., Parodi, L. A., Heinrikson, R. L., and Gurney, M. E. (1999) *Nature* 402(6761), 533-537
103. Lin, X., Koelsch, G., Wu, S., Downs, D., Dashti, A., and Tang, J. (2000) *Proc. Natl. Acad. Sci. USA* 97(4), 1456-1460
104. Cai, H., Wang, Y., McCarthy, D., Wen, H., Borchelt, D. R., Price, D. L., and Wong, P. C. (2001) *Nat Neurosci* 4(3), 233-234
105. Luo, Y., Bolon, B., Kahn, S., Bennett, B. D., Babu-Khan, S., Denis, P., Fan, W., Kha, H., Zhang, J., Gong, Y., Martin, L., Louis, J. C., Yan, Q., Richards, W. G., Citron, M., and Vassar, R. (2001) *Nat Neurosci* 4(3), 231-232
106. Liu, K., Doms, R. W., and Lee, V. M. (2002) *Biochemistry* 41(9), 3128-3136
107. Fluhner, R., Multhaup, G., Schlicksupp, A., Okochi, M., Takeda, M., Lammich, S., Willem, M., Westmeyer, G., Bode, W., Walter, J., and Haass, C. (2003) *J Biol Chem* 278(8), 5531-5538
108. Willem, M., Garratt, A., Novak, B., Citron, M., Kaufmann, S., Rittger, A., De Strooper, B., Saftig, P., Birchmeier, C., and Haass, C. (2006) *Science* 314, 664-666
109. Hu, X., Hicks, C. W., He, W., Wong, P., Macklin, W. B., Trapp, B. D., and Yan, R. (2006) *Nat Neurosci* 9(12), 1520-1525
110. Lichtenthaler, S. F., Dominguez, D., Westmeyer, G., Reiss, K., Haass, C., Saftig, P., De Strooper, B., and Seed, B. (2003) *J Biol Chem* 278, 48713-48719
111. Kitazume, S., Tachida, Y., Oka, R., Shirotani, K., Saido, T. C., and Hashimoto, Y. (2001) *PNAS* 98, 13554-13559
112. Solans, A., Estivill, X., and de La Luna, S. (2000) *Cytogenet Cell Genet* 89(3-4), 177-184
113. Acquati, F., Accarino, M., Nucci, C., Fumagalli, P., Jovine, L., Ottolenghi, S., and Taramelli, R. (2000) *FEBS Lett* 468(1), 59-64
114. Hussain, I., Powell, D. J., Howlett, D. R., Chapman, G. A., Gilmour, L., Murdock, P. R., Tew, D. G., Meek, T. D., Chapman, C., Schneider, K., Ratcliffe, S. J.,

- Tattersall, D., Testa, T. T., Southan, C., Ryan, D. M., Simmons, D. L., Walsh, F. S., Dingwall, C., and Christie, G. (2000) *Mol Cell Neurosci* 16(5), 609-619
115. Farzan, M., Schnitzler, C. E., Vasilieva, N., Leung, D., and Choe, H. (2000) *Proc Natl Acad Sci U S A* 97(17), 9712-9717
116. Yan, R., Munzner, J. B., Shuck, M. E., and Bienkowski, M. J. (2001) *J Biol Chem* 276(36), 34019-34027
117. Edbauer, D., Winkler, E., Regula, J. T., Pesold, B., Steiner, H., and Haass, C. (2003) *Nat. Cell Biol.* 5(5), 486-488
118. Kimberly, W. T., LaVoie, M. J., Ostaszewski, B. L., Ye, W., Wolfe, M. S., and Selkoe, D. J. (2003) *Proc. Natl. Acad. Sci. USA* 100(11), 6382-6387
119. Kim, S. H., Ikeuchi, T., Yu, C., and Sisodia, S. S. (2003) *J. Biol. Chem.* 278(36), 33992-34002
120. Takasugi, N., Tomita, T., Hayashi, I., Tsuruoka, M., Niimura, M., Takahashi, Y., Thinakaran, G., and Iwatsubo, T. (2003) *Nature* 422(6930), 438-441
121. Sato, T., Diehl, T. S., Narayanan, S., Funamoto, S., Ihara, Y., De Strooper, B., Steiner, H., Haass, C., and Wolfe, M. S. (2007) *J Biol Chem*
122. Capell, A., Grunberg, J., Pesold, B., Diehlmann, A., Citron, M., Nixon, R., Beyreuther, K., Selkoe, D. J., and Haass, C. (1998) *J. Biol. Chem.* 273(6), 3205-3211
123. Yu, G., Chen, F., Levesque, G., Nishimura, M., Zhang, D. M., Levesque, L., Rogaeva, E., Xu, D., Liang, Y., Duthie, M., St George-Hyslop, P. H., and Fraser, P. E. (1998) *J. Biol. Chem.* 273(26), 16470-16475
124. Evin, G., Canterford, L. D., Hoke, D. E., Sharples, R. A., Culvenor, J. G., and Masters, C. L. (2005) *Biochemistry* 44(11), 4332-4341
125. Nyabi, O., Bentahir, M., Horre, K., Herreman, A., Gottardi-Littell, N., Van Broeckhoven, C., Merchiers, P., Spittaels, K., Annaert, W., and De Strooper, B. (2003) *J. Biol. Chem.* 278, 43430-43436
126. Li, Y. M., Lai, M. T., Xu, M., Huang, Q., DiMuzio-Mower, J., Sardana, M. K., Shi, X. P., Yin, K. C., Shafer, J. A., and Gardell, S. J. (2000) *Proc. Natl. Acad. Sci. USA* 97(11), 6138-6143.
127. Edbauer, D., Winkler, E., Haass, C., and Steiner, H. (2002) *Proc. Natl. Acad. Sci. USA* 99(13), 8666-8671
128. Lazarov, V. K., Fraering, P. C., Ye, W., Wolfe, M. S., Selkoe, D. J., and Li, H. (2006) *Proc Natl Acad Sci U S A* 103(18), 6889-6894
129. Tolia, A., Chávez-Gutiérrez, L., and De Strooper, B. (2006) *JBC* 281, 27633-27642
130. Sato, C., Morohashi, Y., Tomita, T., and Iwatsubo, T. (2006) *J Neurosci* 26, 12081-12088
131. Laudon, H., Hansson, E. M., Melen, K., Bergman, A., Farmery, M. R., Winblad, B., Lendahl, U., von Heijne, G., and Naslund, J. (2005) *J Biol Chem* 280(42), 35352-35360
132. Oh, Y. S., and Turner, R. J. (2005) *Biochemistry* 44(35), 11821-11828
133. Kaether, C., Capell, A., Edbauer, D., Winkler, E., Novak, B., Steiner, H., and Haass, C. (2004) *Embo J* 23(24), 4738-4748
134. Thinakaran, G., Borchelt, D. R., Lee, M. K., Slunt, H. H., Spitzer, L., Kim, G., Ratovitsky, T., Davenport, F., Nordstedt, C., Seeger, M., Hardy, J., Levey, A. I., Gandy, S. E., Jenkins, N. A., Copeland, N. G., Price, D. L., and Sisodia, S. S. (1996) *Neuron* 17(1), 181-190
135. Saura, C. A., Tomita, T., Davenport, F., Harris, C. L., Iwatsubo, T., and Thinakaran, G. (1999) *J. Biol. Chem.* 274(20), 13818-13823
136. Ratovitski, T., Slunt, H. H., Thinakaran, G., Price, D. L., Sisodia, S. S., and Borchelt, D. R. (1997) *J. Biol. Chem.* 272(39), 24536-24541
137. Steiner, H., Capell, A., Pesold, B., Citron, M., Kloetzel, P. M., Selkoe, D. J., Romig, H., Mendla, K., and Haass, C. (1998) *J. Biol. Chem.* 273(48), 32322-32331
138. Shirotani, K., Edbauer, D., Prokop, S., Haass, C., and Steiner, H. (2004) *J Biol Chem*

139. Steiner, H., Winkler, E., Edbauer, D., Prokop, S., Basset, G., Yamasaki, A., Kostka, M., and Haass, C. (2002) *J. Biol. Chem.* 277, 39062-39065
140. De Strooper, B., Saftig, P., Craessaerts, K., Vanderstichele, H., Guhde, G., Annaert, W., Von Figura, K., and Van Leuven, F. (1998) *Nature* 391(6665), 387-390
141. Naruse, S., Thinakaran, G., Luo, J. J., Kusiak, J. W., Tomita, T., Iwatsubo, T., Qian, X., Ginty, D. D., Price, D. L., Borchelt, D. R., Wong, P. C., and Sisodia, S. S. (1998) *Neuron* 21(5), 1213-1221
142. Shearman, M. S., Beher, D., Clarke, E. E., Lewis, H. D., Harrison, T., Hunt, P., Nadin, A., Smith, A. L., Stevenson, G., and Castro, J. L. (2000) *Biochemistry* 39(30), 8698-8704.
143. Wolfe, M. S., Xia, W., Ostaszewski, B. L., Diehl, T. S., Kimberly, W. T., and Selkoe, D. J. (1999) *Nature* 398(6727), 513-517
144. Steiner, H., Duff, K., Capell, A., Romig, H., Grim, M. G., Lincoln, S., Hardy, J., Yu, X., Picciano, M., Fichteler, K., Citron, M., Kopan, R., Pesold, B., Keck, S., Baader, M., Tomita, T., Iwatsubo, T., Baumeister, R., and Haass, C. (1999) *J. Biol. Chem.* 274(40), 28669-28673
145. Kimberly, W. T., Xia, W., Rahmati, T., Wolfe, M. S., and Selkoe, D. J. (2000) *J. Biol. Chem.* 275(5), 3173-3178
146. Li, Y. M., Xu, M., Lai, M. T., Huang, Q., Castro, J. L., DiMuzio-Mower, J., Harrison, T., Lellis, C., Nadin, A., Neduvelli, J. G., Register, R. B., Sardana, M. K., Shearman, M. S., Smith, A. L., Shi, X. P., Yin, K. C., Shafer, J. A., and Gardell, S. J. (2000) *Nature* 405, 689-694
147. Esler, W. P., Kimberly, W. T., Ostaszewski, B. L., Diehl, T. S., Moore, C. L., Tsai, J.-Y., Rahmati, T., Xia, W., Selkoe, D. J., and Wolfe, M. S. (2000) *Nat. Cell Biol.* 2, 428-433
148. Steiner, H., Kostka, M., Romig, H., Basset, G., Pesold, B., Hardy, J., Capell, A., Meyn, L., Grim, M. G., Baumeister, R., Fichteler, K., and Haass, C. (2000) *Nat. Cell Biol.* 2, 848-851
149. Yamasaki, A., Eimer, S., Okochi, M., Smialowska, A., Kaether, C., Baumeister, R., Haass, C., and Steiner, H. (2006) *J Neurosci* 26(14), 3821-3828
150. Steiner, H., Romig, H., Pesold, B., Philipp, U., Baader, M., Citron, M., Loetscher, H., Jacobsen, H., and Haass, C. (1999) *Biochemistry* 38(44), 14600-14605
151. Nakaya, Y., Yamane, T., Shiraiishi, H., Wang, H., Matsubara, E., Sato, T., Dolios, G., Wang, R., De Strooper, B., Shoji, M., Komano, H., Yanagisawa, K., Ihara, Y., Fraser, P., St George Hyslop, P., and Nishimura, M. (2005) *JBC* 280(May 13), 19070-19077
152. Tu, H., Nelson, O., Bezprozvanny, A., Wang, Z., Lee, S. F., Hao, Y. H., Serneels, L., De Strooper, B., Yu, G., and Bezprozvanny, I. (2006) *Cell* 126(5), 981-993
153. Khachaturian, Z. S. (1989) *Ann N Y Acad Sci* 568, 1-4
154. Kaether, C., Lammich, S., Edbauer, D., Ertl, M., Rietdorf, J., Capell, A., Steiner, H., and Haass, C. (2002) *J. Cell Biol.* in press
155. Cai, D., Leem, J. Y., Greenfield, J. P., Wang, P., Kim, B. S., Wang, R., Lopes, K. O., Kim, S. H., Zheng, H., Greengard, P., Sisodia, S. S., Thinakaran, G., and Xu, H. (2003) *J Biol Chem* 278(5), 3446-3454
156. Levitan, D., Lee, J., Song, L., Manning, R., Wong, G., Parker, E., and Zhang, L. (2001) *Proc Natl Acad Sci U S A* 98(21), 12186-12190
157. Guo, Y., Livne-Bar, I., Zhou, L., and Boulianne, G. L. (1999) *J. Neurosci.* 19(19), 8435-8442
158. Wang, R., Tang, P., Wang, P., Boissy, R. E., and Zheng, H. (2006) *Proc Natl Acad Sci U S A* 103(2), 353-358
159. Nishimura, M., Yu, G., Levesque, G., Zhang, D. M., Ruel, L., Chen, F., Milman, P., Holmes, E., Liang, Y., Kawarai, T., Jo, E., Supala, A., Rogaeva, E., Xu, D. M., Janus, C., Levesque, L., Bi, Q., Duthie, M., Rozmahel, R., Mattila, K., Lannfelt, L.,



- Westaway, D., Mount, H. T., Woodgett, J., St George-Hyslop, P., and et al. (1999) *Nat Med* 5(2), 164-169
160. Noll, E., Medina, M., Hartley, D., Zhou, J., Perrimon, N., and Kosik, K. S. (2000) *Dev Biol* 227(2), 450-464
161. Yu, G., Nishimura, M., Arawaka, S., Levitan, D., Zhang, L., Tandon, A., Song, Y. Q., Rogaeva, E., Chen, F., Kawarai, T., Supala, A., Levesque, L., Yu, H., Yang, D. S., Holmes, E., Milman, P., Liang, Y., Zhang, D. M., Xu, D. H., Sato, C., Rogaeve, E., Smith, M., Janus, C., Zhang, Y., Aebersold, R., Farrer, L. S., Sorbi, S., Bruni, A., Fraser, P., and St George-Hyslop, P. (2000) *Nature* 407(6800), 48-54
162. Chen, F., Yu, G., Arawaka, S., Nishimura, M., Kawarai, T., Yu, H., Tandon, A., Supala, A., Song, Y. Q., Rogaeva, E., Milman, P., Sato, C., Yu, C., Janus, C., Lee, J., Song, L., Zhang, L., Fraser, P. E., and St George-Hyslop, P. H. (2001) *Nat. Cell Biol.* 3(8), 751-754.
163. Shirotani, K., Edbauer, D., Kostka, M., Steiner, H., and Haass, C. (2004) *J. Neurochem.* in press
164. Yu, G., Nishimura, M., Arawaka, S., Levitan, D., Zhang, L., Tandon, A., Song, Y. Q., Rogaeva, E., Chen, F., Kawarai, T., Supala, A., Levesque, L., Yu, H., Yang, D. S., Holmes, E., Milman, P., Liang, Y., Zhang, D. M., Xu, D. H., Sato, C., Rogaeve, E., Smith, M., Janus, C., Zhang, Y., Aebersold, R., Farrer, L. S., Sorbi, S., Bruni, A., Fraser, P., and St George-Hyslop, P. (2000) *Nature* 407(6800), 48-54.
165. Shah, S., Lee, S. F., Tabuchi, K., Hao, Y. H., Yu, C., LaPlant, Q., Ball, H., Dann, C. E., 3rd, Sudhof, T., and Yu, G. (2005) *Cell* 122(3), 435-447
166. Chávez-Gutiérrez, L., Tolia, A., Maes, E., Li, T., Wong, P., and De Strooper, B. (2008) *J Biol Chem* 283(29), 20096-20105
167. Francis, R., McGrath, G., Zhang, J., Ruddy, D. A., Sym, M., Apfeld, J., Nicoll, M., Maxwell, M., Hai, B., Ellis, M. C., Parks, A. L., Xu, W., Li, J., Gurney, M., Myers, R. L., Himes, C. S., Hiebsch, R. D., Ruble, C., Nye, J. S., and Curtis, D. (2002) *Dev. Cell* 3(1), 85-97
168. Watanabe, N., Tomita, T., Sato, C., Kitamura, T., Morohashi, Y., and Iwatsubo, T. (2005) *J Biol Chem* 280(51), 41967-41975
169. Kim, S. H., and Sisodia, S. S. (2005) *J Biol Chem* 280(51), 41953-41966
170. Prokop, S., Shirotani, K., Edbauer, D., Haass, C., and Steiner, H. (2004) *J. Biol. Chem.* 279, 23255-23261
171. Hasegawa, H., Sanjo, N., Chen, F., Gu, Y. J., Shier, C., Petit, A., Kawarai, T., Katayama, T., Schmidt, S. D., Mathews, P. M., Schmitt-Ulms, G., Fraser, P. E., and St George-Hyslop, P. (2004) *J Biol Chem* 279(45), 46455-46463
172. Fortna, R. R., Crystal, A. S., Morais, V. A., Pijak, D. S., Lee, V. M., and Doms, R. W. (2004) *J. Biol. Chem.* 279(5), 3685-3693
173. Goutte, C., Tsunozaki, M., Hale, V. A., and Priess, J. R. (2002) *Proc. Natl. Acad. Sci. USA* 99(2), 775-779.
174. Lee, S. F., Shah, S., Li, H., Yu, C., Han, W., and Yu, G. (2002) *J. Biol. Chem.* 277(47), 45013-45019
175. Hebert, S. S., Serneels, L., Dejaegere, T., Horre, K., Dabrowski, M., Baert, V., Annaert, W., Hartmann, D., and De Strooper, B. (2004) *Neurobiol Dis* 17(2), 260-272
176. Shirotani, K., Tomioka, M., Kremmer, E., Haass, C., and Steiner, H. (2007) *Neurobiol Dis* 27(1), 102-107
177. Gu, Y., Chen, F., Sanjo, N., Kawarai, T., Hasegawa, H., Duthie, M., Li, W., Ruan, X., Luthra, A., Mount, H. T., Tandon, A., Fraser, P. E., and St George-Hyslop, P. (2003) *J. Biol. Chem.* 278, 7374-7380
178. LaVoie, M. J., Fraering, P. C., Ostaszewski, B. L., Ye, W., Kimberly, W. T., Wolfe, M. S., and Selkoe, D. J. (2003) *J. Biol. Chem.* 278(39), 37213-37222
179. Hu, Y., and Fortini, M. E. (2003) *J. Cell Biol.* 161(4), 685-690
180. Capell, A., Beher, D., Prokop, S., Steiner, H., Kaether, C., Shearman, M. S., and Haass, C. (2005) *J Biol Chem* 280(8), 6471-6478

181. Morais, V. A., Crystal, A. S., Pijak, D. S., Carlin, D., Costa, J., Lee, V. M., and Doms, R. W. (2003) *J. Biol. Chem.* 278, 43284-43291
182. Luo, W. J., Wang, H., Li, H., Kim, B. S., Shah, S., Lee, H. J., Thinakaran, G., Kim, T. W., Yu, G., and Xu, H. (2003) *J. Biol. Chem.* 278(10), 7850-7854
183. Kim, S. H., Yin, Y. I., Li, Y. M., and Sisodia, S. S. (2004) *J Biol Chem* 279(47), 48615-48619
184. Chyung, J. H., Raper, D. M., and Selkoe, D. J. (2005) *J Biol Chem* 280(6), 4383-4392
185. Bergman, A., Hansson, E. M., Pursglove, S. E., Farmery, M. R., Lannfelt, L., Lendahl, U., Lundkvist, J., and Naslund, J. (2004) *J. Biol. Chem.* 279(16), 16744-16753
186. Sato, K., Sato, M., and Nakano, A. (2003) *Mol Biol Cell* 14(9), 3605-3616
187. Spasic, D., Raemaekers, T., Dillen, K., Declerck, I., Baert, V., Serneels, L., Fullekrug, J., and Annaert, W. (2007) *J Cell Biol* 176(5), 629-640
188. Kaether, C., Scheuermann, J., Fassler, M., Zilow, S., Shirotani, K., Valkova, C., Novak, B., Kacmar, S., Steiner, H., and Haass, C. (2007) *EMBO Rep* 8(8), 743-748
189. Meyer, E. L., Strutz, N., Gahring, L. C., and Rogers, S. W. (2003) *J Biol Chem* 278(26), 23786-23796
190. Scheinfeld, M. H., Ghersi, E., Laky, K., Fowlkes, B. J., and D'Adamio, L. (2002) *J Biol Chem* 277(46), 44195-44201
191. Saxena, M. T., Schroeter, E. H., Mumm, J. S., and Kopan, R. (2001) *J Biol Chem* 276(43), 40268-40273
192. Lammich, S., Okochi, M., Takeda, M., Kaether, C., Capell, A., Zimmer, A. K., Edbauer, D., Walter, J., Steiner, H., and Haass, C. (2002) *J Biol Chem* 277(47), 44754-44759
193. Ikeuchi, T., and Sisodia, S. S. (2003) *J Biol Chem* 278(10), 7751-7754
194. Marambaud, P., Shioi, J., Serban, G., Georgakopoulos, A., Sarnier, S., Nagy, V., Baki, L., Wen, P., Efthimiopoulos, S., Shao, Z., Wisniewski, T., and Robakis, N. K. (2002) *Embo J.* 21(8), 1948-1956
195. Ni, C. Y., Murphy, M. P., Golde, T. E., and Carpenter, G. (2001) *Science* 294(5549), 2179-2181
196. May, P., Reddy, Y. K., and Herz, J. (2002) *J Biol Chem* 277(21), 18736-18743
197. Kim, D. Y., Ingano, L. A., and Kovacs, D. M. (2002) *J Biol Chem* 277(51), 49976-49981
198. Taniguchi, Y., Kim, S. H., and Sisodia, S. S. (2003) *J Biol Chem* 278(33), 30425-30428
199. Schulz, J. G., Annaert, W., Vandekerckhove, J., Zimmermann, P., De Strooper, B., and David, G. (2003) *J Biol Chem* 278(49), 48651-48657
200. Gowrishankar, K., Zeidler, M. G., and Vincenz, C. (2004) *J Cell Sci* 117(Pt 18), 4099-4111
201. Niwa, M., Sidrauski, C., Kaufman, R. J., and Walter, P. (1999) *Cell* 99(7), 691-702
202. Tomita, T., Tanaka, S., Morohashi, Y., and Iwatsubo, T. (2006) *Mol Neurodegener* 1, 2
203. Kuhn, P. H., Marjaux, E., Imhof, A., De Strooper, B., Haass, C., and Lichtenthaler, S. F. (2007) *J Biol Chem* 282(16), 11982-11995
204. De Strooper, B., Annaert, W., Cupers, P., Saftig, P., Craessaerts, K., Mumm, J. S., Schroeter, E. H., Schrijvers, V., Wolfe, M. S., Ray, W. J., Goate, A., and Kopan, R. (1999) *Nature* 398(6727), 518-522
205. Jarriault, S., Brou, C., Logeat, F., Schroeter, E. H., Kopan, R., and Israel, A. (1995) *Nature* 377(6547), 355-358
206. Joutel, A., and Tournier-Lasserre, E. (1998) *Semin Cell Dev Biol* 9(6), 619-625
207. Levitan, D., and Greenwald, I. (1995) *Nature* 377(6547), 351-354
208. Blaumueller, C. M., Qi, H., Zagouras, P., and Artavanis-Tsakonas, S. (1997) *Cell* 90(2), 281-291

209. Saxena, M. T., Schroeter, E. H., Mumm, J. S., and Kopan, R. (2001) *J. Biol. Chem.* 276(43), 40268-40273.
210. Logeat, F., Bessia, C., Brou, C., LeBail, O., Jarriault, S., Seidah, N. G., and Israel, A. (1998) *Proc. Natl. Acad. Sci. USA* 95(14), 8108-8112.
211. Okochi, M., Fukumori, A., Jiang, J., Itoh, N., Kimura, R., Steiner, H., Haass, C., Tagami, S., and Takeda, M. (2006) *J Biol Chem* 281(12), 7890-7898
212. Culty, M., Miyake, K., Kincade, P. W., Sikorski, E., Butcher, E. C., and Underhill, C. (1990) *J Cell Biol* 111(6 Pt 1), 2765-2774
213. Thomas, L., Byers, H. R., Vink, J., and Stamenkovic, I. (1992) *J Cell Biol* 118(4), 971-977
214. Gunthert, U., Hofmann, M., Rudy, W., Reber, S., Zoller, M., Haussmann, I., Matzju, S., Wenzel, A., Ponta, H., and Herrlich, P. (1991) *Cell* 65, 13-24
215. Kajita, M., Itoh, Y., Chiba, T., Mori, H., Okada, A., Kinoh, H., and Seiki, M. (2001) *J Cell Biol* 153(5), 893-904
216. Nagano, O., Murakami, D., Hartmann, D., De Strooper, B., Saftig, P., Iwatsubo, T., Nakajima, M., Shinohara, M., and Saya, H. (2004) *J Cell Biol* 165(6), 893-902
217. Nakamura, H., Suenaga, N., Taniwaki, K., Matsuki, H., Yonezawa, K., Fujii, M., Okada, Y., and Seiki, M. (2004) *Cancer Res* 64(3), 876-882
218. okamoto, I., Kawano, Y., Tsuiki, H., Sasaki, J., Nakao, M., Matsumoto, M., Suga, M., Ando, M., Nakajima, M., and Saya, H. (1999) *oncogen* 18, 1435-1446
219. Okamoto, I., Tsuiki, H., Kenyon, L. C., Godwin, A. K., Emllet, D. R., Holgado-Madruga, M., Lanham, I. S., Joynes, C. J., Vo, K. T., Guha, A., Matsumoto, M., Ushio, Y., Saya, H., and Wong, A. J. (2002) *Am J Pathol* 160(2), 441-447
220. Okamoto, I., Kawano, Y., Murakami, D., Sasayama, T., Araki, N., Miki, T., Wong, A. J., and Saya, H. (2001) *J Cell Biol* 155(5), 755-762
221. Struhl, G., and Adachi, A. (2000) *Mol. Cell* 6, 625-636
222. Esler, W. P., Kimberly, W. T., Ostaszewski, B. L., Ye, W., Diehl, T. S., Selkoe, D. J., and Wolfe, M. S. (2002) *Proc. Natl. Acad. Sci. USA* 99, 2720-2725.
223. Beher, D., Fricker, M., Nadin, A., Clarke, E. E., Wrigley, J. D., Li, Y. M., Culvenor, J. G., Masters, C. L., Harrison, T., and Shearman, M. S. (2003) *Biochemistry* 42(27), 8133-8142
224. Kornilova, A. Y., Bihel, F., Das, C., and Wolfe, M. S. (2005) *Proc Natl Acad Sci U S A* 102(9), 3230-3235
225. Hong, L., Koelsch, G., Lin, X., Wu, S., Terzyan, S., Ghosh, A. K., Zhang, X. C., and Tang, J. (2000) *Science* 290(5489), 150-153
226. Demeule, M., Regina, A., Jodoin, J., Laplante, A., Dagenais, C., Berthelet, F., Moghrabi, A., and Beliveau, R. (2002) *Vascul Pharmacol* 38(6), 339-348
227. Hussain, I., Hawkins, J., Harrison, D., Hille, C., Wayne, G., Cutler, L., Buck, T., Walter, D., Demont, E., Howes, C., Naylor, A., Jeffrey, P., Gonzalez, M. I., Dingwall, C., Michel, A., Redshaw, S., and Davis, J. B. (2007) *J Neurochem* 100(3), 802-809
228. Stachel, S. J., Coburn, C. A., Steele, T. G., Crouthamel, M. C., Pietrak, B. L., Lai, M. T., Holloway, M. K., Munshi, S. K., Graham, S. L., and Vacca, J. P. (2006) *Bioorg Med Chem Lett* 16(3), 641-644
229. Lewis, H. D., Perez Revuelta, B. I., Nadin, A., Neduelil, J. G., Harrison, T., Pollack, S. J., and Shearman, M. S. (2003) *Biochemistry* 42(24), 7580-7586
230. Hadland, B. K., Manley, N. R., Su, D., Longmore, G. D., Moore, C. L., Wolfe, M. S., Schroeter, E. H., and Kopan, R. (2001) *Proc Natl Acad Sci U S A* 98(13), 7487-7491
231. Wong, G. T., Manfra, D., Poulet, F. M., Zhang, Q., Josien, H., Bara, T., Engstrom, L., Pinzon-Ortiz, M., Fine, J. S., Lee, H. J., Zhang, L., Higgins, G. A., and Parker, E. M. (2004) *J Biol Chem* 279(13), 12876-12882
232. Nickoloff, B. J., Osborne, B. A., and Miele, L. (2003) *Oncogene* 22(42), 6598-6608

233. Weggen, S., Eriksen, J. L., Das, P., Sagi, S. A., Wang, R., Pietrzik, C. U., Findlay, K. A., Smith, T. E., Murphy, M. P., Bulter, T., Kang, D. E., Marquez-Sterling, N., Golde, T. E., and Koo, E. H. (2001) *Nature* 414(6860), 212-216
234. Takahashi, Y., Hayashi, I., Tominari, Y., Rikimaru, K., Morohashi, Y., Kan, T., Natsugari, H., Fukuyama, T., Tomita, T., and Iwatsubo, T. (2003) *J Biol Chem* 278(20), 18664-18670
235. Weggen, S., Eriksen, J. L., Sagi, S. A., Pietrzik, C. U., Ozols, V., Fauq, A., Golde, T. E., and Koo, E. H. (2003) *J Biol Chem* 278(34), 31831-31837
236. Behr, D., Clarke, E. E., Wrigley, J. D., Martin, A. C., Nadin, A., Churcher, I., and Shearman, M. S. (2004) *J Biol Chem* 279(42), 43419-43426
237. Lleo, A., Berezovska, O., Herl, L., Raju, S., Deng, A., Bacskai, B. J., Frosch, M. P., Irizarry, M., and Hyman, B. T. (2004) *Nat Med* 10(10), 1065-1066
238. Weggen, S., Eriksen, J. L., Sagi, S. A., Pietrzik, C. U., Golde, T. E., and Koo, E. H. (2003) *J Biol Chem* 278(33), 30748-30754
239. Zhou, S., Zhou, H., Walian, P. J., and Jap, B. K. (2005) *Proc Natl Acad Sci U S A* 102(21), 7499-7504
240. Chen, F., Hasegawa, H., Schmitt-Ulms, G., Kawarai, T., Bohm, C., Katayama, T., Gu, Y., Sanjo, N., Glista, M., Rogaeva, E., Wakutani, Y., Pardossi-Piquard, R., Ruan, X., Tandon, A., Checler, F., Marambaud, P., Hansen, K., Westaway, D., St George-Hyslop, P., and Fraser, P. (2006) *Nature* 440(7088), 1208-1212
241. Gabison, E. E., Hoang-Xuan, T., Mauviel, A., and Menashi, S. (2005) *Biochimie* 87(3-4), 361-368
242. Vetrivel, K. S., Zhang, X., Meckler, X., Cheng, H., Lee, S., Gong, P., Lopes, K. O., Chen, Y., Iwata, N., Yin, K. J., Lee, J. M., Parent, A. T., Saido, T. C., Li, Y. M., Sisodia, S. S., and Thinakaran, G. (2008) *J Biol Chem* 283(28), 19489-19498
243. Vetrivel, K. S., Gong, P., Bowen, J. W., Cheng, H., Chen, Y., Carter, M., Nguyen, P. D., Placanica, L., Wieland, F. T., Li, Y. M., Kounnas, M. Z., and Thinakaran, G. (2007) *Mol Neurodegener* 2, 4
244. Grigorenko, A. P., Moliaka, Y. K., Korovaitseva, G. I., and Rogaev, E. I. (2002) *Biochemistry (Mosc)* 67(7), 826-835
245. Ponting, C. P., Hutton, M., Nyborg, A., Baker, M., Jansen, K., and Golde, T. E. (2002) *Hum. Mol. Genet.* 11(9), 1037-1044
246. Weihofen, A., Binns, K., Lemberg, M. K., Ashman, K., and Martoglio, B. (2002) *Science* 296(5576), 2215-2218
247. Haass, C., and Steiner, H. (2002) *Trends Cell Biol.* 12, 556-562
248. LaPointe, C. F., and Taylor, R. K. (2000) *J. Biol. Chem.* 275(2), 1502-1510
249. LaPointe, C. F., and Taylor, R. K. (2000) *J Biol Chem* 275(2), 1502-1510
250. Strom, M. S., Nunn, D. N., and Lory, S. (1993) *Proc Natl Acad Sci U S A* 90(6), 2404-2408
251. Bieber, D., Ramer, S. W., Wu, C. Y., Murray, W. J., Tobe, T., Fernandez, R., and Schoolnik, G. K. (1998) *Science* 280(5372), 2114-2118
252. Friedmann, E., Lemberg, M. K., Weihofen, A., Dev, K. K., Dengler, U., Rovelli, G., and Martoglio, B. (2004) *J Biol Chem* 279(49), 50790-50798
253. Nyborg, A. C., Jansen, K., Ladd, T. B., Fauq, A., and Golde, T. E. (2004) *J Biol Chem* 279(41), 43148-43156
254. Nyborg, A. C., Kornilova, A. Y., Jansen, K., Ladd, T. B., Wolfe, M. S., and Golde, T. E. (2004) *J Biol Chem* 279(15), 15153-15160
255. Nyborg, A. C., Herl, L., Berezovska, O., Thomas, A. V., Ladd, T. B., Jansen, K., Hyman, B. T., and Golde, T. E. (2006) *Mol Neurodegener* 1, 16
256. Krawitz, P., Haffner, C., Fluhrer, R., Steiner, H., Schmid, B., and Haass, C. (2005) *J Biol Chem*
257. Weihofen, A., and Martoglio, B. (2003) *Trends Cell Biol.* 13, 71-78
258. McLauchlan, J., Lemberg, M. K., Hope, G., and Martoglio, B. (2002) *Embo J* 21(15), 3980-3988

259. Lemberg, M. K., Bland, F. A., Weihofen, A., Braud, V. M., and Martoglio, B. (2001) *J Immunol* 167(11), 6441-6446
260. Fluhrer, R., Grammer, G., Israel, L., Condrón, M. M., Haffner, C., Friedmann, E., Bohland, C., Imhof, A., Martoglio, B., Teplow, D. B., and Haass, C. (2006) *Nat Cell Biol* 8(8), 894-896
261. Friedmann, E., Hauben, E., Maylandt, K., Schlegler, S., Vreugde, S., Lichtenthaler, S. F., Kuhn, P. H., Stauffer, D., Rovelli, G., and Martoglio, B. (2006) *Nat Cell Biol* 8(8), 843-848
262. Martin, L., Fluhrer, R., Reiss, K., Kremmer, E., Saftig, P., and Haass, C. (2007) *J Biol Chem*
263. Vidal, R., Frangione, B., Rostagno, A., Mead, S., Revesz, T., Plant, G., and Ghiso, J. (1999) *Nature* 399(6738), 776-781
264. Weihofen, A., Lemberg, M. K., Ploegh, H. L., Bogoy, M., and Martoglio, B. (2000) *J. Biol. Chem.* 275(40), 30951-30956
265. Hecimovic, S., Wang, J., Dolios, G., Martinez, M., Wang, R., and Goate, A. M. (2004) *Neurobiol Dis* 17(2), 205-218
266. Kopan, R., Schroeter, E. H., Weintraub, H., and Nye, J. S. (1996) *Proc Natl Acad Sci U S A* 93(4), 1683-1688
267. Okochi, M., Steiner, H., Fukumori, A., Tanii, H., Tomita, T., Tanaka, T., Iwatsubo, T., Kudo, T., Takeda, M., and Haass, C. (2002) *EMBO J.* in press
268. Herreman, A., Hartmann, D., Annaert, W., Saftig, P., Craessaerts, K., Serneels, L., Umans, L., Schrijvers, V., Checler, F., Vanderstichele, H., Baekelandt, V., Dressel, R., Cupers, P., Huylebroeck, D., Zwijsen, A., Van Leuven, F., and De Strooper, B. (1999) *Proc. Natl. Acad. Sci. USA* 96(21), 11872-11877
269. Fenteany, G., Standaert, R. F., Lane, W. S., Choi, S., Corey, E. J., and Schreiber, S. L. (1995) *Science* 268(5211), 726-731
270. Kukar, T., Murphy, M. P., Eriksen, J. L., Sagi, S. A., Weggen, S., Smith, T. E., Ladd, T., Khan, M. A., Kache, R., Beard, J., Dodson, M., Merit, S., Ozols, V. V., Anastasiadis, P. Z., Das, P., Fauq, A., Koo, E. H., and Golde, T. E. (2005) *Nat Med* 11(5), 545-550
271. Tian, G., Sobotka-Briner, C. D., Zysk, J., Liu, X., Birr, C., Sylvester, M. A., Edwards, P. D., Scott, C. D., and Greenberg, B. D. (2002) *J. Biol. Chem.* 277(35), 31499-31505
272. Seubert, P., Vigo-Pelfrey, C., Esch, F., Lee, M., Dovey, H., Davis, D., Sinha, S., Schlossmacher, M., Whaley, J., Swindlehurst, C., and et al. (1992) *Nature* 359(6393), 325-327
273. Citron, M., Teplow, D. B., and Selkoe, D. J. (1995) *Neuron* 14(3), 661-670
274. Haass, C., Lemere, C. A., Capell, A., Citron, M., Seubert, P., Schenk, D., Lannfelt, L., and Selkoe, D. J. (1995) *Nat Med* 1(12), 1291-1296
275. Thinakaran, G., Harris, C. L., Ratovitski, T., Davenport, F., Slunt, H. H., Price, D. L., Borchelt, D. R., and Sisodia, S. S. (1997) *J. Biol. Chem.* 272(45), 28415-28422
276. Wiltfang, J., Smirnov, A., Schnierstein, B., Kelemen, G., Matthies, U., Klafki, H. W., Staufenbiel, M., Huther, G., Ruther, E., and Kornhuber, J. (1997) *Electrophoresis* 18(3-4), 527-532
277. Page, R. M., Baumann, K., Tomioka, M., Perez-Revuelta, B. I., Fukumori, A., Jacobsen, H., Flohr, A., Luebbers, T., Ozmen, L., Steiner, H., and Haass, C. (2007) *J Biol Chem*
278. Czirr, E., Cottrell, B. A., Leuchtenberger, S., Kukar, T., Ladd, T. B., Esselmann, H., Paul, S., Schubel, R., Torpey, J. W., Pietrzik, C. U., Golde, T. E., Wiltfang, J., Baumann, K., Koo, E. H., and Weggen, S. (2008) *J Biol Chem*
279. Czirr, E., Leuchtenberger, S., Dorner-Ciossek, C., Schneider, A., Jucker, M., Koo, E. H., Pietrzik, C. U., Baumann, K., and Weggen, S. (2007) *J Biol Chem* 282(34), 24504-24513

280. Eriksen, J. L., Sagi, S. A., Smith, T. E., Weggen, S., Das, P., McLendon, D. C., Ozols, V. V., Jessing, K. W., Zavitz, K. H., Koo, E. H., and Golde, T. E. (2003) *J Clin Invest* 112(3), 440-449
281. Murakami, D., Okamoto, I., Nagano, O., Kawano, Y., Tomita, T., Iwatsubo, T., De Strooper, B., Yumoto, E., and Saya, H. (2003) *Oncogene* 22(10), 1511-1516
282. Bachmair, A., Finley, D., and Varshavsky, A. (1986) *Science* 234(4773), 179-186
283. Oberg, C., Li, J., Pauley, A., Wolf, E., Gurney, M., and Lendahl, U. (2001) *J Biol Chem* 276(38), 35847-35853
284. Gupta-Rossi, N., Le Bail, O., Gonen, H., Brou, C., Logeat, F., Six, E., Ciechanover, A., and Israel, A. (2001) *J Biol Chem* 276(37), 34371-34378
285. Blat, Y., Meredith, J. E., Wang, Q., Bradley, J. D., Thompson, L. A., Olson, R. E., Stern, A. M., and Seiffert, D. (2002) *Biochem Biophys Res Commun* 299(4), 569-573
286. Chandu, D., Huppert, S. S., and Kopan, R. (2006) *J Neurochem* 96(1), 228-235
287. Aberle, H., Bauer, A., Stappert, J., Kispert, A., and Kemler, R. (1997) *Embo J* 16(13), 3797-3804
288. Xia, W., Ray, W. J., Ostaszewski, B. L., Rahmati, T., Kimberly, W. T., Wolfe, M. S., Zhang, J., Goate, A. M., and Selkoe, D. J. (2000) *Proc. Natl. Acad. Sci. USA* 97, 9299-9304
289. Kimberly, W. T., LaVoie, M. J., Ostaszewski, B. L., Ye, W., Wolfe, M. S., and Selkoe, D. J. (2002) *J. Biol. Chem.* 277(38), 35113-35117
290. Leem, J. Y., Vijayan, S., Han, P., Cai, D., Machura, M., Lopes, K. O., Veselits, M. L., Xu, H., and Thinakaran, G. (2002) *J. Biol. Chem.* 277(21), 19236-19240
291. Tomita, T., Katayama, R., Takikawa, R., and Iwatsubo, T. (2002) *FEBS Lett* 520(1-3), 117-121
292. Brunkan, A. L., Martinez, M., Wang, J., Walker, E. S., Beher, D., Shearman, M. S., and Goate, A. M. (2005) *J Neurochem* 94(5), 1315-1328
293. Brunkan, A. L., Martinez, M., Wang, J., Walker, E. S., and Goate, A. M. (2005) *J Neurochem* 92(5), 1158-1169
294. Wang, J., Beher, D., Nyborg, A. C., Shearman, M. S., Golde, T. E., and Goate, A. (2006) *J Neurochem* 96(1), 218-227
295. Ikeuchi, T., Dolios, G., Kim, S. H., Wang, R., and Sisodia, S. S. (2003) *J Biol Chem* 278(9), 7010-7018
296. Xia, W., Ostaszewski, B. L., Kimberly, W. T., Rahmati, T., Moore, C. L., Wolfe, M. S., and Selkoe, D. J. (2000) *Neurobiol Dis* 7(6 Pt B), 673-681
297. Lemieux, M. J., Fischer, S. J., Cherney, M. M., Bateman, K. S., and James, M. N. (2007) *Proc Natl Acad Sci U S A* 104(3), 750-754
298. Wu, Z., Yan, N., Feng, L., Oberstein, A., Yan, H., Baker, R. P., Gu, L., Jeffrey, P. D., Urban, S., and Shi, Y. (2006) *Nat Struct Mol Biol* 13(12), 1084-1091
299. Baker, R. P., Young, K., Feng, L., Shi, Y., and Urban, S. (2007) *Proc Natl Acad Sci U S A* 104(20), 8257-8262
300. Ben-Shem, A., Fass, D., and Bibi, E. (2007) *Proc Natl Acad Sci U S A* 104(2), 462-466
301. Wang, Y., Zhang, Y., and Ha, Y. (2006) *Nature* 444(7116), 179-180
302. Feng, L., Yan, H., Wu, Z., Yan, N., Wang, Z., Jeffrey, P. D., and Shi, Y. (2007) *Science* 318(5856), 1608-1612
303. Urban, S., Lee, J. R., and Freeman, M. (2001) *Cell* 107(2), 173-182.
304. Narayanan, S., Sato, T., and Wolfe, M. S. (2007) *J Biol Chem* 282(28), 20172-20179
305. Ng, S. Y., Chaban, B., VanDyke, D. J., and Jarrell, K. F. (2007) *Microbiology* 153(Pt 2), 305-314
306. Javadpour, M. M., Eilers, M., Groesbeek, M., and Smith, S. O. (1999) *Biophys J* 77(3), 1609-1618
307. Eilers, M., Shekar, S. C., Shieh, T., Smith, S. O., and Fleming, P. J. (2000) *Proc Natl Acad Sci U S A* 97(11), 5796-5801

308. Russ, W. P., and Engelman, D. M. (2000) *J Mol Biol* 296(3), 911-919
309. Sternberg, M. J., and Gullick, W. J. (1990) *Protein Eng* 3(4), 245-248
310. Senes, A., Gerstein, M., and Engelman, D. M. (2000) *J Mol Biol* 296(3), 921-936
311. Kienlen-Campard, P., Tasiaux, B., Van Hees, J., Li, M., Huysseune, S., Sato, T., Fei, J. Z., Aimoto, S., Courtoy, P. J., Smith, S. O., Constantinescu, S. N., and Octave, J. N. (2008) *J Biol Chem*
312. Munter, L. M., Voigt, P., Harmeier, A., Kaden, D., Gottschalk, K. E., Weise, C., Pipkorn, R., Schaefer, M., Langosch, D., and Multhaup, G. (2007) *Embo J* 26(6), 1702-1712
313. Lee, S. F., Shah, S., Yu, C., Wigley, W. C., Li, H., Lim, M., Pedersen, K., Han, W., Thomas, P., Lundkvist, J., Hao, Y. H., and Yu, G. (2004) *J Biol Chem* 279(6), 4144-4152
314. Edbauer, D., Kaether, C., Steiner, H., and Haass, C. (2004) *J Biol Chem* 279(36), 37311-37315
315. Niimura, M., Isoo, N., Takasugi, N., Tsuruoka, M., Ui-Tei, K., Saigo, K., Morohashi, Y., Tomita, T., and Iwatsubo, T. (2005) *J Biol Chem* 280(13), 12967-12975
316. Araki, W., Saito, S., Takahashi-Sasaki, N., Shiraishi, H., Komano, H., and Murayama, K. S. (2006) *J Mol Neurosci* 29(1), 35-43
317. Senes, A., Engel, D. E., and DeGrado, W. F. (2004) *Curr Opin Struct Biol* 14(4), 465-479
318. Mendrola, J. M., Berger, M. B., King, M. C., and Lemmon, M. A. (2002) *J Biol Chem* 277(7), 4704-4712
319. Jozwiak, K., Krzysko, K. A., Bojarski, L., Gacia, M., and Filipek, S. (2007) *ChemMedChem*
320. Sato, C., Takagi, S., Tomita, T., and Iwatsubo, T. (2008) *J Neurosci* 28(24), 6264-6271

## Acknowledgements

I am grateful to thank Prof. Dr. Christian Haass for the opportunity to join his lab and work on this exciting research project as well as for his suggestions during the achievement of this thesis.

I would also like to thank Prof. Dr. Ralf-Peter Jansen who kindly became my supervisor and made possible that this thesis was accepted in the Faculty of Pharmacy and Chemistry.

I am indebted and I have to express my deepest gratitude to Prof. Dr. Harald Steiner for his kind support, help and advice during these years. His ideas and suggestions, has been great value for the achievement of this dissertation.

Without my colleagues from the lab Edith, Gabi, Richard, Beni, Masanori, Akio as well as the former lab members Aya and Keiro I could not have enjoyed the time working as much as I did. They all have given good advices and tips for my work and I have really enjoyed their company in and outside the lab.

I also have to thank my friends from outside the lab, Juampa, Emiliano, Laura, Mercedes, Belén, have always supported and encouraged me here and in the distance.

I would also like to thank my parents, my sister and my godmother because they always have believed in me and had given me the opportunity to reach what I have reached and for the long telephonic conversations which had helped me to be less homesick.

Last, but not least, I would also want to thank Sebastian for his tender care, love, support as well as for his enduring patience.



## CURRICULUM VITAE

### **Personal data:**

Name: Blanca Isabel Pérez Revuelta  
 Sex: Female  
 Address: Edlingerplatz 1, 81543 München  
 E-mail: bperezre@med.uni-muenchen.de  
 Date of birth: 14.07.1977  
 Place of birth: Salamanca, Spain  
 Nationality: Spanish  
 Marital status: Single

### **Education:**

#### ***Dissertation***

2002-2008: Ludwig-Maximilians-University Munich, Adolf-Butenandt Institute, Prof. Dr. C. Haass

#### ***Visiting scientist***

2001-2002. Merck Sharp and Dohme, Essex, UK

#### ***Leonardo da Vinci programme***

2001. Merck Sharp and Dohme, Harlow, Essex, UK

#### ***MSc in Biology***

2001. University of Salamanca, Spain, Faculty of Biology, department of Physical-Chemistry, Prof. Dr. Licesio J. Rodríguez, Spain.

#### ***BSc in Biochemistry***

1995-2000. University of Salamanca, Spain

#### ***High school***

1991-1995: Maristas Champagnat School, Salamanca, Spain

#### ***Elementary school***

1988-1991: Maristas Champagnat School, Salamanca, Spain

1983-1988: Santísima Trinidad School, Salamanca, Spain

### **Presentations/Conferences:**

July 2006: Poster presentation at the 10<sup>th</sup> International Conference on Alzheimer's Disease and Related Disorders, Madrid, Spain

May 2006: Presentation at SFB meeting, "Meeting of the Alzheimer's Disease Research Focus, Fourth Progress Report". Adolf-Butenandt Institute

**Publications:****Effect of PVP K-25 on the formation of the naproxen:beta cyclodextrin complex.**

Valero M, Pérez-Revuelta BI, Rodríguez LJ.

*Int J Pharm.* 2003 Mar 6;253(1-2):97-110

**Catalytic site-directed gamma secretase complex inhibitors do not discriminate pharmacologically between Notch S3 and beta-APP cleavages.**

Lewis HD, Pérez Revuelta BI, Nadin A, Neduveilil JG, Harrison T, Pollack SJ, Shearman MS.

*Biochemistry.* 2003 Jun 24;42(24):7580-6

**Scaffold of the cyclooxygenase-2 (COX-2) inhibitor carprofen provides Alzheimer gamma-secretase modulators.**

Narlawar R, Pérez Revuelta BI, Haass C, Steiner H, Schimdt B, Baumann K.

*J Med Chem* 2006 Dec 28;49(26):7588-91

**N-Substituted carbazolyloxyacetic acids modulate Alzheimer associated gamma-secretase.**

Narlawar R, Pérez Revuelta BI, Baumann K, Schubeneil R, Haass C, Steiner H, Schimdt B.

*Bioorg Med Chem Letters* 2007 Jan 1;17(1):176-82.

**Generation of Abeta 38 and Abeta 42 is independently and differentially affected by FAD-associated presenilin 1 mutations and gamma secretase modulation.**

Page RM, Baumann K, Tomioka M, Pérez Revuelta BI, Fukumori A, Jacobsen H, Flohr A, Luebbers T, Ozmen L, Steiner H, Haass C.

*J Biol Chem* 2008 Jan 11;283(2):677-83

**PUBLICATIONS**